MOLECULAR BASIS OF INHIBITORY MODULATION OF P2X2 RECEPTORS BY ZINC AND COPPER

by

Sukanya Srinivasa Rao Arun Punthambaker

A dissertation submitted in partial fulfillment
of the requirements for the degree of
Doctor of Philosophy
(Molecular, Cellular, and Developmental Biology)
in The University of Michigan
2012

Doctoral Committee:

Professor Richard I. Hume, Chair
Associate Professor Matthew R. Chapman
Associate Professor Haoxing Xu
Assistant Professor Gabrielle Rudenko
Assistant Professor Michael M. Sutton

OM TAMASO MA JYOTIRGAMAYA

“From darkness to light”

(Brhadaranyaka Upanishad)

To my parents, brother and everyone who made this possible

ACKNOWLEDGEMENTS

This Ph.D. was made possible by the support and wishes from a lot of people. I would like to thank everyone who helped me get this far and made this degree a reality.

I would like to thank my parents and younger brother for their unconditional love and support throughout the testing times of my degree.

I would like to express my deep and sincere gratitude to my advisor Dr. Richard Hume for being an excellent mentor and guide and for his constant support and encouragement. His trust in me and confidence that I could succeed despite coming from a different academic background, kept me going.

I would like to thank all past and present members of the Hume lab; Dr. Rachel Tittle, Dr. Sean Low, Dr. Sean Friday with special thanks to Dr. Naomi Nagaya and Dr. Shlomo Dellal for their helpful discussions about my projects and being great friends and colleagues in the lab. Thank you Jamila Power for the all-round help with general technical expertise in the lab. Thank you to all the past and present undergraduate students in the lab especially those who directly worked with me; Divya Gehi, Jacob Blum, Nahid Rashid and Connie Truong. Jacob Blum is second author on chapter 2 of this thesis which is published in the Journal of Biological Chemistry, 2012.

I would like to sincerely thank Dr. Gabby Rudenko who was my collaborator mentor during the initial years of my PhD thesis. I learnt a tremendous lot of biochemical techniques and general lab procedures during my project in her lab. I also received a lot of help on my project from all other members in her lab especially Sha Huang and Prashant Rajbhandari.

I would like to thank my thesis committee members Dr. Matt Chapman, Dr. Haoxing Xu and Dr. Gabby Rudenko for their invaluable advice, insight and suggestions towards the

progress of my projects. A special thank you to Dr. Mike Sutton who graciously agreed to join my committee during the last minute of my thesis defense.

Thank you Dr. Ken Cadigan for showing me the doors to Rich's lab and convincing me that I will be able to do well.

I would like to thank all my dear students from MCDB 222 and MCDB 423 particularly the ones who supported me for being selected for the Outstanding GSI award (2012) awarded by Rackham graduate school. Special thanks to my student Rebecca Wachter from MCDB 222 (2011) for nominating me for the award.

Life in the MCDB department was made more fun thanks to my MCDB colleagues especially Dr. Elisabeth Ashman-Epstein, Dr. Yan Liu and Marcelo de Oliveira.

Thank you to all my near and dear friends especially Divya Purushotham, Ashwina Mahanti and Abishek Bhat for staying by my side no matter what.

I would like to thank all my Ann Arbor friends Malavika Tripathi, Dr. Chandan Bhambhani, Dr. Ojas Kulkarni, Abha and Prashant Rajbhandari, Dr. Aditi Dave, Ishani Chatterjee, Ana Pinheiro and all my other friends from across the globe who thought of me in their prayers and always wished the best for me.

Thank you to my Bollyfit friends especially Susan and Steve Gray for being my guardian parents in the USA.

The initial source of inspiration to choose biology as my subject was derived from my former biology school teachers Rema Ma'm and Sneha Ma'm that made me embark on this journey.

Finally, a big thank you to everyone who made this possible.

TABLE OF CONTENTS

LIST OF FIGURES

CHAPTER 2: High potency zinc modulation of human P2X2 and low potency zinc modulation of rat P2X2 share a common molecular mechanism

CHAPTER 3: Potent and long lasting inhibition of human P2X2 receptors by copper

LIST OF TABLES

CHAPTER 1: Introduction

CHAPTER 2: High potency zinc modulation of human P2X2 and low potency zinc modulation of rat P2X2 share a common molecular mechanism

ABSTRACT

P2X receptors are ion channels gated by ATP. The channels are also modulated by the trace metals zinc and copper. These metals are released along with neurotransmitter at certain synapses and can bind to the receptors and thus modulate neuronal activity. Rat P2X2 (rP2X2) receptors show reversible potentiation by 2-100 μM zinc in the presence of a submaximal concentration of ATP but are inhibited by zinc at concentrations above 100 μM while human P2X2 (hP2X2) receptors are strongly inhibited by zinc over the range of 2-100 μM. The biological role of zinc modulation is unknown in either species. In Chapter 2 of this dissertation, I used the known 3D crystal structure of the zebrafish P2X4.1 receptor as a template to identify candidate residues that might be involved in zinc inhibition of hP2X2 receptors, and then tested the effect of these residues using site directed mutagenesis followed by biochemical and electrophysiological analysis. I demonstrated that a cluster of residues at the subunit interface controls zinc modulation. I also showed that the low affinity zinc inhibition of rP2X2 receptors can be converted to high affinity inhibition by a single residue change. I explored whether the zinc binding site lies within the vestibules running down the central axis of the receptor. Elimination of all negatively charged residues from the upper vestibule had no effect on zinc inhibition. In contrast, mutation of several residues in the hP2X2 middle vestibule resulted in dramatic changes in the potency of zinc inhibition.

In particular, the zinc potency of P206C could be reversibly shifted from extremely high (~10 nM) to very low (>100 μM) by binding and unbinding MTSET.

In Chapter 3 of this dissertation I showed that hP2X2 receptors are potently inhibited by copper. This high affinity inhibition is also long-lasting with extremely slow recovery after washout of copper. ATP seemed to facilitate copper binding but was not required for copper to leave its inhibitory binding site. The first six cysteines of the extracellular domain were not required for normal copper inhibition. The same three histidine residues required for normal zinc inhibition were also required for normal copper inhibition. Furthermore, DTT, a reducing agent, dramatically accelerated recovery from copper inhibition. Humans with Wilson's disease have excess amounts of copper accumulation in the brain. The copper sensitivity of hP2X2 suggests that these patients have non-functional P2X2 receptors.

CHAPTER 1

Introduction

In this introduction, I begin by reviewing the basic facts about neurotransmission at a level appropriate for a non-neurobiologist. I then review the properties of the skeletal neuromuscular junction of vertebrates because studies at this synapse established most of the paradigms for how synaptic transmission is studied. Next, I introduce the concept of an allosteric modulator, and describe the full array of ligand gated channels that are now known to be present in vertebrate nervous systems. Greater detail is given for P2X receptors, the focus of this thesis. I then review the role of the trace metals zinc and copper in nervous system function. Finally, I describe the Goals of the thesis.

Basic facts about Synaptic neurotransmission

The nervous system contains billions of nerve cells (neurons) which receive signals from the environment, integrate them and thus govern the behavior and the physiological responses of the body. Most neurons have one or more long processes (axons), which use electrical signals referred to as action potentials to very rapidly transmit information down the axon. Stated simply, the way this works is the surface membrane of neurons separates an extracellular region high in sodium and low in potassium from an intracellular region low in sodium and high in potassium. The action potential very rapidly allows first sodium then potassium to flow down their respective concentration gradients. As both are positively charged ions, this quickly changes the membrane potential in the positive direction then the negative direction, in a pattern that causes the

response to propagate down the axon. Axons end in nerve terminals, which form intricate patterns of connections with other neurons or with non-neuronal target cells such as muscle cells or a gland cell. The point of contact between an axon terminal and its target cell is called a synapse. Neuronal communication at synapses usually occurs via the release of chemical neurotransmitter molecules from the nerve terminal (the presynaptic cell) which then activates receptors present on the target (post-synaptic) cell. Because the space between neurons (the synaptic cleft) is very narrow, this communication can be very fast (< 1 msec in mammals with a 37 ^{o}C body temperature). Thus, neurons are the fundamental units of the nervous system and chemical synapses form the basis of most neural circuits that transfer information. However, a small fraction of neurons have electrical synapses which allow signals to pass from cell to cell without the need for a chemical transmitter.

Chemical transmission can work by two distinct receptor mechanisms (metabotropic and ionotropic). At metabotropic receptors, the binding of the neurotransmitter activates a biochemical cascade of several steps. This complexity makes metabotropic receptor chemical signaling relatively slow, typically requiring more than 10 msec for a response to become detectable, and often taking several seconds for the response to reach its peak. In contrast, at ionotropic receptors neurotransmitter binding directly induces a shape change in the receptor that allows the movement of charged molecules through a tiny hole (the pore) which generates an electrical potential. This conformational change can occur within microseconds of transmitter binding, so all the fast chemical synaptic responses of neurons are ionotropic. The class of receptors that produce ionotropic responses are called ligand-gated ion channels (LGIC).

Development of key concepts in our understanding of synaptic transmission

The first microscopic image of the neuron was depicted by Gabriel Gustav Valentin (Valentin, 1836). Later, Wilhelm Friedrich Kuhne described how the synaptic terminals from motor neurons formed junctions onto skeletal muscle cells at the end-plate and he named it the neuromuscular junction (NMJ) (Kuhne, 1862; Kuhne, 1871). The

mammalian neuromuscular junction (NMJ) was the first synapse to have its properties characterized in detail, and these classical studies established most of the paradigms for how neurobiologists study other synapses. The reason is because of its simple anatomy. The cell bodies of motor neurons lie within the spinal cord, and are relatively inaccessible, because of the bony vertebral column that surrounds it. The bony skull similarly protects the neurons of the brain. However, the axons of motor neurons exit the spinal cord and travel long distances through the soft tissues of the body in peripheral nerves to reach their targets, and it is easy to dissect out the muscle from a frog or rat together with a long piece of the axon that remains functional for several hours when placed into a recording chamber. In this way synaptic responses were first recorded and characterized.

Discovery of acetylcholine as the neuromuscular synaptic transmitter

Until the early 20th century, direct electrical transmission was considered to the likely means of communication at all synapses. However, acetylcholine (ACh) was identified as the first neurotransmitter by Otto Loewi in 1921. The classic experiment conducted by Loewi was as follows. He dissected two beating hearts out of frogs. One was denervated while the other had its vagus nerve (which controls heart rate) intact. Loewi showed that the heart of frog that was denervated could be made to slow down or even stop beating when a fluid taken from the surrounding of an innervated heart was passed over it. This indicated that some soluble substance present in the fluid of the innervated heart was responsible for controlling the heart rate of the denervated heart. He called this unknown chemical "Vagusstoff" (Loewi, 1921). This "stuff" was soon identified as acetylcholine (Loewi and Navratil, 1926). Very soon thereafter, acetylcholine was shown by Henry Dale to also be the neurotransmitter released by motor neurons onto skeletal muscle (Dale and Dudley, 1929). It was also established during this period that the duration of the response to ACh depended on the activity of the enzyme acetylcholinesterase (AChE), which breaks ACh down to acetate and choline. Indeed, the reason that the classic experiment by Loewi worked was that AChE activity is very low

in the frog heart. In contrast, at the skeletal NMJ there is a very high concentration of AChE, and so the effect of any single release of ACh lasts only a few milliseconds. The mechanism by which acetylcholine is released from the presynaptic nerve terminal and the way the acetylcholine receptors operate to generate a postsynaptic response were the focus of intensive investigation from the 1950s-1970s, and resulted in Nobel Prizes for Bernard Katz in 1970, and for Erwin Neher and Bert Sakmann in 1991. Some of the work for which John Eccles received his Nobel Prize in 1963 also involved studies at the neuromuscular junction.

As far as the postsynaptic response at the NMJ, it was established by Dale that the binding of ACh was to receptors with a specific type of pharmacology referred to as nicotinic. These receptors are also irreversibly bound and inactivated by certain snake venoms, and this eventually allowed biochemical isolation of the nicotinic AChR from muscle. It consists of four evolutionarily related subunits of 40-60 kD referred to as α, ß, γ and δ that come together as a pentamer with the stoichiometry α_2ßγδ. The structure of these AChR has been unraveled using two completely different strategies. The earlier approach pursued by Nigel Unwin was to purify receptors from an incredibly rich natural source where they form an almost crystalline array (the Torpedo fish electric organ) and to use electron microscopy to analyze receptors in two dimensional sheets. Optimization of this approach resulted in structures that did not quite reach atomic resolution. However, the serendipitous discovery of a naturally occurring soluble protein from snails that is the structural and functional homologue of the N-terminal ligand-binding domain of the nAChr, called the acetylcholine-binding protein (AChBP) gave rise to an atomic level understanding of ACh binding. The reason this protein is soluble is that it lacks the transmembrane domains of the receptors that make solubilizing intact receptors difficult. When the AChBP was overexpressed in yeast and purified, the crystal structures of the AChBP showed that ligand binding is intersubunit and supported a model of the conformational changes that occur upon binding of the ligand that had previously been inferred from the lower resolution structures (Unwin, 2005). The x-ray structure of a nicotinic receptor with intact transmembrane domains is still lacking but a number of homologs of these channels have been crystallized in bacteria (Tasneem et al, 2005),

including a homolog from *Gloeobacter violaceus* (GLIC) which is a proton-gated channel (Bocquet et al, 2007) and another homolog from *Erwinia chrysanthemi* (ELIC) whose function is not known. This has paved the path for the ease of expression using the *E. coli* expression system and crystallization of these intact receptors. The X-ray structure of ELIC was determined at 3.3 Å resolution (Hilf & Dutzler, 2008) and of the GLIC at 2.9 Å (Bocquet *et al.* 2009) and 3.1 Å (Hilf & Dutzler, 2009). The overall 3D architecture resembles that of the nAChR inferred by Unwin. The structural comparison from these bacterial homologs suggests that activation of the channel leads to a twist and tertiary deformation of the subunits which then couples the opening and closing of the channel (Bocquet et al, 2009).

Binding of two molecules of ACh to nicotinic AChR receptors results in the opening of a hole through the membrane (an ion channel) that allows small cations (sodium, potassium and to a lesser extent calcium) to flow across the cell membrane but completely impedes the flow of anions as well as larger cations. Because of the ion gradients across the muscle cell membrane, each opening causes the cell to very slightly depolarize (become less negative) than the resting potential of about -90 mV. When many AChR channels open simultaneously, they drive the membrane potential to about -10 mV, which is sufficient to activate the contractile machinery of the muscle cell and make it twitch. In 1976, Neher and Sakmann reported a method that allowed for the recording of single AChR channels, and showed that each opening allows about 1 pA (1 trillionth of an Ampere) to flow for a 1-10 msec.

As far as the presynaptic release of ACh, the pre-synaptic terminal contains vesicles filled with neurotransmitters. These synaptic vesicles are docked at areas called active zones at the plasma membrane of the presynaptic cell. Katz and his collaborators Fatt and Del Castillo provided the first evidence that these vesicles are occasionally released spontaneously. These quantal releases are typically about 1 mV in amplitude, and the role of the nerve action potential is to cause the rapid, synchronous release of many vesicles to produce the 80 mV depolarization that activates the muscle. Katz and his colleague Miledi showed that the signaling process begins when the wave of an action potential travels down the axon and reaches the synapse. This results in depolarization

(membrane potential becoming more positive) of the presynaptic membrane that opens voltage gated calcium channels. Calcium ions rush in to the presynaptic cell and the intracellular calcium rises, activating the biochemical machinery of release. However, the biochemical machinery of transmitter release remained unknown until the 1990s, when a series of cell biological studies showed that the release machinery of nerve terminals uses proteins homologous with proteins that mediate fusion of intracellular vesicles with various organelles. These core fusion proteins are called SNARES. In contrast to neurotransmitter release, under the typical conditions found in a cell, the fusion of these other vesicles typically occurs at a very slow and steady rate (constitutive fusion). The key specialized feature of vesicles of the nerve terminal is that additional proteins allow the fusion rate to be nearly zero at the calcium concentration found in resting terminals, but to occur in less than 1 ms if calcium rises high enough. The family of proteins called synaptotagmins is believed to be the essential calcium sensors of nerve terminals.

In the following years, other neurotransmitters were identified. Norepinephrine (NE) was established as the neurotransmitter onto some glands and onto many smooth muscles soon after the discovery of ACh and was eventually shown to play a role in a small number of neurons of the brain. However, the discovery of the major neurotransmitters of the brain occurred much later. By far the most important brain transmitters are gamma-amino-butyric acid (GABA) (Awapara et al, 1950; Roberts and Frankel, 1950) and glutamate (Curtis and Watkins, 1960). In the 1970's, the characterization of Substance P (Chang and Leeman, 1970) and opioid peptides (Hughes 1975; Hughes et al. 1975) paved the way for the identification of neuropeptides such as gastrin, cholecystokinin, etc (Krieger, 1983). The discovery of these diverse groups of neurotransmitters thus established different modes of chemical neurotransmission.

Allosteric modulation of ion channels

The site at which a neurotransmitter binds is referred to as the orthosteric binding site. All molecules that bind to this site and activate a response are called agonists. Molecules that bind to this site but do not cause a response are referred to as competitive

inhibitors; because when they are co-applied with an agonist they make the response smaller, by making some receptors unavailable for agonist binding. However, all receptors that have been studied in detail also can bind molecules that affect their function at other positions than the agonist binding site. These ligands are referred to as allosteric modulators. The role of allosteric modulators on channel function is generally to enhance or inhibit the action of the agonist but by themselves most allosteric modulators have little or no intrinsic activity. Often they can change the range of concentrations of agonist that have an effect, without changing the maximal response possible with very high agonist concentration. In the terms of pharmacology, this would mean that they alter the potency but not the efficacy. As for any type of ligand binding, the effect of the allosteric modulator is saturable, in that, the maximum effect is reached once all the allosteric binding sites are occupied.

The effect of an allosteric modulator can be tested experimentally in several different ways. One approach is to pick a fixed concentration of agonist, and measure the response a variety of concentrations of the modulator. The data are then plotted as a concentration response relation with the Y axis normalized to the response with no modulator. The major parameter derived from this type of experiment is the EC_{50} or IC_{50} (the concentration of modulator necessary to elicit 50 % of the maximal potentiation or inhibition). It is important to note that for an allosteric effect, the EC_{50} or IC_{50} is not a fixed parameter. Indeed, the usual pattern is that the higher the agonist concentration, the less modulation that is possible.

Alternatively, a fixed concentration of modulator can be used, and agonist concentration varied. The agonist EC_{50} of in the presence or absence of modulator is then compared. A positive allosteric modulator typically lowers the EC_{50}, and a negative allosteric modulator typically raises it.

Allosteric modulators are extremely attractive as pharmaceutical agents because unlike receptor agonists or antagonists, they typically still leave some level of endogenous response at high doses. An example of an allosteric modulator in wide use

clinically is valium, which is an allosteric potentiator of some subtypes of GABA-A receptors.

Ligand-gated ion channels other than nAChR

Although studies of the nicotinic AChR of muscle established the basic principles of how fast synaptic transmission works, over the last 30 years, the molecular basis of signaling at almost all synapses in mammals has been established. One surprise is that relatively few molecules serve as fast transmitters. In addition to acetylcholine, the only other well established fast transmitters are GABA (gamma-amino butyric acid), glycine, serotonin, glutamate, and ATP. For each transmitter there are multiple receptor types encoded by separate genes. However, all the known fast receptors fall into one of three superfamilies, which can be classified based on either the number of subunits that assemble to make a functional protein, or by the number of transmembrane domains that each subunit contains (as either criterion gives the same groupings). The family with the largest number of genes in humans consists of proteins that assemble as pentamers, and have four transmembrane domains per subunit. This cys-loop family (because they contain a 13-amino acid loop of highly conserved residues in the extracellular domain that contain a pair of disulphide bonded cysteines) includes nicotinic acetylcholine receptors, GABA-A receptors, glycine receptors and 5HT3 receptors. There are also glutamate gated cys-loop receptors in some invertebrates (Jones et al, 2010), but no known vertebrate glutamate receptors belong to this superfamily. The second most diverse superfamily encodes glutamate receptors, which assemble as tetramers, with each subunit having three transmembrane domains plus a reentrant pore loop segment that enters and leaves the membrane without crossing. Although there are three distinct subclasses of glutamate receptor subunits (AMPA, kainate, NMDA) with 4 or more members per subclass, all form channels that require glutamate as an agonist. The NMDA subclass requires glycine as a co-agonist. The smallest family, the P2X receptors has the simplest molecular architecture, assembling as trimers, with each subunit crossing the membrane only twice. All known P2X receptors are gated by ATP.

Ligand binding to GluR family members

The molecular mechanism of ligand binding to nAChR was discussed above. Over the past 20 years, there also has been major progress in understanding ligand binding by GluR family members. In the case of the glutamate receptors, the first major step was overexpression in bacterial cells of a fusion construct of two pieces of the extracellular domain of an AMPA receptor that normally are separated by several transmembrane domains (Kuusinen et al, 1995). This type of construct was then used by the Gouaux lab to solve the structure by X- ray crystallography (Armstrong, 1998). The crystallization of this protein revealed that the ligand bound within each subunit of the receptor in a clam-shell fashion (reviewed by Madden et al, 2002). They then used a similar approach to crystallize the ligand binding cores of kainite (Armstrong, 1998) and NMDA receptors (Armstrong and Gouaux, 2000). Most recently, another member of the Gouaux lab successfully crystallized a nearly full length AMPA receptor, with intact extracellular and membrane domains, rather than a synthetic linker on just parts of the extracellular domains. Agonist binding within each ligand binding domain induces closing of the clam shell thus separating the transmembrane domains and resulting in opening of the channel (Sobolevsky et al, 2009).

ATP as a neurotransmitter

In 1963, the presence of an unknown neurotransmitter released from the neurons of the gut and bladder was indicated by the observation that when the nerves supplying the smooth muscles of the guinea pig teania coli were stimulated, inhibitory junction potentials were observed in the presence of the blockers of the two neurotransmitters known to be present (acetylcholine and norepinepherine), (Burnstock et al, 1963).

The next step was to identify the neurotransmitter which had to satisfy several criteria in order for it to be called one: it had to be synthesized and stored at nerve terminals, released by calcium, upon external application of the transmitter the nerve stimulated responses had to be mimicked and it had to be cleared from its zone of release.

The fact that adenosine triphosphate (ATP), which is found inside cells as an energy provider molecule, might serve as a neurotransmitter had recently been suggested by studies that demonstrated the release of ATP upon stimulation of sensory nerves in the rabbit ear (Holton, 1959). At the smooth muscle synapses Burnstock and colleagues tested many substances including amino acids, neuropeptides and neuroamines but only ATP was able to completely satisfy the criteria expected for a neurotransmistter and in 1972, Burnstock proposed the concept of purinergic signaling (Burnstock, 1972). Based on additional pharmacological work completed in the 1970 and 1980s, it was proposed that multiple types of purinergic receptors might exist. Furthermore, it was suggested that the fastest acting receptors (referred to as P2X) might be ion channels, and the slower acting receptors (referred to as P2Y) might be metabotropic (Abbracchio and Burnstock, 1994). By 1990, additional receptor types (P2T, P2U, P2Z,) had been proposed (Gordon, 1986; O'Connor et al, 1991). The first ATP receptors to be cloned were 7 transmembrane, G protein coupled proteins of the P2Y family (Webb et al, 1993, Lustig et al, 1993, Boyer et al, 1994). Cloning of cDNAs indicated that P2Y and P2U receptors were part of the same gene family. The completed genome project indicates that humans have 12 members of this family, although only 10 respond to ATP or some other nucleotide (Simon and Barnard, 2003). The cloning of members of the P2X family followed very soon thereafter (Brake et al, 1994, Valera et al, 1994) and when the rest of this family was cloned, it became clear that the molecules that gave rise to P2T and P2Z responses were actually members of the P2X family. As one of the P2X receptors is the focus of this thesis, a more extensive review of this family will be presented next.

P2X receptor family of ion-channels

P2X receptors are ligand-gated cation channels that open upon the binding of extracellular ATP. P2X receptors are expressed in organisms ranging from amoeba to humans (Fountain et al., 2007). However, they are absent in some of the higher invertebrates, including *Drosophila melanogaster* and *C. elegans*. This absence is presumed to be due to a loss during evolution, as some other arthropods and nematode

worms have P2X receptors. There are seven P2X receptor genes (named P2X1 through P2X7) found in most mammals, although about 70% of humans have two copies of a non-functional allele for P2X5 (Le et al, 1997).

In chordates, P2X receptors are involved in functions of both neuronal and non-neuronal tissues (Khakh and North, 2006). Based on data from knock-out mice (Table 1.1), P2X receptors are known to be involved in many physiological processes including triggering smooth muscle contraction (Ren et al, 2003), taste sensation (Finger et al., 2005) and pain detection and transmission (Cockayne et al., 2005). These channels are involved in different pathological conditions and hence they form attractive drug targets for several diseases including chronic pain (North, 2003), irritable bowel syndrome (Galligan, 2004) and cancer (White and Burnstock, 2006).

Table 1.1: **Summary of phenotypic effects of P2X knockout mice**

Gene	Species with gene knocked out	Phenotypic Effect	Reference
p2rx1	mouse	Reduced contraction of vas deferens and male infertility. Platelet formation reduced. Renal autoregulation reduced.	Mulryan, 2000 Hechler et al, 2003 Inscho et al, 2004
p2rx2	mouse	Taste sensation abolished. Reduced ventilator response to hypoxia.	Finger, 2005, Huang et al, 2011 Rong et al, 2000
p2rx3	mouse	Mechanical allodyna reduced. Increased thermal pain. Reduced bladder distension. Peristalsis lost in the intestine.	Cockayne et al, 2000 Souslova et al, 2000 Vlaskovska et al, 2001 Bian et al, 2003
p2rx4	mouse	LTP at Schaeffer collateral synapses reduced.	Sim et al, 2006
P2rx5	human	The most common human allele produces a non-functional protein.	Bo et al, 2003
p2rx7	mouse	Reduced inflammatory response. Mechanical hyperalgesia and lipopolysaccharide induced hypersensitivity lost. Rod and cone photoresponse increased.	Labasi et al, 2002 Clark et al, 2010. Vessey KA and Fletcher et al, 2012.

A functional P2X channel consists of three subunits (Nicke et al, 1998) which can be identical (homomers) or a mixture of subunits (heteromers) (Nicke et al, 1998, Stoop et al, 1999). Each subunit consists of two transmembrane domains with the N- and C-termini inside the cell. The intracellular portions of these receptors have a Protein kinase C recognition site near the N terminal and a conserved YXXXK motif in the C terminal that is thought to stabilize the receptors at the surface (Chaumont et al, 2004).

The bulk of the receptor (around 70%) consists of its large extracellular domain (ECD). The ECD of all the P2X receptor types is glycosylated and these sugars are necessary for efficient trafficking of the receptors to the membrane (Newbolt et al, 1998, Torres et al, 1998b, Rettinger et al, 2000). As ATP is membrane impermeant, it acts only from the outside, hence it must bind somewhere in the ECD (North, 2002; Khakh and North, 2006). So do a variety of allosteric modulators that bind at sites other than the ATP binding site (reviewed in North, 2002). P2X receptors are modulated by trace metals, micro and macro metals, protons, alcohol, ivermectin, lipids and reactive oxygen species (reviewed in Coddou et al 2011).

Review of structural information on P2X receptors

The first structural information of a member of the P2X receptor family came from the Gouaux lab. This was the report of the X-ray crystal structure of the zebrafish P2X4.1 (zP2X4.1) solved at a resolution of 3.1 Å (Kawate et al, 2009). Since most P2X receptors formed aggregates in solution, 35 different P2X receptor orthologues were initially screened by fluorescence detection size-exclusion (FSEC) chromatography to quickly determine the proteins that were most stable in solution and showed mono disparity (Kawate et al, 2009). The candidate that appeared to be most promising from this screen was a truncated form of zP2X4.1 (26 residues from the N-termini and 8 residues from the C termini removed) that formed crystals and diffracted to a resolution of 3.5 Å. Further amino acid substitutions of C51F, N78K and N197R were introduced in this construct to reduce N-linked glycosylation and ectopic disulfide bond formation and this protein then generated crystals that diffracted to a resolution of 3.1 Å. The structure

was solved in the absence of the ligand ATP and it does not show an obvious pathway for ions in the pore of the transmembrane regions, so they concluded that they had a structure for a closed state of the channel.

The 3D structure of the zP2X4.1 channel not only confirmed many inferences made from site-directed mutagenesis and biochemical studies but also revealed several novel features. The receptor is composed of three subunits each spanning the transmembrane regions where the TM2 regions intersect at an angel of 45 degrees with respect to the membrane. The region in the extracellular domain extends about 70 Å above the membrane and each subunit wraps around each other resulting in extensive regions of contact between subunits.

A striking feature in the structure is the presence of three fenestrations (~8 Å in diameter) located just above the transmembrane domains. Apart from these fenestrations, there are three vestibules (upper, central and extracellular) present in the extracellular domain that run down the central axis of the receptor. The dimensions and the presence of negatively charged residues in the central vestibule make it an attractive idea to hypothesize that this region might help draw positively charged molecules into the pore.

For ions to reach the vestibules two pathways for ion access have been suggested; one is down the central axis and the other is via the three fenestrations. Ion accessibility was assessed by introducing cysteine residues and testing if cys-modifying agents can access these residues. In the central vestibule, H330C (human numbering) was accessible by MTSET but not by MTS-TPAE (a larger molecule) which produced a potentiating response on the ATP-activated currents. Thus ions reached the central vestibule through the fenestrations and not through the central pathway (Kawate et al, 2011). In another study using human P2X4, MTSET was not able to access any residues in the upper and central vestibules. In contrast, MTSET was able to access and modify residues of the lateral portals (Samways et al, 2011).

This ligand free structure provided no direct evidence or where ATP binds, but it supported inferences drawn using other approaches. P2X receptors lack consensus sequences for ATP binding such as Walker motifs that many ATP-binding proteins are

known to contain. Based on mutagenesis data, eight basic and polar residues that are highly conserved have been suggested to participate in ATP binding. These residues line a region at the interface between subunits in the extracellular domain in the crystal structure. In zP2X4.1 these include residues Lys 70, Lys 72, Phe 188 and Thr 189 from one subunit and Asn 296, Phe 297, Arg 298 and Lys 316 from the adjacent subunit. In other P2X receptors mutations at all these positions had profound effects on the ATP potency (Jiang et al, 2000; Roberts et al, 2008; Roberts and Evans, 2004; Roberts et al, 2009; Zemkova et al, 2007). Hence, the putative ATP binding site is likely to be formed by these residues.

The solved structure of P2X4.1 also confirmed a surprising homology to another class of channels. Acid-sensing ion channels (ASIC) are cation channels that open by the binding of protons. Like P2X subunits, the ASIC subunits cross the membrane twice, and have N and C termini inside. However, because the ASIC and P2X channels share no sequence homology, it was thought for some time to just be a coincidence. However, a series of studies beginning in 2006 forced a re-examination of this conclusion. A number of ASIC1 deletion mutants were screened by FSEC and the chicken ASIC1 was selected because it gave a sharp and symmetric elution profile (Kawate and Gouaux, 2006). This mutant construct included the N-terminus and stopped just after the second TM domain.

The crystal structure of this chicken ASIC1 deletion mutant was solved at pH 6.5 at 3 Å resolution (Jasti et al, 2007). Since on prolonged exposure to protons the channel enters a desensitized state and the chicken ASIC1 deletion mutant did not produce any currents, the crystal structure was deemed to be in a closed desensitized state Similar to P2X receptors, the ASIC channels also have subunits that assemble as trimers. When the P2X4.1 structure was solved, superimposition of the TM domains of zP2X4.1 and ASIC1 structures gave a root mean square value of 2.3 Å indicating that they are very similar (Gonzales, 2009). The other common feature is the presence of vestibules and fenestrations in the structure of ASIC1. The vestibules are located along the three-fold symmetric axis, and are similar in size. The central vestibule of both P2X and ASIC1 is lined by acidic residues and is predicted to bind cations (Jasti et al, 2007; Kawate et al, 2009). The residues in the central vestibule of rat ASIC3 were shown to be accessible in

the resting but not the desensitized state (Cushman et al, 2007). This suggested that conformational movements are required for the central vestibule to be accessible when the channel shifts from the resting to the desensitized state (Gonzales et al, 2009). In contrast, there is no structural similarity between Asic1 and zP2X4.1 in the parts of the extracellular domains beyond the pore region. The pore lining portion of these proteins is coded for by sequences near their beginning and end of the gene, while the ligand binding domains are encoded by sequences in the middle. It therefore seems likely that these two groups of proteins diverged from a common ancestor as the result of a large insertion into the middle of the ancestral gene creating new ligand binding properties.

Modulation of ligand gated ion channels by protein-protein interactions

Comparison of recombinant AMPAR's expressed in heterologous systems and native receptors showed that when the channels were expressed in the commonly used cell lines (such as HEK cells) they had faster gating kinetics as compared to the native receptors (Mosbacher et al, 1994, Colquhoun et al, 1992). Also, the single channel properties of the recombinant proteins (Swanson et al, 1997) were different from that of the native receptors (Wyllie et al, 1993). These results suggested that the differences might be arising because the channels are associated with and modulated by auxiliary proteins that were absent in the transfected cells. This would make ligand gated channels similar to voltage-gated ion channels that require beta subunits as auxiliary proteins in order to display their normal physiological properties. The identification of proteins that can modulate AMPA receptor function began when it was demonstrated that a transmembrane protein called stargazin was essential for the surface expression of AMPA receptors (AMPAR's) (Chen et al, 1999, Chen et al, 2000). Stargazin was subsequently shown to belong to a family of proteins called transmembrane AMPA receptor regulatory proteins (TARPs) (Tomita et al, 2003) that also regulate the physiological properties of AMPA receptors on the cell surface.

Stargazin was originally discovered from the mutant mouse stargazer which showed a characteristic phenotype of epilepsy including ataxia, head-tossing and spike-

wave discharges (Noebels et al, 1990). This mouse does not express functional AMPAR's on cerebellar granule cells. The protein encoding the single recessive mutation, stargazin, was identified as a four-pass transmembrane protein that is specifically expressed in the brain (Letts et al, 1998). Chen et al (2000) showed that stargazin is necessary for efficient trafficking and surface expression of functional AMPAR's to the membrane. In the cerebellar granule cells of the stargazer mice, AMPAR's are absent at the synapses but these could be rescued by transfection by stargazin (Chen et al, 2000).

Co-immunoprecipitation experiments suggested that TARP's bound to subunits of GluA receptors in both native tissues (Tomita et al, 2003) and heterologous cells (Chen et al, 2000). Biochemical data further suggested that stargazin is physically associated with AMPAR's as these proteins migrated as a heavier band on a native protein gel which was absent in the protein extracted from the stargazer mice (Vandenberghe et al, 2005a). The surface expression of AMPAR's increased when different proteins of the TARPS family were co-expressed with GluA subunits (Chen et al, 2003; Tomita et al, 2004). The last four residues in the cytosolic tail of the stargazin protein were shown to be critical for the trafficking of AMPAR's to synapses (Chen et al, 2000). Not only do the stargazins play a role as a chaperone for the AMPAR's, they also potentiate the glutamate-evoked currents and increase the single-channel conductance (Yamazaki et al, 2004; Tomita et al, 2005). Hippocampal slices infected with a virus encoding stargazin showed that these proteins slowed the deactivation and desensitization of AMPAR's expressed on neurons (Tomita et al, 2005). Since the kinetics of AMPAR's determine the synaptic currents and plasticity of neurons (Jonas, 2000), this suggests a physiological relevance for the modulation of AMPAR's by TARPS. Furthermore, in *C. elegans*, AMPA receptors are completely non-functional unless they are bound to one of the *C. elegans* TARPS (Wang et al, 2008; Walker et al, 2006).

Interaction of P2X receptors with other proteins

Given the importance of TARPS in modulating AMPA receptor expression and function, an area of current interest is whether the functional properties of P2X receptors

also are modulated by accessory proteins. Co-immunoprecipitation studies have demonstrated that P2X receptors interact with other proteins. For example, P2X2 interacts and is regulated by Fe65 which is a beta-amyloid precursor protein interacting protein (Masin et al, 2006) and beta III tubulin (Gendreau et al, 2003) which suggests that P2X2 also interacts with microtubules. In search for P2X7 interacting proteins, a proteomic screen was conducted in HEK cells that identified 11 proteins that consisted of heat-shock proteins, a laminin, an integrin, an actin, an actinin, phosphatidylinositol 4-kinase and a protein tyrosine phosphatase (Kim et al, 2001). Whether any of these interactions have consequences for the function of P2X receptors is unknown.

Another protein-protein interaction that has been proposed to modulate P2X receptor function is between P2X7 and pannexin 1 (a member of the pannexin family of proteins that show low-sequence homology and considerable structural homology to the gap junction proteins called innexins). P2X7 receptors have the most extreme version of a feature that is also present in some other P2X receptors (P2X2 and P2X4) (Khakh et al, 1999). When short applications of ATP are given, the channels that are opened are permeable to small cations such as sodium, potassium and calcium, but moderately sized organic cations such as N-methyl-D-glucamine (NMDG, molecular weight 195) are impermeable. However, in response to prolonged applications of ATP the cell becomes highly permeable to NMDG and molecules with a molecular weight up to about 900 can cross the membrane, and cells also show extensive membrane blebbing. Some fluorescent dyes (including propidium iodide and Lucifer yellow) are smaller than this, and so entry into this high permeability state can be measured in dye uptake experiments (North, 2002). An association between P2X7 and epithelial membrane protein-2 was proposed to mediate the blebbing phenomenon (Wilson et al, 2002). It was subsequently hypothesized that the increase in NMDG and dye permeation might be due to interactions of P2X7 with pannexin 1, because over-expression or knock down of PANX-1 resulted in increase or decrease of dye-uptake respectively (Pelegrin and Suprenant, 2006; Iglesias, 2008). This suggested that PANX-1 formed the major dye-uptake pathway. However, a more recent study using PANX-1 knock-out mice showed that dye-uptake was not affected in these mice (Qu et al, 2011), suggesting that PANX-1 is not required for P2X7 membrane permeabilization. Indeed, the most recent evidence suggests that the P2X7

pore itself dilates with prolonged ATP application to form the pathway for NMDG and dye entry (Chaumont and Khakh, 2008; Yan et al, 2008).

Although the role of accessory proteins in modulating P2X7 remains unclear, a protein-protein interaction that clearly does modulate P2X receptor function is that of P2X2 with some members of the cys-loop family of receptors, including neuronal nicotinic receptors, GABA-A receptors and 5HT-3 receptors (Zhou and Galligan, 1998; Barajas-Lopez et al, 1998; Searl et al, 1998; Khakh et al, 2000; Sokolova et al, 2001; Barajas-Lopez et al, 2002; Boue-Grabot et al, 2003). For example, the interaction of nAChR and P2X2 receptors on sympathetic ganglion neurons from guinea pigs was demonstrated by showing that when agonist for one type of receptors (either nicotine or ATP) was applied at high concentration, subsequent responses to the other agonist were greatly diminished (Searl et al, 1998). This was interpreted to mean that the gating mechanisms of the two channels must be interacting. Using FRET microscopy, it was subsequently shown that the subunits of nACHR and P2XRs can form dimers within a distance of 80 Å (Khakh et al, 2000; Khakh, 2005). The exact mechanism of interaction is not known. However, it has been suggested that the C-terminal tail might play a role in the interaction (reviewed in Murrell-Lagnado and Quesreshi, 2008). For P2X3 receptors a QST motif in the C-terminal tail has been shown to be required for coupling with $GABA_A$ receptors (Toulme et al, 2007).

Trace metals as allosteric modulators of ligand gated channels

Trace metals are found in very small quantities (1-10 ppm; 10 – 100 µM) as important constituents in the body. These are chromium, cobalt, copper, iron, manganese, molybdenum, nickel, selenium and zinc and of particular relevance for ion channel function are zinc, copper and iron (Mathie et al, 2006). In contrast to the equivocal evidence for Cu and Fe release, it is very well established that zinc is stored in synaptic vesicles by the transporter Znt-3 and released along with neurotransmitter (Palmitier and Huang, 2004).

Physiological relevance of zinc

Zinc is an essential trace metal found ubiquitously in the body and is important for a number of biological functions that include its role in stabilizing not just enzymes and proteins but also DNA and RNA (MacDonald, 2000). In the nervous system, zinc is stored and concentrated in synaptic vesicles. Much of this vesicular zinc is found within neurons called "gluzinergic" neurons (Fredrickson, 1989; Fredrickson and Bush, 2001) because these neurons also release the neurotransmitter glutamate. While most of the zinc in the brain is protein-bound, vesicular zinc is in free form and hence can be selectively visualized (Fredrickson, 1989). This free zinc was first identified in the brain as focal deposits following a histochemical process that stained only free zinc (Maske, 1955). The most obvious zinc-dithizonate staining was observed in the hippocampal mossy fiber region (Maske, 1955). The co-localization of zinc and glutamate suggested that zinc may play a role in neurotransmission and synaptic plasticity.

Synaptic release of zinc

The first demonstration of release of zinc into the synaptic cleft came from *in vitro* preparations of hippocampal slices (Assaf and Chung, 1984; Howell et al, 1984). In these experiments, depolarization of neurons was stimulated either electrically (Howell et al, 1984) or chemically (Assaf and Chung, 1984). Either treatment led to an increase in zinc in the bath containing the slices. Later, *in vivo* studies were performed that confirmed these results (Charton et al, 1985; Amiksztejn et al, 1987). Based on these experiments, the amount of zinc in the synaptic cleft was suggested to reach as high as 300μM (Assaf and Chung, 1984). A more direct method to visualize synaptic zinc release has been by the use of fluorescent probes. Several laboratories (Budde et al, 1997; Li et al, 2001b; Varea et al 2001; Ueno et al 2002; Komatsu et al, 2005; Qian and Noebels. 2005, 2006; Fredrickson et al, 2006a) have used this technique and the amount of zinc estimated from such studies was found to be in the range of 10 – 30 μM (Li et al, 2001b; Ueno et al, 2002; Fredrickson et al, 2006b). In contrast to the above results, another study (Kay, 2003) reported that the zinc released from vesicles reached only about 2 – 6 nM.

These experiments were done on hippocampal slices using a membrane impermeant fluorimetric probe called FluoZin-3 that was synthesized such that it is highly specific for zinc and its affinity for calcium and magnesium is reduced. This was used along with Ca-EDTA (that has a high affinity for zinc and is a slow zinc chelator) to reduce background fluorescence. The fluorescence intensity of the probe was then measured following stimulation of hippocampal slices (Kay, 2003). In a more recent study, the use of FluoZin-3 was deemed not trust worthy which included a problem of high background fluorescence due to dead cells (Bastian and Li, 2007).

Zinc transporters

There are two groups of proteins that are known to be involved in the transport of zinc. One is the zinc transporter (ZnT) family that transports zinc out of the cytoplasm into the extracellular space or into intracellular compartments like vesicles. The other is the Zip (Zrt-Irt-like proteins) family of proteins that increases intracellular cytoplasmic zinc by accumulating zinc from the extracellular space (Liuzzi and Cousins, 2004).

There are 10 members (ZnT1-10) of the ZnT group of proteins in mammals (Cousins, 2006). Of these proteins, the best characterized is the ZnT3 transporter. ZnT3 is specifically found on synaptic vesicles of glutamatergic neurons (Palmitier and Huang, 2004). This transporter is responsible for moving zinc from the cytoplasm and loading them into synaptic vesicles (Palmitier et al, 1996). The pattern of ZnT3 expression overlaps with that of vesicular zinc, i.e., regions of high zinc concentrations of the hippocampus and the cortex also have increased expression levels of ZnT3 (Palmitier et al, 1996). The importance of ZnT3 and its co-localization with vesicular zinc was confirmed by genetic deletion of the ZnT3. The ZnT3 KO mice lacked histochemical staining of vesicular zinc and the total amount of zinc in the brain was reduced by 20% (Cole et al, 1999). Interestingly, these mice did not show any major defects in behavioral (Cole et al, 1999, 2001) or electrophysiological (Lopantsev et al, 2003) properties which suggest that either vesicular zinc via ZnT3 is not required for cognitive functions or that there were compensatory mechanisms that were able to overcome the loss of ZnT3. One

abnormality seen with the ZnT3 mice was that these mice showed a higher susceptibility to seizures induced by kainic acid as compared to the wild-type. A more recent study on the ZnT3 KO mice (Adlard et al, 2010) hypothesized that the lack of impairment in cognitive functions was due to the fact that the mice used in the Cole et al study were young (6-10 weeks old) and that this phenotype was age-related. This was the first report that showed that ZnT3 ablation results in deficits in learning and memory and that vesicular zinc is indeed required for normal cognitive function in adulthood. A more recent study also supports this idea that vesicular zinc plays a role in the long-term potentiation in the hippocampal mossy fibers (Pan et al, 2011).

Role of zinc in synaptic plasticity

The co-localization of glutamate expressing neurons and zinc in the cortex and limbic areas suggests a role of zinc in synaptic plasticity involving learning and memory (Xie and Smart, 1994; Weiss et al, 1989). A number of laboratories have tested the role of zinc in long term potentiation (LTP) at the hippocampal mossy fibers with varying results among the different studies. Three of the studies reported no change in LTP using zinc chelators (Quinta-Ferreira et al, 2004; Vogt et al, 2000; Xie and Smart, 1994). One group found that chelation of zinc resulted in impairment of LTP (Lu et al, 2000) while yet another group reported that LTP could be blocked by removing zinc or increased by adding zinc (Smart et al, 1994). A new study reported that zinc released from synaptic vesicles plays a critical role in LTP (Pan et al, 2011). The authors synthesized a water-soluble zinc chelator that was membrane impermeable and had a high affinity for zinc (unlike Ca-EDTA that can bind calcium and magnesium as well) such that it could bind zinc rapidly before it could get turned over following its release at the synapse (Pan et al, 2011). With such an appropriate tool in hand, the authors tested the effect of the zinc chelator on LTP at the hippocampal mossy fibers and found that vesicular zinc is required for presynaptic mossy fiber LTP while it inhibits post-synaptic LTP. These results indicate that zinc plays a dual role at the synapse of hippocampal mossy fiber neurons.

This conclusion was further supported by studies in the ZnT3 knockout mice where LTP is reduced as compared to the wild-type mice (Pan et al, 2011).

Physiological relevance of copper

Similar to zinc, copper is a transition metal that is essential for life. It is required for several processes including mitochondrial respiration, neurotransmitter biosynthesis, pigment production, connective tissue and blood vessel formation (Pena et al, 1999). Copper is essential but is toxic at excess amounts; hence copper homeostasis is critical to prevent the accumulation of this metal to toxic levels. In humans, this toxicity is marked by two known inherited diseases of copper metabolism, Menkes disease and Wilson disease.

Copper metabolism

Copper is absorbed through the diet and is removed from the hepatic circulation system in the liver. This mode of removal is the only physiological means of eliminating copper and at steady state the copper levels found in the bile is equal to the amount that is absorbed from the intestine (Gitlin, 2003). If the copper content increases in the diet, then the amount of copper excreted through the bile also increases and excess of copper results in toxicity and metabolic disorders (Gollan and Deller, 1973). Hence, copper homeostasis is important in relation to dietary intake that could lead to neurological diseases like Alzheimer's (Sparks and Shreurs, 2003).

Copper is found in many regions of the brain, including the cerebral cortex, hippocampus and cerebellum and is also found in the synaptic membranes of afferent nerves (Kozma et al 1981; Sato et al 1994; Trombley and Shephard, 1996). In cultured hippocampal neuronal cells, copper acts as an antagonist at NMDA receptors (Vlachova et al.1996; Weiser and Wienrich, 1996). Several properties of synaptic transmission in the CA1 region of the rat hippocampus were found to be altered when copper (1-100 µM)

was added to the bathing solution (Doreulee et al, 1997). The amplitude of the NMDA component of evoked EPSPs was reduced by 10 µM copper to about 50% of control. Furthermore, a protocol that produced robust short term and long term potentiation in control slices (50 pulses at 100 Hz, 3 times at 20 second intervals) showed significantly reduced potentiation at 5 minutes and a complete loss of potentiation at 90 minutes when 1 µM copper was present. As robust LTP is essential for learning, it therefore seems that copper must not normally reach 1 µM at the excitatory synapses of the CA1 region.

There have been three papers that demonstrated that copper can be released from potassium stimulated nerve terminals of rat neurons. All assessed total copper (Cu^{+1} and Cu^{+2} in both the bound and free forms). One study looked at release from slices of rat hypothalamus that had been preloaded with radioactive ^{67}Cu, and detected the released material with a gamma counter (Hartter and Barnea, 1998), while two studies looked at release from synaptosomes and used an analytical chemistry instrument to detect copper. The earlier of the two studies using synaptosomes detected copper with atomic absorption spectroscopy (Kardos et al, 1998) while the more recent study used ICS-mass spectroscopy (Hopt et al, 2003).

All three studies made a set of assumptions and then extrapolated from their measurements to produce an estimate of the concentration of copper that would be present in the synaptic cleft shortly after release. The Harter and Hopt studies both estimated total copper at about 15 µM, while the Kardos et al. study estimated that total copper reaches 100-250 µM. This latter number seems suspect because the actual amount of copper detected in the Kardos et al study was 10fold less than the amount observed by Hopt et al. It therefore seems likely that one of their assumptions produced a 10-fold overestimate.

The Hopt et al study also used a molecule that has its fluorescence quenched by copper, and enhanced by zinc to estimate free copper and free zinc in response to depolarization of synaptosomes. They estimated that synaptic free copper is 2-3 µM, about 20% of total copper. A measurement of free Cu^{2+} represented an important result, because Cu^{2+} is the form of copper that is known to bind to and modulate several ion

channels including rat P2X2. They estimated that about 20 times as much zinc is released as copper, so the predicted synaptic zinc concentration is over 50 μM. The importance of measuring zinc and copper with the same method is that the concentration of zinc released at intact synapses has been measured using fluorescent sensors. The fact that the extrapolated synaptic zinc concentration reported by Hopt et al. is similar to the concentration that has been reported in some studies supports the assumptions made to estimate synaptic copper.

It is important to point out that these calculations assume that all synapses release similar amounts of copper. If some synapses release none, then the concentration at the synapses that release copper will be higher than these average estimates. It is well established that only a subset of nerve terminals contain zinc (Frederickson et al, 2000) but it is unclear whether copper is also unevenly distributed. It is also important to point out that none of the methods used so far were sufficiently sensitive to detect copper release at a functioning synapse. The explanation for this is that making an optical sensor for Cu^{2+} with the appropriate properties (soluble in physiological solutions, membrane impermeable, large increase in fluorescence upon binding copper, insensitivity to other divalent cations) is difficult because of the chemical properties of Cu^{2+} (Que et al, 2008). Thus, the role of endogenous copper at synapses (if any) is unknown. However, it is clear that brain copper levels that are too high or too low can cause human diseases.

Menkes disease

Menkes disease is an X-linked autosomal recessive disorder that is caused by mutations in the ATP7A gene (Vulpe et al, 1993; Mercer et al, 1993) which encodes a copper transporter expressed in many tissues. This transporter is responsible for controlling copper levels in the body because it absorbs copper in the intestine. Most known Menkes mutations are due to alterations that diminish or abolish transporter function. When only a severe mutation is present (males with an affected X chromosome or homozygous females) death usually occurs early in infancy.

Copper is essential for the development of the central nervous system and a deficiency during embryonic and fetal development such as the one produced in Menkes disease results in perinatal mortality, retardation and neurodegeneration (Keen et al, 1998). In vivo experiments using mice show that copper is essential for perinatal development and that the timing of deficiency affects neurological development (Prohaska and Brokate, 2002).

Wilson disease

Wilson disease is caused by mutations in the autosomal ATP7B gene, which encodes a copper transporter primarily expressed in the liver. Individuals homozygous for mutant alleles typically develop normally, and then show either behavioral or hepatic symptoms (or both) in their late teens or twenties. The mutant alleles lead to copper overload in many tissues, but the mechanism by which this leads to changes in brain function, and why some patients show neurological symptoms and other psychiatric symptoms remain unclear. If untreated, this disease is fatal but it often responds well to copper chelation therapy. The mouse knock out of the ATP7B gene has hepatic symptoms similar to the human disorder, but there is no indication of any neurological symptoms (Huster et al, 2006). The reason for this species difference is unknown.

Modulatory actions of zinc on ligand gated ion channels other than P2X receptors

Cys- loop family of receptors: nAChR's

Zinc can modulate nAchR's (Hsao et al, 2001; Garcia-Colunga et al, 2001). Zinc has a biphasic mode of action on nAchR's depending on the subunit composition of the receptors and the zinc concentration (Hsiao et al, 2001). Zinc at potentiates α2β2, α2β4, α2β 4, α4β2 nicotinic receptors at concentrations less than 100 μM and inhibits the receptors at concentrations higher than 100 μM (Hsiao et al, 2001). The α3β2 receptors are only inhibited by zinc (Hsiao et al, 2001). The potentiating zinc binding site is

suggested to lie at the subunit interface of the receptors that alternate with the Ach binding sites (Hsiao, 2006) with a key role of H162 of the a4 subunit. Moreover, modulation of zinc depends on the stoichiometry of the receptor. While (a4)2(b2)3 are inhibited by zinc, (a4)3(b2)2 are either potentiated or inhibited depending on the concentration of zinc (Moroni et al, 2008).

Cys- loop family of receptors: $GABA_A$

Ionotropic GABA receptors are classified into $GABA_A$ and $GABA_C$. Zinc inhibits both $GABA_A$ and $GABA_C$ receptors through an unknown mechanism (Xie and Smart, 1991; Kaneda, 1997). The inhibition of zinc is modulated based on the neuronal developmental stage. Zinc inhibits GABA receptors on embryonic neurons more strongly than in the adult neurons (Smart and Constanti, 1990; Smart et al, 1991). The expression pattern of α1, α4, and γ2 subunits in embryonic neurons is much less than in adult neurons (Brooks-Kayal, 2001) which indicate that zinc inhibition is subunit dependent on GABA receptors. Since the δ subunit is selectively found in the extra-synaptic regions (Wei et al, 2003), this indicated that zinc could modulate the tonic conductance of these GABA receptors that are located far away from the synapse (Farrant and Nusser, 2005).

Cys- loop family of receptors: GlycineR

Zinc co-locailzes with glycine in inhibitory neurons in the spinal cord (Birinyi et al, 2001). Zinc shows a concentration dependent bimodal action on glycine receptors as well. Low micromolar zinc concentrations (< 10 μM) potentiate currents and higher zinc concentrations inhibit the glycine receptor by reducing the affinity of glycine (Bloomenthal et al, 1994; Laube et al, 1995; Trombley and Shephard, 1996). For the GlyR α1 subunit, the residue D80 was shown to be required for zinc potentiation (Laube et al, 2000) while two histidines at positions H107 and H109 were shown to be important determinants for zinc inhibition (Harvey et al, 1999). These experiments were conducted using low concentrations of glycine that do not desensitize the receptor. A recent study

that used hippocampal primary cell cultures showed that co-application of zinc with higher concentrations of glycine had no effect on the glycine receptor (Trombley et al, 2011). This study also showed that pre-application of zinc followed by glycine resulted in slow inhibition of the currents. Since zinc released at the synapse is known to enter post-synaptic neurons (Li et al, 2001), the authors decided to examine the effect of intracellular zinc. They first used a fluorescent probe to show an increase in intracellular zinc. The response of extracellular zinc on the currents in the presence of intracellular zinc chelators was then tested and it was found that intracellular zinc can potentiate glycine receptors (Trombley et al, 2011). The inhibitory effect was not significantly different with or without the presence of intracellular chelators. This suggests that the increase in intracellular zinc had no effect on the inhibitory effect of the receptor or that the action of the chelators was slow. The most likely possibility could be that the inhibitory binding site could be extracellular (Trombley et al, 2011). A knock in mice containing the D80 mutation in the alpha 1 subunit which eliminated potentiation of the glycine receptor was generated by the Laube laboratory. These mice developed neuromotor abnormalities resembling human hyperekplexia (Hirzel et al, 2006). This study shows that zinc is required for normal glycinergic function.

Cys- loop family of receptors: SerotoninR

Zinc modulates serotonin receptors of the 5-HT3 subtype in a biphasic manner. Zinc potentiates 5-HT3 receptors at lower concentrations (1-10 μM) while inhibits at higher concentrations (100 μM) (Gill et al, 1995; Uki and Narahashi, 1996; Hubbard and Lummis, 2000). The differential modulation of zinc is subunit dependent. Zinc inhibits the $5\text{-}HT_{3B}$ subunit (Lovinger et al, 1991) while it potentiates the $5\text{-}HT_{3A}$ subunit depending on the concentration (Gill et al, 1995). The zinc binding site is thought to be extracellular as zinc ions were negligibly permeable through the $5\text{-}HT_3$ channel (Hubbard and Lummis, 2000).

Glutamate Receptor Family: AMPA Receptors

AMPA receptors are potentiated by low concentrations of zinc (300 μM) and inhibited at higher (> 500 μM) concentrations of zinc (Mayer et al, 1989; Lin et al, 2001). The modulation of zinc on AMPA receptors is dependent on its subunit composition (Blakemore and Trombley, 2004). AMPA receptors consist of four subunits, GluA1-4. AMPA receptors composed of the GluA1 subunit show little potentiation, while GluA3 subunit are potentiated by very low concentrations of zinc (5 μM) and GluA2 subunits show no response to zinc (Dreixler and Leonard, 1994).

Glutamate Receptor Family: Kainate Recceptors

There is some discrepancy on the effect of zinc on kainite receptors. Initial experiments conducted showed that micromolar zinc concentrations (~50 μM) potentiated currents in kainite receptors while very high concentrations (up to 3 mM) showed inhibition or no response (Mayer et al, 1989; Peters et al, 1987). However, a study by Mott et al (2008) indicated that inhibition of kainite receptors is subunit and pH dependent. At acidic pH, zinc inhibition of recombinant kainite receptors was reduced (Mott et al, 2008). Zinc inhibited kainite receptors on hippocampal mossy fibers and this inhibition was reversible using zinc chelators. Also, this effect was not seen in ZNT3 mutant mice suggesting that endogenously released zinc can inhibit kainite receptors (Mott et al, 2008).

Glutamate Receptor Family: NMDA Receptors

Initial studies on zinc and NMDA receptors indicated inhibition by low concentrations of zinc in hippocampal cultures (Peters et al, 1987; Westbroook and Mayer, 1987). Zinc inhibits NMDA receptors at two distinct sites; in a voltage-independent and a voltage dependent manner (Williams, 1996; Choi et al, 1999). The high affinity voltage independent zinc inhibition is in the nanomolar range for NR1/NR2A while it is in the micromolar range for NR1/NR2B receptors (Choi et al, 1999). The high affinity zinc binding site has been determined to be two adjacent

histidine residues on the of the NR2A subunit of the large amino-terminal domain of NR2 (Choi et al, 1999; Fayyazuddin et al, 2000; Gielen, 2008). In 2000, Vogt et al demonstrated that endogenous zinc at the synapse of hippocampal mossy fibers can modulate the low and high affinity zinc binding sites in a differential manner (Vogt et al, 2000). The low affinity voltage dependent zinc inhibition was suppressed by the zinc chelator Ca-EDTA while the high affinity voltage independent inhibition remained unaffected (Vogt et al, 2000). The authors also ionophoretically applied glutamate to evoke large NMDA current responses and observed increase in the mossy fiber activity in the presence of Ca-EDTA in the stratum lucidum while no such increase in NMDA activity was seen in the ZNT3 knockout mice (Vogt et al, 2000). This suggested that the increase in mossy fiber activity was due to the suppression of inhibition caused by chelation of endogenous zinc.

Allosteric modulation of P2X receptors by Copper and Zinc

P2X receptors are modulated by essential trace metals, heavy metals and macro metals (Coddou et al, 2011). The first evidence for modulation of P2X receptors by zinc predates cloning of cDNAs for P2X receptor (Li et al, 1993; Koizumi et al, 1995). Based on patterns of expression that were characterized more recently, it seems likely that in both of these studies the receptor being studied was P2X2. Li et al studied the role of zinc in mammalian neurons and showed that micromolar levels of zinc caused potentiation of ATP-gated currents (Li et al, 1993). Another study reported that zinc potentiated the ATP-evoked release of dopamine in PC12 cells and that the potentiation is due to increase in calcium through ATP-gated channels (Koizumi et al, 1995). I will review the available information on the allosteric modulation of cloned P2X receptors by zinc and copper, the metals most likely to be of physiological and pathophysiological significance. This information is summarized in Table 1.2, and details about the cited studies follow.

Table 1.2: **Summary of effects of zinc and copper on P2X receptors**					
Subunit	Zinc	Reference		Copper	Reference
P2X1	Inhibits rat P2X1 receptors in a time-dependent manner.	Wildman et al, 1999		No data reported	
P2X2	Rat P2X2 receptors potentiated at low micromolar levels, inhibited at higher zinc concentrations. Human P2X2 receptors inhibited	Wildman et al, 1999; Nakazawa and Ohno, 1996; Clyne et al, 2002 Tittle and Hume, 2008		Potentiates rat P2X2 receptors at low micromolar levels.	Xiong et al, 1999, Lorca et al, 2005
P2X3	Rat P2X3 receptors are potentiated. The effect becomes biphasic after incubation for 20 minutes.	Wildman et al, 1999		No data reported	
P2X4	Rat P2X4 receptors are potentiated.	Acuna-Castillo, 2000		Rat P2X4 receptors are inhibited	Acuna-Castillo et al, 2000
P2X5	Biphasic effect on rat P2X5 receptors.	Wildman et al, 2002		No data reported.	
P2X6	Cannot form functional homomeric receptors.				
P2X7	Inhibits rat and mouse P2X7.	Acuna-Castillo et al, 2007, Liu et al, 2008, Moore and Mackenzie, 2008		Inhibited by submicromolar concentrations	Acuna-Castillo, 2007, Liu et al, 2008

Zinc modulation of P2X receptors

P2X1: Rat P2X1 receptors are inhibited by zinc in a time-dependant manner with a 20 min preincubation time being optimal (Wildman et al, 1999). The IC_{50} for zinc was about 1 µM.

P2X2: Zinc has a biphasic effect on rat P2X2 receptors (Wildman et al, 1998). At concentrations between 10-100 µM, the ATP-evoked responses are potentiated while at concentrations higher than 100 µM the currents are inhibited (Wildman et al, 1998; Xiong et al, 1999; Clyne et al, 2002a; Lorca et al, 2005). Zinc also shows potentiation of currents from P2X2 and heteromeric P2X2/3 receptors expressed on native tissues such as parasympathetic ganglia (Ma et al, 2005), dorsal motor neurons (Ueno et al, 2001) and hypothalamus (Vorobjev et al, 2001). Recently, Lorca et al, have studied the role of P2X

receptors in long term potentiation (LTP) in the CA1 region of rat hippocampal slices. The authors suggest that 5-50 µM zinc enhances LTP while 100-300 µM inhibits LTP by acting on rat P2X4 neurons (Lorca et al, 2011).

Two histidine residues, H120 and H213, were identified to be important for the potentiation by zinc (Clyne et al, 2002a) and copper (Lorca et al, 2005) in rP2X2. The binding site of zinc involved in potentiation was shown to be at the interface of subunits (Nagaya et al, 2005). Further, the flexibility of the zinc binding site has also been tested by moving the two essential histidines H120 and H213 either 13 residues upstream or downstream from their original positions (Tittle et al, 2007). The effect of zinc on P2X2 differs by species. Tittle and Hume (2008) demonstrated that while rP2X2 receptors are potentiated by zinc, human P2X2 receptors are strongly inhibited by the same concentrations of zinc. The molecular mechanisms that allow zinc for it to cause inhibition is the focus of chapter 2.

P2X3: Rat P2X3 receptors are potentiated by zinc with an EC_{50} value of 11 µM (Wildman et al, 1999). When oocytes expressing P2X3 receptors are pre-incubated with zinc for 20 min, the response becomes biphasic.

P2X4: P2X4 receptors are differentially modulated by zinc and copper. These receptors are potentiated by zinc but inhibited by copper. At concentrations between 30 µM -1000 µM, zinc inhibits rP2X4 (Acuna-Castillo, 2000). There are three histidine residues in the extracellular domain of the rP2X4 receptor but mutation of only His140 abolished inhibition by copper. This mutation also changed the zinc effect from a biphasic response to a sigmoidal response (Coddou et al, 2003). Further mutagenesis studies on arginines and threonines identified Asp138 as also likely to be a part of the copper inhibitory site. One the extracellular cysteines (Cys132) was suggested to be involved in the zinc induced potentiation of P2X4 receptors (Coddou, 2007), although studies of several other P2X receptors, including the crystal structure of P2X4.1 suggest that the homolog of this residue is disulfide bonded and thus unavailable for metal binding.

P2X5: Rat P2X5 receptors are modulated in a biphasic fashion by zinc (Wildman et al, 2002).

P2X6: P2X6 subunits cannot make functional homomeric receptors.

P2X7: Zinc potently inhibits rP2X7 receptors (Acuna-Castillo et al, 2007; Liu et al, 2008) and mouse P2X7 (Moore and Mackenzie, 2008). A dramatic attenuation by zinc was seen in H62A and D197A mutant and a complete loss of inhibition was seen in the H62A/D197A double mutant (Liu et al, 2008).

Copper modulation of P2X receptors

P2X1: No data has been reported for the effects of copper.

P2X2: At low micromolar levels (1-100 μM), copper potentiates rat P2X2 receptors (Xiong et al, 1999; Lorca et al, 2005). Copper resulted in a left-shift of the EC_{50} of the ATP on the concentration-response curve. But, this shift was not seen when a maximal concentration of zinc was co-applied with copper. In other words, the increase in current by copper and zinc together was no greater than the increase in current seen by zinc itself. This suggests that copper and zinc might bind to the same site or have a similar mechanism of action on P2X receptors (Xiong et al, 1999; Lorca et al, 2005). Site-directed mutagenesis of all the histidine to alanine residues in the extracellular domain revealed that H120A and H213A were critical to the potentiation action of copper. H192, H245 and H319 showed a reduction in the potentiation of the ATP-evoked current by copper (Lorca et al, 2005).

P2X3: No data reported for effects of copper.

P2X4: This receptor has an interesting mode of action by trace metals in that it is potentiated by zinc and inhibited by copper (Acuna-Castillo et al, 2000). This receptor contains only 3 extracelluar histidines, which are known to be common high affinity binding sites for copper. Of these three histidine residues, only H140 has been shown to be involved in copper inhibition (Coddou et al, 2003). In the H140 mutant, not only was the copper induced inhibition abolished, but there was a significant increase in the potentiation evoked by zinc that changed the zinc concentration-response from a bell-

shaped curve to a sigmoidal curve. Based on these results, two separate and distinct binding sites for zinc and copper were proposed. One is an inhibitory binding site that binds copper with high affinity while a second site is responsible for the potentiation (Acuna-Castillo et al, 2000). Further studies revealed that Asp138 is also involved in the inhibitory action by copper on the P2X4R (Coddou et al, 2007). When these three residues were mapped onto a homology model using the zebrafish P2X4.1 as a template, it was observed that Asp138, His140 and Cys132 are located close to each other and also close to the proposed ATP binding site composed of residues Asn294, Arg295, Lys313 from the same subunit and Lys65, Lys69 and Phe185 from the adjacent subunit (Coddou et al, 2011).

P2X5: There is no data reported for the role of copper on P2X5 receptors.

P2X6: No functional channel is formed by homomeric P2X6 receptors.

P2X7: P2X7 receptors are inhibited by submicromolar concentrations of copper (Acuna-Castillo, 2007). Site-directed mutagenesis revealed H267A to be resistant to copper inhibition while H201A and H130A showed significantly less inhibition by copper (Acuna-Castillo et al, 2007). Liu et al examined 14 potential metal binding residues in the extracellular domain of the rP2X7 receptor and observed that H62A and D197A were significantly reduced in copper inhibition and copper inhibition was abolished in the H62A/D192A double mutant (Liu et al, 2008). These differences might be due to the differences in the expression systems (HEK cells versus oocytes) (Coddou et al, 2011).

Goals of this thesis

P2X receptors are present in many tissues in the body and mediate a number of physiological functions. The receptors are involved in many pathological conditions and hence form attractive drug targets for several diseases ranging from pain to cancer. Hence, one of the initial goals to my thesis project was to attempt to understand these receptors in a 3D form by crystallization of the protein with the hope of also being able to

directly identify the ATP binding site. At the time I initiated thesis research, no structural information was available for any P2X receptor. My initial goal for this thesis was to find a way to make a soluble protein that included the ATP binding domains of a P2X receptor, and then to characterize it in detail. The approach I pursued was similar to the approach of Armstrong et al. (1998) that had been successful for the glutamate receptors, and I obtained promising initial results. However, when a full length crystal structure for a P2X receptor became available in 2009, I decided not to pursue this approach. The Appendix documents the progress made on this project.

For my remaining studies, I decided to use the new information provided by the crystal structure to answer two other interesting questions. As reviewed above, zinc has opposite modulatory effects on rodent and human P2X2 receptors, potentiating rP2X2 and mP2X2, and inhibiting hP2X2. I also reviewed the substantial information available about the molecular basis of potentiation in the rodent receptors, and indicated that prior to this thesis there was no molecular information available giving insight into how zinc acts to inhibit hP2X2. Furthermore, there was no information available about whether hP2X2 was potentiated or inhibited by copper. In Chapter 2, I show that building a homology model of hP2X2 based on the zP2X4.1 structure provided a new idea about how zinc inhibition might work, and then describe a series of molecular, biochemical and electrophysiological experiments that tested this idea. In Chapter 3, I show that copper is an extremely potent inhibitor of hP2X2, and that the molecular mechanisms of inhibition by zinc and copper involve some of the same residues. Finally, in Chapter 4, I describe some of the possible functional consequences of modulation of hP2X2 by these metals, and future experiments that might be done to test these ideas.

CHAPTER 2

High potency zinc modulation of human P2X2 and low potency zinc modulation of rat P2X2 share a common molecular mechanism

Introduction

In humans, seven different genes (P2RX1-P2RX7) code for subunits of P2X receptors. The proteins these genes encode (P2X1-P2X7) form ATP-gated cation channels, by assembling into homomeric or heteromeric trimers (North, 2002). Different subunit combinations have distinct physiological and pharmacological properties. The characterization of the crystal structure of one member of this gene family (Kawate et al, 2009) provides a framework to allow a more sophisticated exploration of the molecular basis of properties specific to particular subunit combinations.

It is well established that rodent and human P2X2 receptors expressed in Xenopus oocytes or transfected cells are modulated by extracellular zinc (reviewed in Coddou et al, 2011), but the actions of zinc on P2X2 receptors vary dramatically by species. Mouse and rat P2X2 receptors (rP2X2) show a biphasic response to zinc. When exposed to zinc concentrations in the range of 2-100 μM the response to ATP shows dramatic potentiation, while at higher zinc concentrations the ATP response is inhibited (Nakazawa and Ohno, 1996; Wildman et al, 1998; Clyne et al, 2002). In contrast, human P2X2 receptors (hP2X2) show no potentiation at any zinc concentration; rather over the same concentration range that potentiates the rat receptor (2-100 μM) the response to ATP is inhibited by zinc (Tittle and Hume, 2008).

Substantial evidence indicates that zinc is co-released with neurotransmitters from many synaptic terminals (Palmitier and Huang, 2004) and upon release can bind to receptors and modulate neuronal excitability of several types of neurotransmitter receptors (Mathie et al, 2006). Some regions of high P2X2 expression also have a high density of zinc containing nerve terminals (for example the cerebral cortex and hippocampus) but evidence for zinc modulation of P2X2 receptors *in vivo* or in brain slices is lacking. Indeed, the role of P2X2 receptors in the brain is unclear. Although P2X2 receptors are highly expressed in many parts of the central nervous system (Burnstock and Knight, 2004; Koles et al, 2011), with the assays used so far most regions of the brain where these receptors are expressed function normally in P2X2 knock-out mice (Cockayne et al, 2005).

The molecular basis for high potency zinc potentiation of rP2X2 is zinc binding to H120 and H213, which lie on opposite sides of each subunit interface (Clyne et al, 2002b; Nagaya et al, 2005). However, the molecular mechanism for high potency zinc inhibition of hP2X2 is unclear. All of the extracellular histidines of hP2X2 have been mutated (Tittle and Hume, 2008) and two sites were identified (H204 and H209) at which replacement with an alanine resulted in a modest decrease in the extent of zinc inhibition. However, in neither of these mutants nor in the H204A/H209A double mutant was the potency of zinc dramatically shifted from wild type hP2X2.

One striking feature of the structure of zP2X4.1 is the presence of three cavities referred to as vestibules that run down the threefold symmetric central axis from the top of the molecule to just above the pore region in the membrane (Kawate et al, 2009). In the ligand-free closed state that was crystallized, the upper and middle vestibules are separated by a constriction that would prevent ion flow, and a relatively narrow region that might impede ion flow also separates the middle vestibule from the lowest cavity, which is referred to as the extracellular vestibule. The reason for this designation is that just above the membrane there are three fenestrations between subunits that appear large enough to allow the unimpeded flow of ions directly into the extracellular vestibule even when the channel gate (which lies midway through the membrane) is closed. Two recent

papers have supported the idea that the pathway for ion movements through open P2X channels is via the fenestrations (Kawate et al, 2011; Samways et al, 2011). However, there must be a pathway that allows ions to enter the middle vestibule, since Gd^{3+}, an inhibitor of zP2X4.1 channel function was shown to bind to Glu98 from all three subunits at the top of the middle vestibule (Kawate et al, 2009). It is possible that the movements associated with channel opening might also allow access to the upper vestibule. Thus these vestibules are potential locations for the high potency inhibitory zinc binding site of hP2X2.

Our goal for this study was to use a homology model of hP2X2 based on the structure of zP2X4.1 to suggest candidate residues for involvement in inhibitory zinc binding, with the hope of identifying mutations that dramatically enhance or attenuate zinc inhibition of hP2X2. Identification of such mutants might provide a framework for understanding the molecular basis of zinc inhibition, and also offer the possibility of using them as tools to probe the role of P2X receptors *in vivo*.

Materials and Methods

Homology modeling of the human P2X2 receptor

The human P2X2 homology model was generated using the SWISS-MODEL server "Automated Protein Modeling Server" (http://swissmodel.expasy.org, (Arnold, Bordoli et al. 2006; Bordoli, Kiefer et al. 2009). The amino acid sequence for hP2X2b (GenBank AAF74202.1) was used as the input and the template was the single chain structure of zebrafish P2X4.1 (3H9V.pdb, Bordoli et al, 2009). The program COOT (Crystallographic Object-Oriented Toolkit, (Emsley et al, 2010) was then used to superimpose the hP2X2b monomer single chain onto the zP2X4.1 trimer template (3I5D.pdb) to generate the hP2X2b trimer structure. Molecular graphics images of the structure were drawn using the UCSF Chimera software (http://www.cgl.ucsf.edu/chimera) from the Resources for Biocomputing, Visualization and Informatics at the University of California, San Francisco (supported by NIH P41 RR001081).

Site Directed Mutagenesis

The source of the human P2X2b and rat P2X2a cDNAs has been previously described (Tittle and Hume, 2008). Mutations were made using the QuickChange mutagenesis kit (Agilent Technologies, Santa Clara, CA) and are referred to by the original single letter amino acid codon followed by the residue number and the substituted single letter codon. All mutations were confirmed by DNA sequencing from the University of Michigan DNA sequencing core.

Expression

RNAs encoding wild-type and mutant P2X2 receptors were synthesized using the mMessage Machine T7 kit (Life Technologies Corporation, Grand Island, NY) and expressed in stage V-VI *Xenopus laevis* oocytes. Oocytes were surgically extracted and harvested following methods approved by the University of Michigan Committee on the Use and Care of Vertebrate Animals. Each oocyte was injected with 50 nl of RNA (50-100 ng/µl unless it is stated that a lower concentration was used).

Crosslinking and Western blotting

Prior to protein isolation, oocytes injected with RNA (50 ng/µl) encoding either wild type or mutant hP2X2 receptors were exposed at room temperature to ND96 buffer alone (96 mM NaCl, 2 mM KCl, 1.8 mM $CaCl_2$, 1 mM $MgCl_2$, 5 mM sodium pyruvate and 5 mM HEPES, pH 7.6) or to ND96 buffer supplemented with either the long arm cys-reactive cross-linker $BM(PEG)_3$ (1,11-bismaleimidotriethyleneglycol Thermo Fisher Scientific, Rockford IL, 1mM), the short arm cys-reactive cross-linker BMOE (Bismaleimidoethane Thermo Fisher Scientific, Rockford IL, 1mM,) or H_2O_2 (0.1% w/v) for 10 minutes. Oocytes were washed five times in ND96 buffer and

homogenized in buffer H (100 mM NaCl, 20 mM Tris.Cl pH 7.4, 1% w/v Triton X-100, 10 µl/ml protease inhibitor cocktail (P8340, Sigma-Aldrich, St. Louis MO) in a volume of 10 µl/ oocyte. The samples were centrifuged at 16,000g at 4°C for 2 min and the supernatant was transferred into clean microfuge tubes. 15 µl of the supernatant was mixed with 4X SDS-PAGE loading sample buffer (50 mM Tris.Cl, pH 6.8, 50 mM DTT, 2% w/v SDS, 10% v/v glycerol) and stored on ice for SDS-PAGE analysis of total protein. Protein samples were heated to 95° C for 3 min, and loaded on pre-cast NuPAGE 4-12% w/v Bis-Tris gels (Life Technologies Corporation, Grand Island, NY). Gels were transferred to nitrocellulose membranes and probed using a polyclonal antibody (1:200) against an epitope in the extracellular domain of human P2X2 (Santa Cruz Biotechnology, Santa Cruz, CA) and then visualized by chemiluminescence with the SuperSignal West Pico Chemiluminescent Substrate kit (Thermo Fisher Scientific, Rockford IL) that was detected on film.

In Fig. 2.2, for each construct, the treated and untreated samples illustrated were always taken from adjacent lanes on the same gel and shown at identical exposures, so there is no separation between them. However, white bars separate the images from different constructs, to indicate that they were selected from films of several different gels exposed for different periods of time, so that a similar amount of P2X2 immunoreactivity could be illustrated in each lane. This was necessary because the amount of protein expressed varied widely among mutants (likely because of variation in the quality of the RNA injected). The position of molecular weight markers (in kD) are shown on the left, and because commercial precast gels were always run for the same length of time, their positions on all gels used were superimposable.

Electrophysiological recordings

Two-electrode voltage clamp studies were performed on oocytes expressing wild-type or mutant receptors 1-5 days after injection. For all recordings, the holding potential was -50 mV. Recording electrodes consisted of thin-walled borosilicate glass pipettes pulled on a P-97 Flaming Brown puller (Sutter Instrument Company, Novato, CA) that

had resistances of 0.5-1 MΩ. Currents were recorded using a Turbo-Tec3 or Turbo-Tec10 amplifier (npi electronic GmBH, Tamm, Germany). Data acquisition was done using a Digidata 1322A interface controlled by Clampex 9 or 10 (Molecular Devices, Sunnyvale, CA).

Solutions

The external recording solution consisted of (in mM): 90 NaCl, 1 KCl, 1.3 $MgCl_2$ and 10 HEPES, pH 7.5. Disodium ATP (Sigma-Aldrich, St. Louis MO) was prepared as a 100 mM stock in external recording solution and stored at -20°C. The ATP solutions were made by diluting the stock in external recording solution and adjusting the pH to 7.5 to obtain the desired concentrations. Recording electrodes were filled with an internal solution of 3 M KCl. Zinc Chloride was prepared as a 10 mM stock in external recording solution that was acidified with 0.01 M HCl to prevent precipitation.

At the flow rates typically used, the time constant for solution exchange in the recording chamber was approximately 3 seconds. In most experiments, a computer controlled, gravity fed 8-valve array (ALA Scientific Instruments, Farmingdale, NY) regulated solution delivery. For electrophysiological studies of the effect of modification of accessible cysteines, the oocytes were studied while impaled in the recording chamber, but to conserve materials, flow through the recording chamber was stopped, and a concentration of reagent sufficient to cause maximum modification within a 2 minute incubation was added from a P-200 pipetter in a volume sufficient to cause a nearly complete solution change within a few seconds. At the end of the incubation period, a wash of at least 30 s occurred before recording resumed. The modifiers tested were BMOE, $BM(PEG)_3$ and MTSET [(2-(Trimethylammonium)ethyl]Methanethiosulfonate Chloride, Toronto Research Chemicals, North York, ON, Canada). The modifier stocks were made in DMSO and kept on ice, and then freshly diluted at least 1:100 into room temperature recording solution immediately before testing.

Data analysis

Preliminary data analysis was performed using Clampfit 10 (Molecular Devices, Sunnyvale, CA), with additional analysis done with Microsoft Excel. Concentration-response relations were fit using the non-linear curve fitting program of Sigmaplot 9.0 or 10.0 (Systat Software, San Jose, CA). For ATP, the 3 parameter Hill equation was used. For zinc inhibition the 3 parameter Hill equation was used when the inhibition was complete at high zinc, and the 4 parameter Hill equation was used when the maximal effective concentration of zinc did not completely eliminate the ATP activated current.

For analysis of the magnitude of zinc inhibition, the data from each cell were normalized to the maximum value of the ATP response, which was assigned a value of 100%. When parameters of the fit are given in text or figure legends, they were obtained by finding the best IC_{50} for each cell, and then reporting the average IC_{50} ± the standard error of the mean and the sample size. For display in figures, the normalized points at each zinc concentration from all cells were averaged and plotted with error bars indicating the standard error of the mean. The fits shown on the graphs are to these averaged data, and therefore the IC_{50} of these fits sometimes differed slightly from the mean value of the IC_{50} reported in text.

Correcting the zinc IC_{50} for changes in ATP potency

The IC_{50} for zinc differs depending on whether one tests hP2X2 at the EC_{10}, EC_{50} or EC_{90} for ATP (Tittle and Hume, 2008). To test for differences in zinc potency between mutants, we normally tested each construct for zinc inhibition at its own EC_{10} for ATP. Accomplishing this required pre-screening, because the ATP concentration response relation of oocytes expressing P2X2 varies considerably, so that when the average EC_{50} concentration is used, individual oocytes respond from 20-75% of the maximal current (Clyne et al, 2003). For the pre-screen, a series of oocytes were tested with a concentration of ATP that was the average EC_{10} for a population of cells expressing that

construct and with saturating ATP, and only the oocytes that had ATP responses between 5% and 15% of maximum were used for studying zinc inhibition.

Chemical modification of free cysteines by MTSET or crosslinkers sometimes changed the potency of ATP. Managing the number of solutions needed to test oocytes at both their pre- and post-MTSET EC_{10}s for ATP would have been very difficult to accomplish with the available equipment, and would have been impossible for mutants like P206C, whose sensitivity to ATP changed rapidly following MTSET modification. Instead, we simplified the experiment by using the same ATP concentration (the pre-screen EC_{10}) before and after modification. We then used data in Figure 3 of Tittle and Hume showing the relationship between zinc potency and the dose of ATP used (Tittle and Hume, 2008) to develop a correction for changes in ATP potency. By fitting a power function to these data, we were able to define a scaling factor based on the percentage of the maximum current (EC_x) that the ATP concentration used in each experiment produced after modifier treatment. The scaling factor was calculated by the equation,

$$\text{Scaling Factor} = \frac{y_0 + A * 10^b}{y_0 + A * {EC_2}^b}$$

where EC_2 is the EC_x for ATP after modifier treatment (and so would be 80 if cells were studied at their EC_{80}) and y_0, A and b are empirical constants determined from fitting the data from wild type hP2X2 (y_0 = 8.29, A = $1.19*10^{-4}$ and b = 2.98). Multiplying the scaling factor by the measured IC_{50} for zinc after modifier treatment gave the expected IC_{50} at the post-modification EC_{10} for ATP. This procedure perfectly corrected for the change in zinc potency of wild type hP2X2 when ATP concentration was raised.

Results

A homology model for hP2X2 suggests that H204, H209 and H330 lie close together across the subunit interface

In rP2X2, the zinc binding site that causes potentiation includes two histidines on opposite sides of the subunit interface. When the sequence of hP2X2 was used to create a homology model based on the structure of zP2X4.1, H330 from one subunit was predicted to lie close to H204 and H209 across the interface between adjacent subunits (Fig. 2.1A), raising the possibility that this histidine cluster might contribute to the zinc

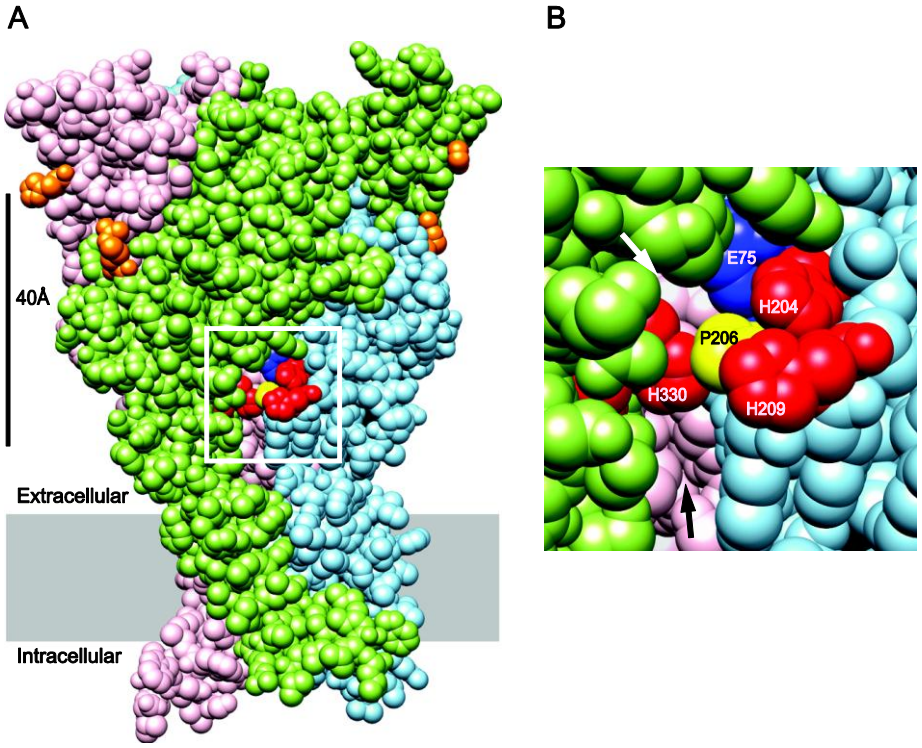

FIGURE 2.1: Location of candidate residues for participation in the inhibitory zinc binding of hP2X2. A. Homology model of hP2X2 based on the structure of zP2X4.1 in the closed state. The three identical subunits of this trimeric protein are shown in pink, green and light blue. The positions shown in orange (H132 and R225) are equivalent to the two histidines of rP2X2 that are required for the potentiating effect of zinc. The positions of the three histidines to be tested for participation in the inhibitory zinc binding site are shown in red. The white box shows the region illustrated in B. B. Higher resolution view of the region around the three candidate histidines. H204 and H209 are close to each other on the light blue subunit while the nearest H330 is on the adjacent green subunit. In this closed state model, P206 (yellow) of the light blue subunit partially shields H330 from access to H204 and H209. The black arrow indicates the top of the fenestration that provides access to the extracellular vestibule. Several residues on the inside of this vestibule arising from the pink subunit are visible. The white arrow indicates a smaller fenestration into the middle vestibule. The visible residue arising from the pink subunit at the back of the middle vestibule is S76. Another middle vestibule residue visible through this opening is E75 (dark blue) from the same subunit as H204 and H206.

binding site responsible for the high potency zinc inhibition seen in hP2X2 receptors. If these residues are part of the inhibitory zinc binding site, it might also explain why zinc inhibition of rP2X2 has such low potency, because in rP2X2 the residue equivalent to H209 is a lysine (K197), which would be expected to disrupt zinc binding.

A challenge to the idea that this histidine cluster contributes to binding zinc is that in the homology model, P206 is positioned in a way that would likely interfere with interactions between H204 or H209 on one side of the subunit interface and H330 on the other (Fig 2.1B). However, the homology model was based on the unliganded, closed, channel, so the interference might be absent in other conformations. To test if hP2X2 can take on a conformation in which H330 closely approaches H204 or H209, we expressed the double cysteine mutants H204C/H330C and H209C/H330C in oocytes and then used physiological and biochemical methods to explore whether these positions were close enough to form ectopic disulfide bonds.

In some cases an ectopic disulfide bond across a subunit interface can form spontaneously and constrain the conformation of a channel such that the electrophysiological properties are altered. For instance, the H120C/H213C double mutant in rP2X2 dramatically right shifts the ATP concentration response curve by spontaneously forming disulfide bonds (Nagaya et al, 2005). However, the hP2X2 double mutants H204C/H330C and H209C/H330C responded normally to ATP. Both of these mutants still showed potent zinc inhibition. Indeed, when tested in parallel with wild type in the same batch of oocytes, both had an IC_{50} that was slightly left shifted (wild type IC_{50} = 12.9 ± 0.9 µM, N = 17); H204C/H330C IC_{50} = 1.8 ± 0.2 µM; H209C/H330C IC_{50} = 2.0 ± 0.3µM, N = 6 for each). Thus, either ectopic disulfide bonds did not form, or bonds at these positions have little effect on function. To distinguish between these possibilities, total proteins from oocytes expressing either wild type hP2X2, single cysteine mutants or double cysteine mutants were extracted and run on Western blots (Fig. 2.2).

In the absence of an exogenous crosslinking agent, the vast majority of hP2X2 protein in wild type and all single and double mutants was at the monomer size, indicating that spontaneous crosslinking was rare. Occasionally there was a small amount of material, the size expected for a dimer, but trimer sized material was never observed. Since dimer was observed in some preps of wild type hP2X2, whatever caused it was not a consequence of the added cysteines. Very different results were observed when cysteine reactive crosslinkers were used. $BM(PEG)_3$ had no effect on the size of the P2X2 proteins extracted from any of the single cysteine mutants (Fig. 2.2A), nor on the material extracted from the H204C/H209C double mutant (as expected since in this mutant both cysteines are on the same side of the subunit interface, so crosslinking these residues would not create bonds that join two subunits together). In contrast, $BM(PEG)_3$ shifted most of the hP2X2 protein from H204C/H330C and H209C/H330C to the size of trimers (Fig. 2.2B), demonstrating that the distance between these residues across the subunit interface must be less than the extended length of $BM(PEG)_3$ (17.8 Å). To further probe the distance between these residues, we used H_2O_2, an oxidizing agent that can promote disulfide bond formation between cysteines that are close to each other but do not react

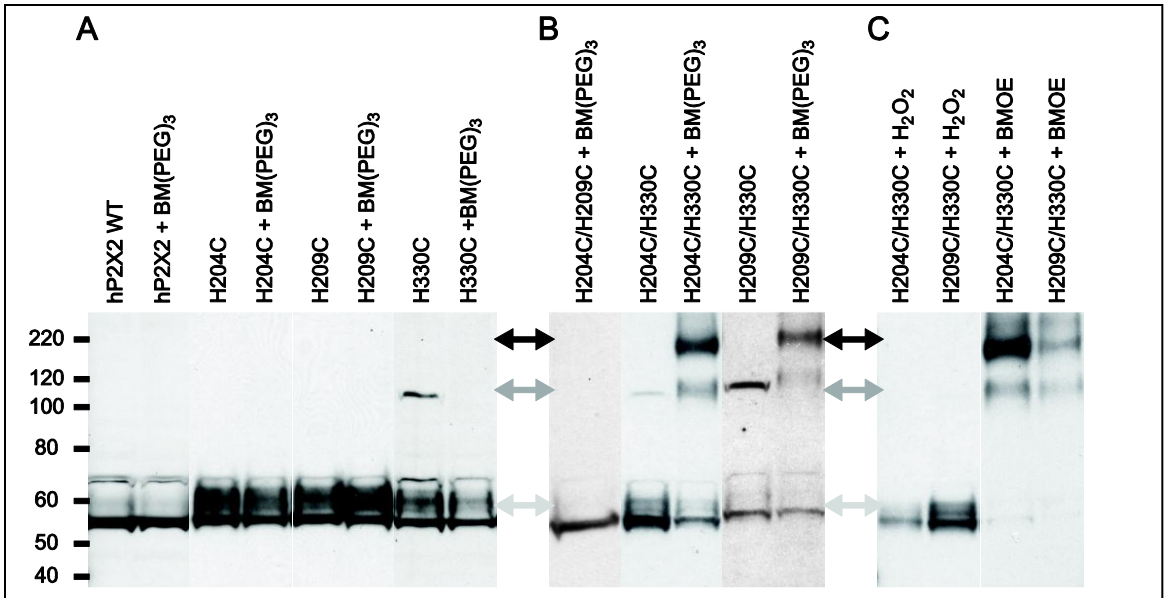

Figure 2.2: Biochemical test of accessibility of H204C or H209C to H330C of the adjacent subunit. A. Lack of effect of the cysteine reactive crosslinker $BM(PEG)_3$ on the indicated single cysteine mutant constructs. The positions of the molecular weight markers (in kD) shown on the left apply to Panels A-C. The double headed arrows between panels A and B and panels B and C indicates the expected position of monomers (light gray arrows), dimers (dark gray arrows) and trimers (black arrows). B. Effect of $BM(PEG)_3$ on double cysteine mutants. C. Effect of the oxidizing agent H_2O_2 and the cysteine reactive crosslinker BMOE on double cysteine mutants.

spontaneously, and BMOE (8 Å), a crosslinker with a shorter span than $BM(PEG)_3$ (Fig. 2.2C). H_2O_2 treated material was monomer sized, while BMOE shifted most of the hP2X2 protein from H204C/H330C and H209C/H330C to trimer size. These results indicate that hP2X2 can take on a conformation in which the distance across the subunit interface between these cysteine pairs is less than the span of BMOE (8 Å), but that these cysteines are farther apart than the maximum distance that allows a disulfide bridge to form between cysteines (2-3 Å).

Mutation of the histidine cluster can dramatically alter zinc inhibition of hP2X2

A challenge to the idea that the histidine cluster H204/H209/H330 contributes to zinc inhibition is that it was previously reported that the H204A and H209A mutants have an IC_{50} for zinc only slightly higher than wild type hP2X2 (Tittle and Hume, 2008). We replicated these results and extended them to H330A. When H330A was studied near its EC_{10} for ATP, zinc caused inhibition with an IC_{50} similar to wild type hP2X2 (Table 2.1). Similarly, at the EC_{10} for ATP, the double mutant H209A/H330A had a zinc IC_{50} similar to wild type (5.5 ± 0.3 μM, N = 5) as had previously been reported for the

Table 2.1: Potency of zinc inhibition for equivalent mutations in human and rat P2X2. All constructs were tested at the EC_{10} concentration for ATP.

Human P2X2	IC_{50} for zinc (μM)	Number of Cells	Rat equivalent	IC_{50} for zinc (μM)	Number of Cells
WT	13 ± 1	17	H120A/ K197H/H213A (Humanized rP2X2)	19 ± 2	15
H209K	77 ± 8	10	H120A/H213A	121 ± 9	8
H204A	19 ± 1	5	H120A/H192A/K197H/H213A	27 ± 2	4
H209A	25 ± 1	5	H120A/197A/H213A	116 ± 12	7
H330A	13 ± 5	4	H120A/K197H/H213A/H319A	16 ± 3	4

H204A/H209A double mutant (Tittle and Hume, 2008). Although wild type hP2X2 and the other mutants reported in this study showed only zinc inhibition at all ATP levels tested, when H330A was tested with ATP at the EC_{40} or above, addition of zinc produced transient inhibition that was followed by growth. At low zinc concentrations the balance at steady state favored inhibition while at higher zinc there was modest potentiation. For example as compared to the amplitude before zinc, the currents at the most effective inhibitory concentration (20 µM zinc) stabilized at 73% ± 8 % and the currents at the most effective potentiating concentration (500 µM) stabilized at 223% ± 75% (N = 5 experiments, each with 4-5 cells at each concentration). Potential explanations for this unexpected observation are considered in Discussion.

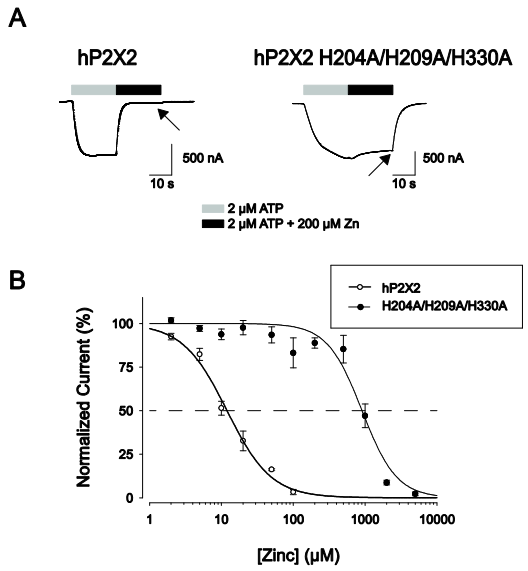

Figure 2.3: Effect of elimination of the three clustered histidines. A. Two electrode voltage clamp recordings from Xenopus oocytes expressing hP2X2 or the hP2X2 H204A/H209A/H330A mutant. In all experiments, the holding potential was -50 mV. The arrow indicates the current at the end of the period of zinc application. B. Concentration response relationship for a series of oocytes studied as in A. In these experiments, a range of concentrations of zinc were tested, while the ATP concentration was held constant at 2 µM. The data were fit to the 3 parameter Hill equation (wild type, IC_{50} = 11 µM; H204A/H209A/H330A, IC_{50} = 979 µM).

In contrast to the relatively normal zinc potency of the single and double alanine mutants at the histidine cluster, the H204A/H209A/H330A triple mutant gave a very different result. Although this mutant had a nearly normal EC_{50} for ATP (20 ± 2 µM, N = 24), when studied at its EC_{10} for ATP the H204A/H209A/H330A triple mutant had very low zinc potency, with its IC_{50} shifted about 100fold to the right as compared to wild type (Fig. 2.3). Thus mutations in the region of the histidine cluster can dramatically alter zinc inhibition of hP2X2.

Reciprocal modification of the potency of zinc inhibition in rat P2X2 and human P2X2

If the difference in the potency of zinc inhibition between the hP2X2 and rP2X2 is due to the fact that rP2X2 receptors lack a histidine in a key position (the homolog of hP2X2 H209 is rP2X2 K197) then placing a histidine at this position of rP2X2 should mimic the high potency zinc inhibition seen in hP2X2 receptors. To test this possibility, it was necessary to first eliminate high potency zinc potentiation in rP2X2, by mutating the two histidines essential for potentiation (Nagaya et al, 2005). As expected based on the previous work, in the rP2X2 H120A/H213A double mutant, zinc potentiation was absent and zinc inhibition was of low potency with an IC_{50} of more than 100 µM. When K197H was introduced into this background, the rH120A/K197H/H213A mutant, which will be referred to as humanized rP2X2, responded to zinc with much higher potency, that was quite similar to wild type hP2X2 (Fig. 2.4A, Table 2.1). The opposite mutation in hP2X2 (H209K) reciprocally converted zinc potency from high to low (Fig. 2.4B, Table 2.1).

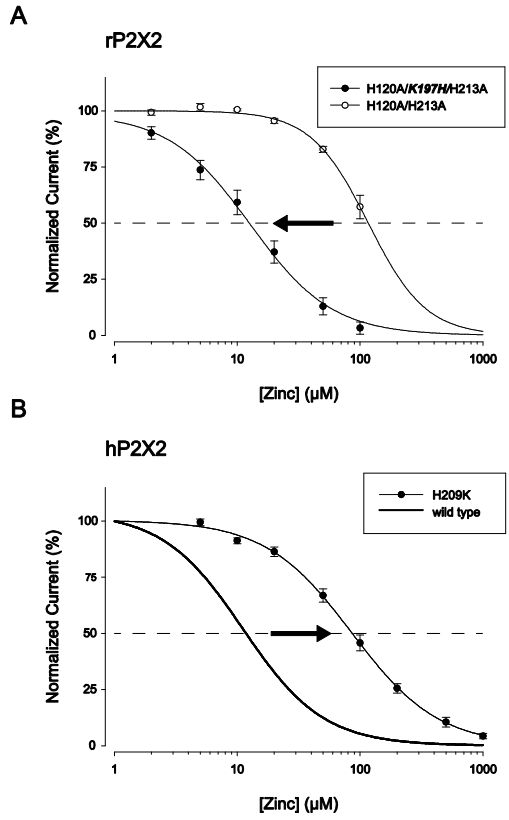

Figure 2.4: Reciprocal effects of mutations of rP2X2 and hP2X2 on zinc inhibition. In both panels the arrow indicates the direction of the change in zinc potency when the endogenous residue is changed to the residue found in the same position in the other species. A. Zinc concentration response relation for two variants of rP2X2 that lacks critical residues at the potentiating zinc binding site (H120A/H213A). The residue at position 197 was either the normal lysine, or was mutated to a histidine, as is found at the equivalent site in hP2X2. B. Zinc concentration response relation for wild type hP2X2 (same data as Fig. 2.3, so only the fit is shown) and for a mutant in which H209 was changed to lysine, as found at the equivalent site (position 197) of rat P2X2.

To further explore similarities between the mechanism of zinc inhibition of rP2X2 and hP2X2 we made alanine mutations of the rat P2X2 residues equivalent to H204A, H209A and H330A and compared them to humanized rP2X2 (Fig. 2.5 and Table 2.1). rH120A/K197H/H213A/H319A was inhibited by zinc with an IC_{50} nearly identical to humanized rP2X2, just as hH330A was inhibited by zinc with an IC_{50} nearly identical to wild type hP2X2. rH120A/H192A/K197H/H213A had a zinc IC_{50} slightly higher than humanized rP2X2, as was also the case for hH204A compared to wild type hP2X2. For both species, the largest effect on zinc inhibition resulted from mutation of the middle histidines. The IC_{50} of hH209A was shifted about 2fold to the right, while the IC_{50} of rH120A/H197A/H213A was shifted over 8fold to the right, and was as zinc insensitive as rH120A/H213A.

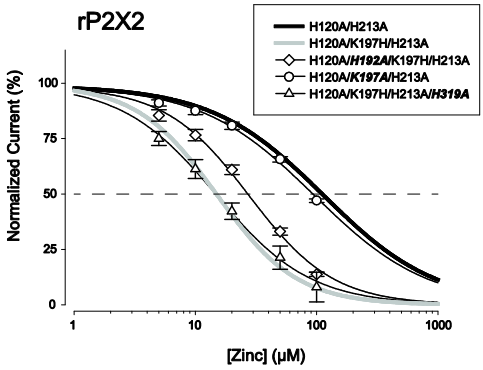

Figure 2.5: Potency of zinc inhibition in a series of rP2X2 mutants. All mutants were made deficient in zinc potentiation by the presence of the H120A and H213A mutations. Effect of substituting an alanine at H192, K197 or H319 (equivalent residues to hP2X2 H204, H209 or H330). The bold part of each label indicates the change from humanized rP2X2. The thick lines without points are reprints of the fits to data from H120A/H213A and H120A/K197H/H213A that were presented in Fig. 2.4.

Tests of potential mechanisms by which mutations in the histidine cluster alter zinc inhibition

The observation that zinc inhibition is barely changed by single alanine mutations to the histidine cluster (H204A, H209A, H330A) and is still present but dramatically right shifted in the H204A/H209A/H330A mutant led us to consider whether this region might be essential for zinc inhibition, and yet not be the zinc binding site. A possible explanation could be that the residues of this cluster control access of zinc to a site elsewhere.

The residues of the histidine cluster sit at a position at which they potentially could control entry into the middle vestibule. We therefore tested whether the inhibitory binding site for zinc might be in the upper or middle vestibule by mutating candidate zinc binding residues.

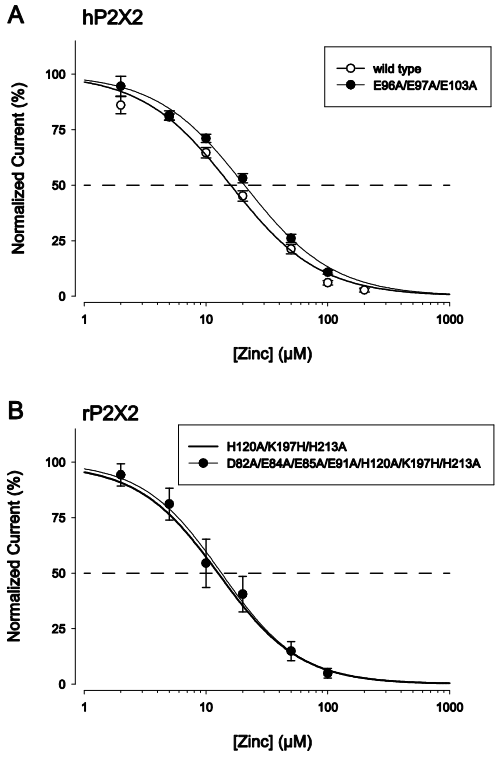

Figure 2.6: Effect of removal of negative charges from the upper vestibule on zinc inhibition. A. Comparison of the zinc concentration response relation for wild type hP2X2 and a variant in which three negative charges in the upper vestibule were mutated to alanine. B. Comparison of the zinc concentration response relation for humanized rP2X2 (H120A/K197H/H213A) and humanized rP2X2 in which all four negative charges in the upper vestibule were mutated to alanine. The average IC_{50} for the mutant lacking negative charges in the upper vestibule was 11 ± 3 μM, N = 5.

In the upper vestibule of hP2X2 there are no histidines or cysteines, but there are several negative charges that might potentially participate in binding zinc. When the hP2X2 residues E96, E97 and E103 were simultaneously mutated to alanines, the IC_{50} of zinc inhibition was very slightly right shifted as compared to that seen in wild type hP2X2 (Fig. 2.6A). When oocytes from the same day were compared, the IC_{50} was 16.2 ± 1.0 μM for hP2X2 and 20.6 ± 1.5 μM for E96A/E97A/E103A (N = 5 each). Similarly, when the rP2X2 homologs of these residues (E84, E85 and E91) plus D82 (the homolog of human D94) were all mutated to alanine in the humanized rP2X2 background, there was no change in zinc inhibition (Fig. 2.6B). Therefore, it seems unlikely that any of the negatively charged residues in the upper vestibule are part of the inhibitory zinc binding site.

In the middle vestibule of hP2X2, there are no cysteines, and the only histidine is H330. However, there are two negative charges (E75 and D326) that might potentially participate in zinc binding. The absence of a negative charge at another middle vestibule

position is noteworthy. The crystal structure of zP2X4.1 identified three negatively charged residues within the middle vestibule that could bind Gd^{3+} (E98 from all three subunits). However, the hP2X2 residue at the homologous position is G104, which is not a zinc binding candidate. As D326 is predicted to form a salt bridge with R324 we also mutated this residue. The R324A mutant responded to ATP similar to wild type (EC_{50} of 14.9 ± 1.2 µM, N = 5), and D326A had a somewhat left shifted ATP concentration response relation (EC_{50} of 2.6 ± 0.6 µM, N = 25). However, when studied at their respective EC_{10} for ATP, both mutants caused only a very slight decrease in the potency of zinc inhibition (Fig. 2.7A). The E75A mutant had slightly enhanced ATP potency (3.7 ± 0.6 µM, N = 4), but zinc inhibition in this mutant was substantially less potent than wild type (Fig. 2.7B).

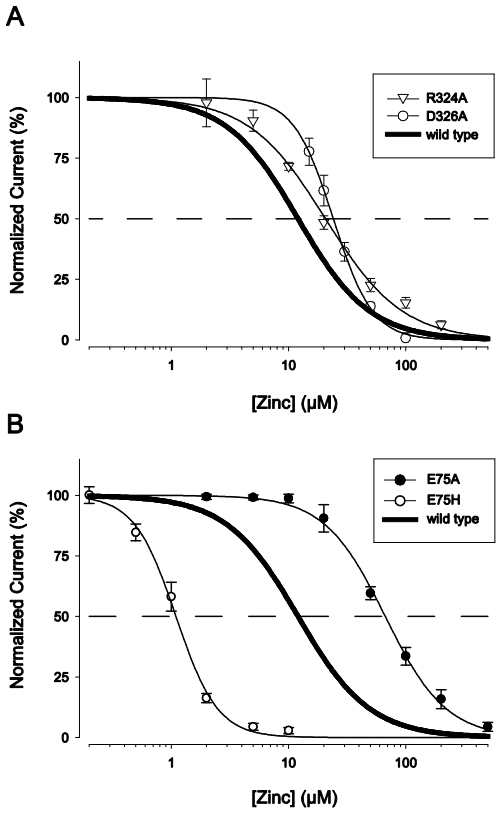

Figure 2.7: Effect of removal of negative charges from the middle vestibule on zinc inhibition. All mutants were made in hP2X2. Data from five cells were averaged for each mutant. A. Zinc concentration response relation for R324A (IC_{50} = 20.1 ± 1.7 µM) and D326A (IC_{50} = 17.9 ± 0.9 µM). B. Zinc concentration response relations for E75 mutants (IC_{50}s were E75A = 68.2 ± 7.0 µM; E75H = 1.6 ± 0.1 µM).

If either D326 or E75 participates in zinc binding or is near the binding site then replacing it with a histidine might enhance zinc inhibition. This was not the case for D326H, which like D326A had an IC_{50} slightly right shifted (21.0 ± 0.8 µM, N=5) compared to wild type. However, the zinc potency of the E75H mutant was 10fold greater than for wild type hP2X2 (Fig. 2.7B).

Effects of mutations of P206 on zinc inhibition

In the homology model of the hP2X2 receptor, P206 protrudes from the middle vestibule into the space between the three residues of the histidine cluster (Fig. 2.1B). If this proline impedes interactions between these histidines, then its replacement with other residues might increase the potency of zinc inhibition. As an initial test of this hypothesis, the glycine mutant of P206 was made, so as to minimize potential steric hindrance. The zinc potency of the P206G mutant (6.1 ± 0.8 µM, N = 7) was similar to wild type hP2X2 (Fig. 2.8A). However P206G was unlike wild type hP2X2 (and most other mutants characterized in this study) in one feature. When tested at the EC_{10} for ATP, wild type hP2X2 showed no residual ATP dependent current at saturating zinc, but in P206G at saturating zinc the residual ATP dependent current was about 25% of the response to ATP alone (Fig. 2.8A). The failure of saturating zinc to completely inhibit EC_{10} ATP in P206G is similar to results seen in wild type hP2X2 when high ATP was used. For instance, at the EC_{90} for ATP, maximal zinc did not eliminate ATP responses, but rather only reduced them to 29% of the response without zinc (Tittle and Hume, 2008). The explanation proposed for this was that the inhibition by zinc was allosteric. That is, zinc binding lowered the potency of ATP, rather than blocking the channel. Viewed in this way, the lowest concentration of ATP that can begin to overcome maximal zinc is an indicator of the efficacy of the allosteric interaction. As EC_{10} ATP could partially overcome maximal zinc in P206G but

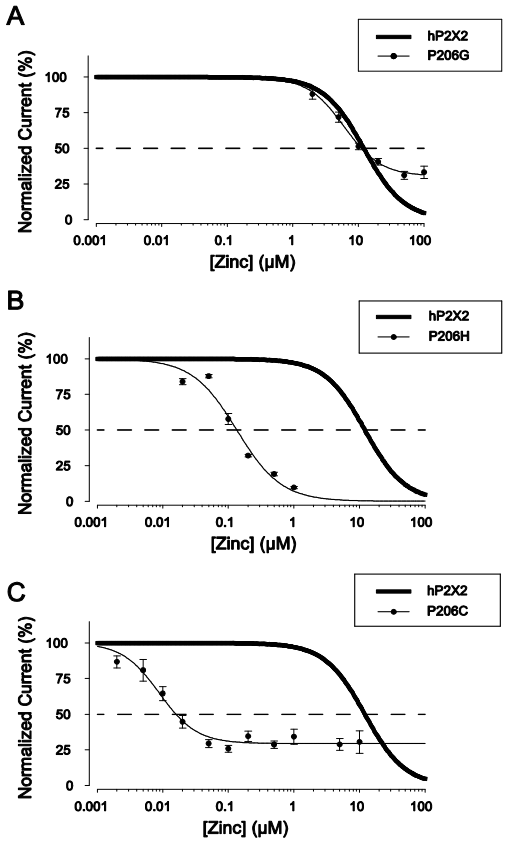

Figure 2.8: Effect of mutations at hP2X2 P206 on zinc potency. A. Zinc inhibition of P206G. Because the final value at high zinc was not 0, the four parameter version of the Hill equation was used to fit these data. The thick line without points in panels A-C is the response of wild type hP2X2 initially shown in Fig. 4. B. Zinc inhibition of P206H (IC_{50} = 0.09 ± 0.02 µM, N=13). C. Zinc inhibition of P206C.

not in wild type, these results show that it is possible for the potency of zinc to be much higher than wild type, and yet the efficacy of allosteric zinc coupling to ATP binding to be lower than wild type.

The P206H mutant increased the potency of zinc inhibition about 100fold compared to wild type hP2X2 and was completely inhibited by saturating zinc (Fig. 2.8B). Possible explanations for this effect are that a histidine at position 206 enhances the potency of the endogenous zinc binding site, or that it creates a novel zinc binding site in this region. If either idea is correct then cysteine, which can also ligate zinc, might have a similar effect on zinc potency and covalent modification of this cysteine might modify zinc potency. As a covalent modifier, we used MTSET, which was originally tested on cysteine modified nicotinic acetylcholine receptors (Akabas et al, 1992) and has subsequently been used extensively to probe the accessibility of specific residues of many ion channels, including P2X receptors (Kawate et al, 2011; Samways et al, 2011). One key property of MTSET is that it reacts specifically and rapidly with the thiols of free cysteines to form mixed disulfides and so blocks any function that requires a free thiol (such as metal binding). A second is that because MTSET is positively charged and relatively bulky, it can often alter permeation through narrow regions of channels due to steric hindrance or charge repulsion of permeant cations. Finally, the mixed disulfide bond is usually stable in the absence of an exogenous reducing agent, producing quasi irreversible modification (Akabas et al, 1992).

The ATP potency of P206C (5.7 ± 0.5 μM, N = 47) was similar to wild type hP2X2. When cells were tested at their EC_{10} for ATP, the zinc potency of the P206C mutant was extremely high (IC_{50} = 11.2 ± 1.6 nM, N = 17, Fig 8C). Thus P206C has zinc potency 1,000 times higher than wild type hP2X2 and about 10 times higher than P206H. However, like the P206G mutant, the ATP dependent currents did not decline to 0 at saturating zinc (average steady state current was 24 ± 3% of the peak).

An unexpected feature of the P206C mutation was that the responses to saturating ATP were usually small (< 3 μA). In contrast, wild type P2X2 injected with comparable amounts of RNA typically give saturating ATP responses over 30 μA. This was not

because the mutant protein had failed to be highly expressed on the cell surface, as when MTSET was applied with the goal of covalently modifying this cysteine, the ATP evoked currents were massively increased (Figure 2.9). For a population of cells studied near their EC_{10} for ATP prior to MTSET application, the average potentiation was 116 ± 14fold, N = 76). It previously had been demonstrated that MTSET had no significant effect on wild type hP2X2 (Tittle and Hume, 2008). As a further control that the effect of MTSET on P206C was due to modification of the cysteine at this position, we also applied MTSET to P206H. After MTSET treatment there was no significant change in the amplitude of the peak current elicited by saturating ATP, the EC_{50} for ATP or the IC_{50} for zinc in oocytes expressing P206H, so the effect on P206C was specific.

Although the effect of MTSET usually reverses very slowly in the absence of an exogenous reducing agent, this was not the case at P206C. When cells were tested with 10 second ATP pulses once per minute, the ATP dependent currents declined back towards the pre-MTSET amplitude along a relatively rapid, exponential time course (Fig. 2.9A). The time constant of this return to baseline varied substantially (Fig. 2.9B) but the average time constant (2.6 ± 0.6 min, N = 17) indicated that by 15 minutes after MTSET treatment most cells tested with this protocol would be close to the original baseline. The decline of current during a long, continuous application of ATP (Fig. 2.9C) was much faster (time constant = 32.7 s ± 0.7 s, N = 5) than when ATP was applied as a series of 10 second pulses, suggesting that the decline in potentiation might be dependent on activation of the channel by ATP. To test this possibility, in a series of cells the first ATP test pulse after MTSET was delayed until 15 minutes of washout had occurred (Fig. 2.9A, bottom). For a series of five cells in which the average potentiation above the pre-MTSET response was 49.8fold, fifteen 10-second pulses of ATP at one per minute brought the average potentiation down to only 2.9fold above the pre-MTSET response. In contrast, waiting 15 minutes without applying ATP left the average potentiation at 53.8fold (N = 4) suggesting that no recovery occurred in the absence of ATP. Once the currents had returned to near baseline, they could be re-potentiated by a second dose of MTSET (Fig. 2.9A, top). For the set of five cells that had declined to 2.9fold potentiation at 15 minutes post-MTSET, the second dose of MTSET took the currents back up to 22.7fold potentiation Thus, either the bond is rapidly cleaved due to the conformation

taken on when ATP is present, or MTSET causes its potentiating effect by interacting with P206C in a non-covalent manner and can only be released when the channel enters the activated state.

The fold potentiation by MTSET depended on the concentration of ATP at which the measurement was made (Fig. 2.9D) and was much greater at lower ATP, but substantial potentiation was still present when a concentration that produced a maximal ATP response prior to MTSET treatment was used (11.9 ± 1.3fold, N = 65).

When low and high concentrations of ATP were applied (Fig. 2.9E) it became clear that ATP was much more potent immediately after MTSET. In the example shown, 1 μM, a concentration that produced about an EC_{10} response prior to MTSET instead produced an EC_{80} response. From a series of two pulse experiments we estimated the ATP potency. Although there was considerable cell to cell variability in the EC_{50} for ATP, on average MTSET treatment caused a 10fold increase in the potency of ATP (Fig. 2.9F) from 5.7 ± 0.4 μM (N = 58) to 0.57 ± 0.04 μM (N = 56).

A similar two pulse paradigm allowed us to estimate the potency of zinc inhibition. For these experiments we used an ATP concentration near the pre-MTSET EC_{10} (0.5 or 1 μM). Prior to MTSET treatment this concentration of ATP gave nearly stable responses, and 200 nM zinc was sufficient to maximally decrease the response, which as noted above plateaus at about 25% of the initial amplitude (Fig. 2.9G, left panels). After MTSET treatment, the response to even a brief application of ATP ran down as receptors returned to the unmodified state, so measuring the extent of zinc inhibition required us to compare the current amplitude at the end of the zinc application to the amplitude that would have occurred had ATP alone been applied (Fig. 2.9G right panels). Oocytes treated with ATP plus 200 nM zinc showed a small, but significant decline. However the extent of the decline did not change in a concentration dependent manner as zinc concentration increased from 200 nM to 20 μM (Fig. 2.9H). To exceed 50% inhibition shortly after MTSET treatment required over 500 μM zinc.

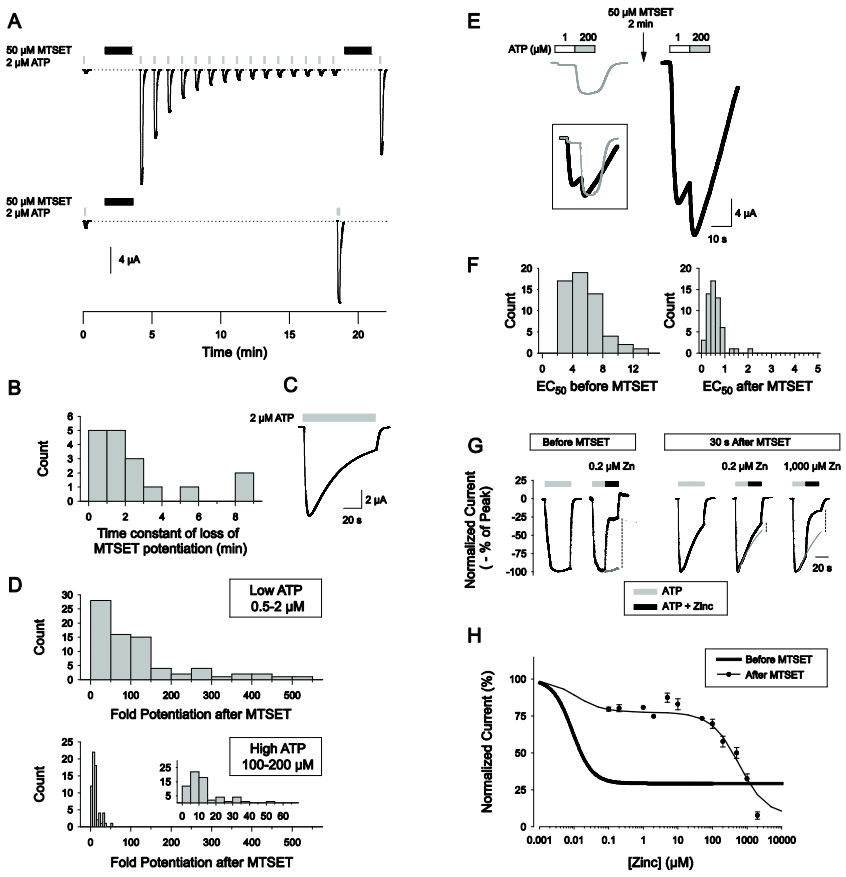

Figure 2.9: Effect of MTSET on responses of hP2X2 P206C to ATP and zinc. A. Massive, but transient potentiation of ATP responses by MTSET. Top: After an initial 10 second application of ATP (grey box) MTSET was applied for 2 minutes (black box), and after a 30 s washout, 10 s ATP pulses were given once per minute. After 15 ATP pulses, MTSET was reapplied, and then a final ATP pulse was given. Bottom: The first ATP pulse after MTSET was delayed until 15 minutes after the washout of MTSET. B. Histogram of the time constant of loss of potentiation after MTSET for a series of cells tested as in the top panel of part A. C. More rapid loss of potentiation when a long ATP pulse was used. D. Histogram of the fold potentiation after MTSET when tested with ATP concentrations near the EC_{10} prior to MTSET treatment (top) or with ATP concentrations that caused a nearly maximal response prior to MTSET treatment (bottom). E. Traces illustrating the shift in the ATP concentration response relation after MTSET treatment. At both concentrations 200 µM produced a maximal response. MTSET treatment shifted the response to 1 µM from 9% of maximal to 81% of maximal. The traces inset within the box show the responses to 200 µM normalized to the same peak amplitude, to accentuate the relative change in the response to 1 µM ATP. F. Histogram of the EC_{50} for ATP before and immediately after MTSET from experiments done as in panel E. G. Recordings illustrating the change in zinc inhibition immediately after MTSET treatment. For each panel 4-5 traces obtained under the indicated condition were normalized to the peak current and then averaged. The gray traces in the panels with zinc represent the extrapolated response amplitudes with ATP only. The top and bottom of the vertical dashed lines indicate the amplitude of the responses with and without zinc that were used to calculate the extent of zinc inhibition. In all panels, ATP was 1 µM. The time calibration applies to all panels. H. Zinc concentration response relation measured after MTSET calculated from data collected and measured as in G. The thick black line is the fit from Fig. 2.8C. The thin black line is the fit to the model described in text. The concentration of ATP used in this experiment was the EC_{10} for ATP prior to MTSET, so it was near the EC_{80} after MTSET.

The complex shape of the zinc concentration response relation was readily explained with a model that took into account the time course of decay of potentiation in the presence of ATP (Fig. 2.9C) and the observation that at maximal ATP, channels in the MTSET modified state carry about 10 times as much current as unmodified channels when studied at equivalent points on the concentration response relation. At the time we applied zinc (30 seconds of washout plus 20 seconds of ATP alone), the decay time constant indicated that the population consisted of approximately 20% modified receptors and 80% receptors that had already returned to the unmodified state. Even though the majority of receptors were in the unmodified state, the amplitude of the current at this time was dominated by the modified receptors, because of their 10 times larger maximal current. The unmodified receptors were maximally inhibited (see Fig. 2.8C) by the lowest concentration of zinc we tested after MTSET (200 nM) so the concentration response curve did not begin to fall until the unmodified receptors began to be affected. Fitting this model gave zinc potency for the MTSET modified receptors of 577 ± 78 μM, which is a 50,000 fold decrease in potency from the pre-MTSET condition.

Because of the shift in ATP potency after MTSET treatment, these measurements were made near the EC_{80} for ATP. It was not practical to examine the zinc concentration response relation before and after MTSET at the post-MTSET EC_{10}, because untreated P206C expressing oocytes did not reliably give measureable responses to ATP at the post-MTSET EC_{10}. When we corrected for the effect of using a relatively high ATP concentration of ATP as described in Methods, the predicted zinc IC_{50} at the post-MTSET EC_{10} for ATP was 76 μM, which is still a decrease in zinc potency of over 6,000fold.

Lack of effect of crosslinking on zinc inhibition

The growth of current in the P206C mutant after MTSET is a property shared with some other cysteine modified residues in the immediate vicinity. In hP2X2, MTSET modification of H209C caused a substantial increase in current, although modification of H204C with this reagent produced inhibition of current (Tittle and Hume, 2008).

Similarly, in rP2X2, MTSET modification of H319C, the residue equivalent to human H330C, caused a modest (less than twofold) increase in current (Kawate et al, 2011). We therefore tested the effect of MTSET on hP2X2 H330C. When tested before and after MTSET at the pre-MTSET EC_{10} for ATP, the amplitude of currents from H330C expressing oocytes were potentiated 12.4fold ± 1.2 (N = 7). In part this was due to an increase in ATP potency from an EC_{50} of 7.0 ± 0.6 μM (N=4) to 1.5 ± 0.8 μM (N = 5), but the current at maximal ATP was also increased 2.2 ± 0.4fold. The IC_{50} of zinc inhibition was slightly right shifted after MTSET treatment (from 3.4 ± 0.3 μM to 6.5 ± 0.9 μM). However, when the change in the ATP concentration response relation was corrected for, the predicted zinc potency at the post-MTSET EC_{10} for ATP was nearly fivefold higher (0.69 μM). Thus modifying this cysteine to give it a substantially larger volume did not impair zinc inhibition.

Finally, we tested whether BMOE and $BM(PEG)_3$, two reagents demonstrated in Figure 2 to form crosslinks across the subunit interfaces, altered receptor function (Table 2.2). BMOE had no effect on any of the measured properties of the H209C/H330C mutant, even though the companion biochemical studies indicated that these double mutant receptors were extensively cross linked by this treatment. In contrast, for the H204C/H209C and H204C/H330C mutants BMOE reduced the currents in response to saturating ATP to approximately 50% of controls, providing physiological evidence that BMOE binding had occurred. However, again there was no significant change in either the ATP or zinc concentration response relations. One possible explanation for the lack of change is that the BMOE modified H204C/H209C and H204C/H330C receptors were completely non-functional. Another is that crosslinking at this location did not alter ATP or zinc potency. The results were less ambiguous for $BM(PEG)_3$. This compound had little effect on wild type hP2X2, as expected because there are no free cysteines on the extracellular side. As with BMOE, there was no change in zinc inhibition in either double mutant after exposure to $BM(PEG)_3$. However, in this case we know that $BM(PEG)_3$ bound receptors were functional, as after treatment the amplitude of the ATP evoked currents from both H204C/H209C and H204C/H330C were dramatically potentiated, similar to the effect of MTSET on H209C and H330C. Therefore we

conclude that zinc inhibition does not require these cysteines to be unmodified, nor to move any further than $BM(PEG)_3$ would allow and infer that this is also the case for the endogenous histidines.

Table 2.2: Effect of the crosslinkers BMOE and $BM(PEG)_3$ on zinc inhibition of double C mutants in the histidine cluster. The same oocytes were studied before and after treatment.

Construct	Current at maximal ATP	ATP EC_{50} (μM)		Zinc IC_{50} (μM)		Number of Cells
	Post-BMOE / Pre-BMOE	Before BMOE	After BMOE	Before BMOE	After BMOE	
H204C/H209C	44% ± 6%	9.9 ± 1.6	11.3 ± 0.9	11.2 ± 1.8	6.5 ± 0. 6	5
H204C/H330C	47% ± 4%	7.6 ± 0.6	9.2 ± 0.3	6.0 ± 0.4	4.8 ± 0. 7	3
H209C/H330C	97% ± 8%	5.5 ± 0.6	7.9 ± 0.7	8.3 ± 0.8	8.2 ± 1.2	4

Construct	Current at 10 μM ATP		Zinc IC_{50} (μM)		Number of Cells
	Post-$BM(PEG)_3$ / Pre-$BM(PEG)_3$		Before $BM(PEG)_3$	After $BM(PEG)_3$	
hP2X2	90% ± 1%		19.5 ± 3.1	19.8 ± 1.3	3
H204C/H330C	363% ± 59%		3.3 ± 0.4	1.7 ± 0.4	3
H209C/H330C	338% ± 31%		3.8 ± 0.5	6.0 ± 0.7	3

Discussion

The biological role of zinc inhibition of hP2X2 is unknown, in part because no mutations that significantly alter this modulation had previously been described (Tittle and Hume, 2008). In seeking a region of the receptor that might be essential for zinc inhibition, our attention was focused on the histidine cluster (H204/H209/H330) because the homology model to zP2X4.1 suggested that these potential zinc binding residues were

close to each other across a subunit interface, and because there was an interesting amino acid difference in this region between the human receptor, which has high potency zinc inhibition and the rat receptor, which has much lower potency zinc inhibition. By focusing on this region of hP2X2, we have been able to produce receptors that respond relatively normally to ATP, and yet spread the sensitivity to inhibition by zinc over a 100,000fold range. At one extreme, P206C has an IC_{50} of about 10 nM and at the other extreme H204A/H209A/H330A has an IC_{50} of about 1 mM. Other mutant receptors spread zinc potency fairly evenly across this range (P206H near 100 nM, E75H near 1 µM, wild type near 10 µM, H209K and E75A near 100 µM). Two issues of interest are what these results indicate about the nature of zinc binding to hP2X2, and how these mutant receptors might be used to further our understanding of the *in vivo* role of P2X2 receptors.

One surprising feature that we have not yet explored experimentally is that unlike wild type hP2X2 and the other mutants studied, in H330A modest potentiation by zinc was uncovered at high ATP and zinc. A possible explanation for this result is that some of the residues that bind zinc to cause potentiation in rP2X2 are retained in hP2X2 (Tittle and Hume, 2008) and that under appropriate conditions H330A allows a residual bit of activity at this site to be detected. Potentially relevant to this issue is that H330 (and its rat equivalent H319) is known to be required for pH potentiation, and so this site clearly has an influence on the gating machinery (Tittle and Hume, 2008; Clyne et al, 2002b). Alternatively, it is possible that in the presence of zinc, the H330A channels are able to slowly enter the same enhanced conductance state that results from binding MTSET to H209C, H330C or P206C. Whatever the cause, the 2fold potentiation shown by this mutant indicates that it is very inefficient at potentiation as compared to zinc potentiation of rat P2X2 and MTSET potentiation of H209C, H330C or P206C, which can be over 100fold when low concentrations of ATP are used.

Although mutations in the vicinity of the histidine cluster had a dramatic effect on zinc potency, it remains unclear how they did this. One possible interpretation of the results with the H204A/H209A/H330A mutant is that these histidines constitute most of the high potency binding site, and the very low potency of zinc inhibition in this mutant

represents residual binding to other residues near them. A related possibility is that these residues are the entire high potency site, and that the residual inhibition is caused by low potency binding elsewhere. Consistent with these ideas, when reciprocal changes were made at the position in the histidine cluster that varies between humans and rats (hH209 or rK197), the zinc potency was reciprocally shifted. Similarly, when P206, which in the closed state model sits between these histidines, was changed to known zinc binding residues (H or C) the potency of zinc inhibition was greatly increased. Finally, MTSET modification of P206C mutant receptors reversibly decreased zinc potency by more than a factor of 50,000. However, two results previously reported as well as several additional results reported here are difficult to explain if this cluster is the zinc binding site. First, Tittle and Hume (2008) found that no single H to A mutation had more than a modest effect on zinc inhibition, nor did the double mutant H204A/H209A. Second, they reported that when either H204 or H209 is mutated to cysteine, the mutants retain potent zinc inhibition that is only subtly altered after MTSET is bound. In contrast, in the high potency potentiating zinc binding site of rP2X2, mutating single essential histidines nearly obliterates the modulation and binding MTSET to these sites greatly attenuates it (Nagaya et al, 2005). We verified the previous results and extended them by showing that MTSET did not significantly interfere with the ability of H330C to respond to zinc and might even enhance it. Furthermore, crosslinking with BMOE or $BM(PEG)_3$ failed to interfere with zinc inhibition. Finally, although BMOE crosslinking showed that cysteines at these locations can come within 8 Å of each other, to bind zinc they would have to come within 2-3 Å (Alberts et al, 1998). The S-S distance in a disulfide bond is also between 2-3 Å, so the failure of H_2O_2 to accomplish crosslinking suggests that H330C does not get close enough to either H204C or H209C to directly engage in zinc binding.

If the histidine cluster is not the zinc binding site, how might modifications to this region increase or decrease the potency of zinc inhibition and where might the binding site be? The homology model suggests that H204 and H209 sit just outside a potential entry into the middle vestibule, and H330 sits just inside it, so these residues are perfectly positioned to control access of zinc to a binding site in the middle or upper vestibule. We therefore tested all of the most common zinc binding residues in these vestibules. The

inhibitory zinc binding site is unlikely to be in the upper vestibule, as simultaneous mutation of all candidate zinc binding residues had virtually no effect in either hP2X2 or in humanized rP2X2. As far as the middle vestibule, it is noteworthy that in zP2X4.1 (Kawate et al, 2009) this region has a gadolinium binding site that is believed to be the cause of Gd^{3+} inhibition of this channel. The homologous position of hP2X2 is a glycine, and so zinc cannot bind there. Of the highest likelihood candidates for binding zinc within the middle vestibule, mutation of E326 and H330 had only minor effects on zinc potency but the substantial effects of mutation of E75 make it an appealing candidate for participation in zinc binding. If so, additional residues would be needed, and the most likely untested candidates are serines, which although extremely rare in nM affinity structural zinc binding sites (< 0.1%) contribute to zinc binding in about 4% of the lower affinity catalytic zinc sites (Andreini et al, 2011). Candidates are S76, S77 and S106, all of which are close to E75 in our homology model. In summary, a plausible explanation for the loss of zinc potency in H204A/H209A/H330A and in MTSET modified P206C is that in these mutants zinc cannot enter the middle vestibule, even though the binding site is intact.

CHAPTER 3

Potent and long lasting inhibition of human P2X2 receptors by copper

Introduction

Copper is found in most regions of the brain including the cerebral cortex, hippocampus and the cerebellum (Kozma et al, 1981; Sato et al 1994). A recent study producing a 3D atlas of copper distribution in the brain further supports this fact (Hare et al, 2012). It is clear is that much of the copper in the brain is tightly bound to enzymes, where it functions as an essential cofactor for catalysis. For this reason, copper is an essential trace metal. When copper levels in the brain are too low, as occurs with Menkes disease, a disorder caused by mutations in the X linked gene encoding the copper transporter ATP7A, serious problems arise during central nervous system development (Keen et al, 1998). Menkes patients who have only null alleles typically are born with severe mental retardation and die perinatally. Copper levels that are too high are also problematic for brain function. In Wilson disease, mutations to the autosomal gene encoding another copper transporter, ATP7B, lead to dramatic, but highly variable effects on the brain. Surprisingly, the major site of expression of the ATP7B protein is the liver, and none is expressed in the brain, so the effect of the mutations on brain function must be indirect. Typically people homozygous for mutations that cause Wilson disease are symptomless until late in their teens. Eventually excess copper begins to build up in the liver, which secondarily leads to increases in copper in the brain. The presentation of symptoms is highly variable, with some patients showing only hepatic symptoms. When brain effects are present, they vary widely from patient to patient, and can sometimes be

neurological (movement disorders, seizures, migraine, dystonia) and sometimes psychiatric (depression, personality changes, psychosis). Interestingly, mice with the ATP7B gene knocked out show only hepatic symptoms (Huster et al, 2006). The reason they do not also show brain symptoms is currently unknown.

In addition to its structural role in enzyme function, it has been suggested that copper may be a neuromodulator (Coddou et al, 2003). Many different types of ligand gated channels are modulated by micromolar levels of copper (Doreulee et al, 1997). Furthermore, based on studies of isolated synaptosomes from the CNS, it has been suggested that copper can be released from nerve terminals in a calcium dependent manner upon depolarization and extrapolations from these data suggest that the concentration of free Cu^{2+} copper in the synaptic cleft would reach 1-3 μM (Hartter and Barnea, 1998; Hopt et al, 2003). Copper is also located on synaptic membranes isolated from afferent nerves (Trombley and Shephard, 1996). Because of limitations with the methods for measuring copper in intact tissue, the copper concentration reached at an active synapse in a brain slice or *in vivo* has not yet been determined.

We have demonstrated that human and rodent P2X2 receptors respond very differently to binding the divalent metal zinc (Tittle and Hume, 2008) and recently worked out some of the molecular reasons for this difference (Punthambaker et al, 2012). As many proteins that bind zinc can also bind Cu^{2+}, we decided to test the effect of this metal on human P2X2. We report here that Cu^{2+} also has opposite effects on the function of human and rodent P2X2 receptors. The inhibitory effects of copper on human P2X2 begin in the low nanomolar range, making copper 100fold more potent than the zinc, and raise the possibility that these receptors may be modulated by copper during normal brain function or in copper overload disorders like Wilson disease. For this reason, we explored the mechanisms that allow such high potency in detail.

Materials and methods

Materials

The source of most materials and their method of preparation was described in detail in Chapter 2. Several additional chemicals, all obtained from Sigma Chemical (St. Louis MO), were used for the studies described in this chapter.

Copper was made up as a 100 mM stock of $CuCl_2$ to generate Cu^{2+}. Under the conditions of these experiments, little or no Cu^{1+} is expected to be present.

Cyclohexamide was prepared as a 100 mg/ml stock in DMSO and diluted 1/100 in Barth's solution just before being added to oocytes.

To treat oocytes with Dithiothreitol (DTT) during recordings, it was prepared as a 100 mM stock in water, and stored frozen in small aliquots. Just before use it was diluted to its final concentration with recording solution. Because over time DTT can degrade, in every experiment that used DTT, a positive control was included to verify that the DTT was present at sufficient concentration to quickly break accessible disulfide bonds.

H_2O_2 was obtained as a 30% solution in water plus stabilizers that are described as keeping it at full strength for 5 years. It was diluted to its final working concentration with recording solution (usually 0.3%) just before use.

Apyrase (~200 units/mg) was prepared in recording solution (which in appropriate conditions also contained ATP and or copper) and used on the day of the experiment. The final concentration used was 1 mg/ml.

Suramin was prepared as a 1 mM stock on the day of each experiment, and then diluted to its final concentration with recording solution.

Methods

Most methods used to make and analyze electrophysiological recordings are described in Chapter 2. The only significant change was in the system used to apply copper containing solutions during recording. In Chapter 2, all solutions were applied to cells through an 8 way mixing valve. When flow is temporarily stopped (for instance when changing oocytes) a very small amount of mixing can occur between the lines. This clears within a second or two or resuming flow, and so was of no consequence when studying rapidly recovering zinc inhibition. However, because of the very slow recovery from copper inhibition, even a very small amount of copper exposure would alter the initial conditions of the experiment. Therefore, in most experiments copper was applied from a single completely isolated tube that had its tip kept just above the surface of the liquid in the recording chamber. When the valve controlling the control solution was shut off and the valve containing the copper solution opened, the solution "dripped" into the recording chamber. The only issue with the method of application is that the turbulence of the drops caused more frequent premature death of the oocyte than our standard drug application method. However, it was easy to monitor the health of the oocytes using the holding potential of the voltage clamp current at -50 mV.

RESULTS

Copper inhibited human P2X2 receptors

Rat P2X2 (rP2X2) receptors are known to be greatly potentiated by micromolar levels of Cu^{2+} (Xiong et al, 1999). When ATP was set to its EC_{10}, and 20 µM copper applied, the potentiation was approximately 10fold (Fig. 3.1A). In

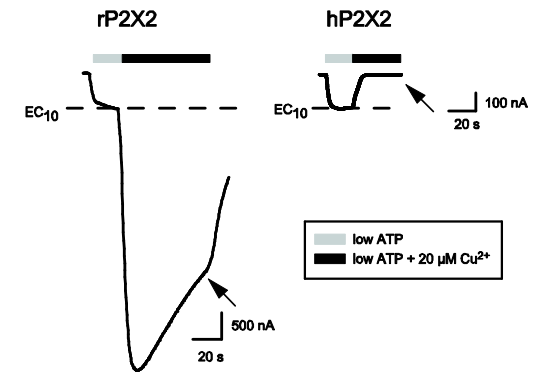

Figure 3.1: Effect of Copper on hP2X2 receptors: In this and all subsequent experiments the holding potential was -50 mV. A) Two-electrode voltage clamp recording from an oocyte expressing rP2X2. The EC_{10} concentration of ATP used was 2 µM. The arrow indicates the current at the end of the copper application. B) Similar recording from an oocyte expressing hP2X2. The EC_{10} concentration of ATP used was 5 µM.

contrast, when we studied human P2X2 receptors (hP2X2) at their EC_{10} for ATP, 20 µM copper caused complete inhibition of the ATP response (Fig 3.1B). We had previously demonstrated that hP2X2 is inhibited by micromolar zinc, and that the IC_{50} was about 8 µM when EC_{10} ATP was used (Tittle and Hume, 2008 and Chapter 2). When oocytes expressing hP2X2 were treated with 5 µM ATP plus 20 µM zinc, washed for two minutes with recording solution and then retested with ATP only, their response amplitude was similar to the initial application of ATP alone (Fig 3.2A). In contrast, when the identical paradigm was given except that 20 µM copper was used as the inhibitor, there was little or no recovery of the ATP response detectable after 2 minutes of washout (Fig 3.2B). On average the response at 1-2 minutes after washing out copper was 0.8 ± 0.02 %, N = 10 of the initial response. We also tested a number of other divalent metals. At 20 µM, cobalt, cadmium and nickel all produced inhibition of hP2X2, but as with zinc, recovery was rapid (Fig 3.2C-E).

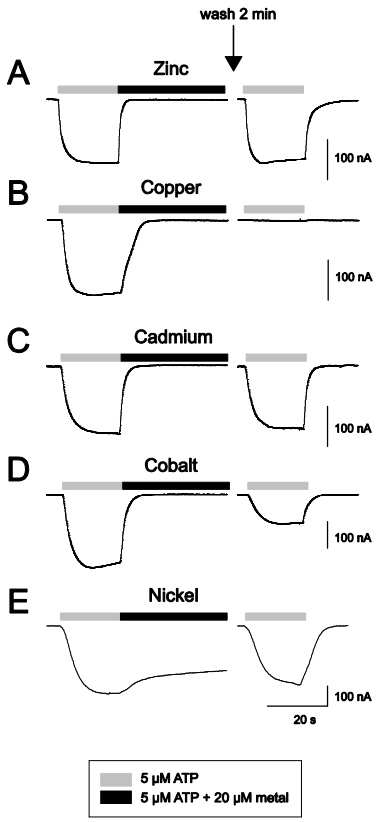

Figure 3.2: Recovery of hP2X2 from inhibition by various divalent metals. Representative traces for five different metals tested with the identical paradigm are shown. After the initial test (ATP followed by ATP plus the metal), the cell was washed for 2 minutes with recording solution, and then retested with ATP alone. Only copper produced long lasting inhibition.

Copper Inhibition was long-lasting

To characterize the time-course of recovery from copper inhibition, short ATP pulses were applied once every 5 minutes beginning 1 minute after a complete inhibition of the ATP-evoked current by copper (Fig 3.3A). By half an hour of washout, recovery

was substantial, and responses had typically nearly reached a final steady state value by 1 hour. In the case illustrated, which was typical, the final value reached was less than 100% of the initial response, as was also true of the average of a series of cells (Fig 3.3B), but some cells stabilized at a final value of 100% or even greater. It was also notable that recovery always followed a sigmoid time course, so that after a lag period with very little recovery, the recovery rate accelerated for a while and then decelerated as the final steady state was approached. The data could usually be well fit by an exponential function raised to a power (the Chapman equation):

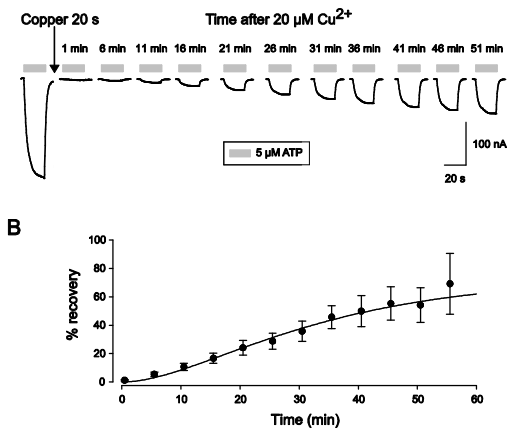

Figure 3.3: Time course of recovery of hP2X2 from copper inhibition. A) An initial 20 sec application of 5µM ATP followed by an application of 20 µM copper after which additional pulses of 5 µM ATP (grey bars) were given every 5 minutes. B) Data were fit to an exponential function raised to a power. The smooth curve was the fit to the averaged data for a series of cells studied as in A. All time points represent the average of data from at least 7 cells, except for the 55 minute point, for which N=4. The parameters of the fit to the Chapman equation are: I_{min} = 0, I_{max} = 73.9%, time constant (τ) = = 24.2 min, N (power) = 2.

$$I(t) = I_{min} + (I_{max} - I_{min}) * (1 - e^{-t/\tau})^N$$

where I_{min} was the current immediately after copper was removed, I_{max} was the final value, τ (tau) was the time constant and N was the power. When ATP was at the EC_{10} and 2 or 20 µM copper was used, I_{min} was very close to 0. For a series of cells tested in this way the time constant of recovery (τ) averaged 19.5 ± 5.1 minutes, the power averaged 2.0 ± 0.3 and I_{max} averaged 83% ± 6 % (N = 11).

Copper inhibition was potent

Because recovery from copper inhibition was extremely slow, to make a concentration response relation for the effect of copper we used protocols where each cell was exposed to copper only once, and then averaged data from many cells tested with the EC_{10} concentration of ATP, and a variety of copper concentrations. The usual protocol

was to first apply a 2 step screening protocol of low ATP followed by saturating ATP (200 µM) to verify that the low concentration was sufficiently close to the EC_{10} (cells in the range EC_5 to EC_{15} were used). All cells that were in range were then given a two-step test protocol of low ATP followed by low ATP + copper (Figure 3.4A). Copper inhibition measured in this way was extremely potent (Figure 3.4B) with an average IC_{50} of 40.1 ± 4.3 nM, N = 9. Furthermore, the rate at which the current declined depended on the concentration of copper used. We also used an alternative protocol in which cells that successfully passed the screening protocol were given a few minutes to recover, and then

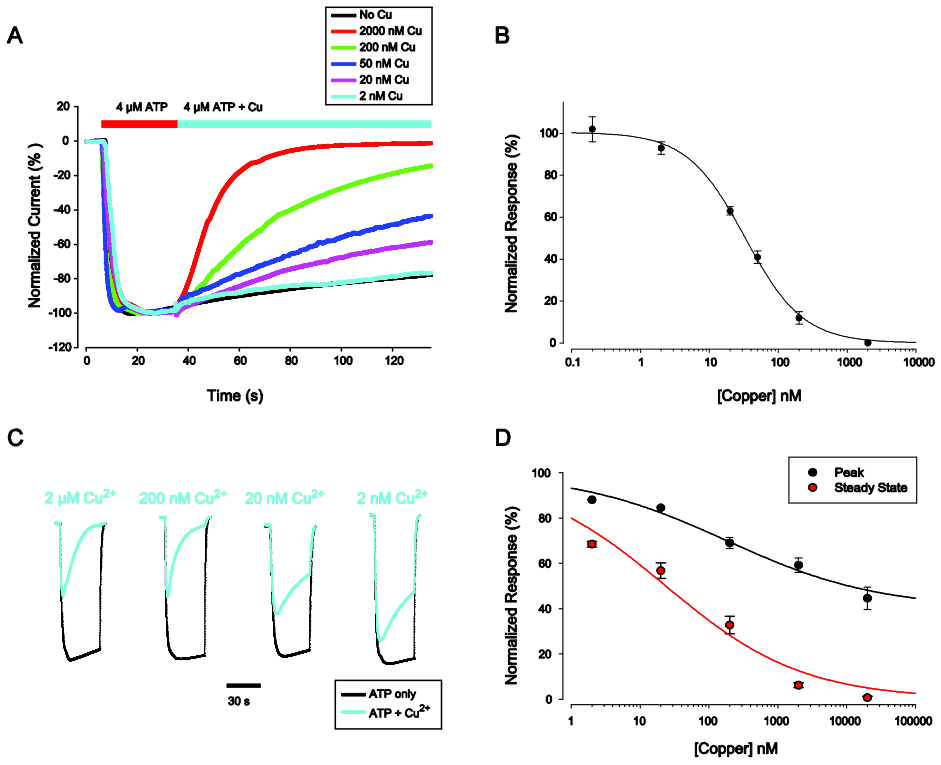

Figure 3.4: Concentration response relation for copper inhibition of hP2X2 when ATP was also present. A) Oocytes at their EC10 for ATP were tested for inhibition by first applying ATP alone, and then ATP plus copper. Each trace is from a different oocyte. To facilitate comparison of the magnitude and rate of inhibition at different copper concentrations, all traces were normalized to their peak response with ATP alone. B) Concentration-response relationship for a range of copper concentrations tested on a series of oocytes as shown in B. Data were fit to the three parameter hill equation (IC50 = 33 nM). C. Responses of hP2X2 expressing oocytes to several different concentrations of copper tested with a one pulse paradigm in which ATP and copper were co-applied. The initial responses to ATP are all normalized to 100%. Each recording is from a separate oocyte. D. Concentration response relations for the peak response and the steady state response for a series of experiments as in C. The data were normalized to an application of ATP alone given at least 2 minutes prior to the coapplication followed by washing with recording solution only.

tested by co-application of ATP and copper without an immediately preceding application of ATP alone (Figure 3.4C). This protocol also indicated that inhibition was very high potency and revealed an additional feature of interest. At all concentrations of copper used, there was an initial response to ATP, which then fell back to some level of steady state inhibition. Both the amplitude of the peak and the steady state response were copper dependent and indicated high potency (Fig 3.4D). The observation that even extremely high copper concentrations were not able to completely suppress the initial responses to ATP indicates that the rate of channel opening is faster than the rate of inhibition and suggests a model in which the channels must be opened by ATP before they can be inhibited by copper.

Effect of copper alone or in the presence of P2X2 receptor inhibitors

If inhibition by copper requires opening of the channel by ATP, one apparent prediction is that pre-applying copper without exogenous ATP, washing, and then testing with ATP alone should give no inhibition. This was not the result that was obtained. Applying 20 μM copper for 1 minute or longer produced nearly complete and longlasting inhibition. The results of one experiment to assess the concentration response relation in which a large number of cells at each copper concentration were tested are shown in Figure 3.5. In this experiment, batches of 7-10 oocytes were first tested with ATP, removed from the recording chamber, washed with ATP free solution, and then incubated in copper containing solutions in 35 mM dishes. Beginning 10 minutes after incubation (long enough for steady state inhibition to become complete when ATP and copper were co-applied during recording, even for low concentrations of copper), we began returning oocytes to the recording

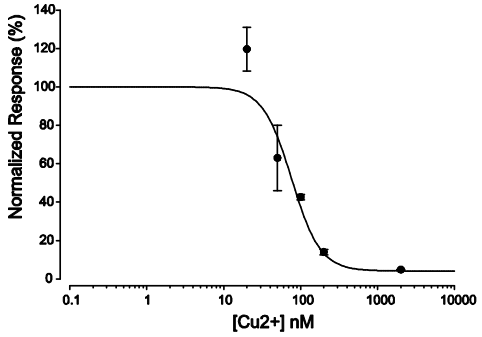

Figure 3.5: Concentration response relation for copper inhibition of hP2X2 when no exogenous ATP was present. See text for details of how this experiment was carried out.

chamber. Once impaled and voltage clamped, each cell was washed with copper free solution for 1 minute and retested for ATP responses. The last cell of each batch was retested about 20 minutes after the first (but also after only a 1-2 minute wash). The % inhibition for the first and the last oocyte tested in each batch was similar. In this experiment, the IC_{50} for copper alone was 76 nM, only slightly higher than observed when ATP and copper were co-applied as in Figure 3.4. However, the results of other experiments testing "copper alone" gave IC_{50}s that were as much as 10fold higher or lower than this. Furthermore, when individual oocytes were kept in the recording chamber for the entire sequence of solution changes, the identical concentration of "copper alone" could cause nearly complete inhibition of some cells, and virtually no inhibition of others.

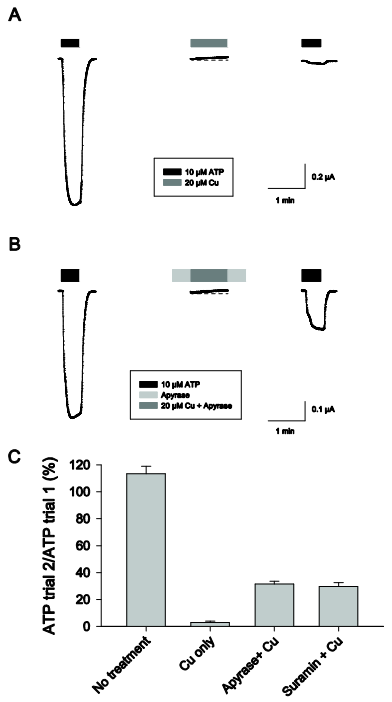

Figure 3.6: Effect of Apyrase and suramin on copper inhibition of hP2X2 when no exogenous ATP was present. A) Effect of copper alone. During the time periods with no drug bar, the cell was superfused with flowing recording solution only. The time scale bar refers to the duration of the washes as well as the duration of the recordings. B) Effect when apyrase was present before, during and after the application of copper. C) Histogram of the extent of recovery of ATP-evoked currents under different conditions. The protocol used to test suramin was identical to the protocol used to test apyrase in B.

A plausible explanation for these variable results was that ATP is required for copper inhibition and that inhibition by copper occurred under "ATP free" conditions because oocytes release enough ATP to reach a concentration at the oocyte surface sufficient to activate some hP2X2 channels in the absence of exogenous ATP. The presence of a basal ATP dependent current in oocytes expressing hP2X2 in the absence of exogenous ATP was confirmed by the observation that in many cells the inward holding current at -50 mV became slightly less negative in the presence of either the ATP degrading enzyme Apyrase, or the hP2X2 antagonist suramin. In a typical experiment, the shift in holding current with 25 µM suramin was +10.7 ± 2.9 nA (N = 7), while when

recording solution was added through the same barrel of the drug application system the shift was negligible (+1.3 ± 0.8 nA, N = 8). Similarly, application of 20 μM copper alone also caused a decrease in inward holding current in most cells (for example Figure 3.6A, middle trace).

We therefore carried out experiments to knock down the effect of any endogenously released ATP. In these experiments, Apyrase or suramin alone was applied for 30s before and after the application of the test compound plus copper. The inhibition by copper was dramatically decreased by either Apyrase or suramin (Figure 3.6B, C), but was not abolished. One interpretation of these results is that inhibition can occur without ATP, but at a much slower rate than in its presence. We favor an alternative interpretation that the highest inhibitor concentrations that were practical to use (due to cost and solubility issues) still allowed some hP2X2 receptors to be activated by endogenously released ATP and then inhibited by the exogenous copper. Evidence that supports this idea is that when copper was applied in the presence of Apyrase (Figure 3.6B, middle trace) it still often elicited a small outward current (which we interpret to be channels that were activated by the basal ATP that managed to elude the Apyrase and then get inhibited when copper was added).

As ATP seemed to be necessary to allow copper to bind to the channel, we also tested whether ATP could promote copper leaving the channel. After inhibiting nearly 100% of the hP2X2 channels with 20 μM copper, we gave a series of test pulses of 2 μM ATP (approximately the EC_{10}), to determine the time course of recovery from copper as in Figure 3.3, or gave a single 1 minute pulse of very high ATP (500 μM) soon after the removal of copper and then resumed the test pulses. Although 500 μM ATP produced a large response (Figure 3.7), the next test pulse fell back down to exactly the amplitude expected if the high ATP had not been given, indicating that no enhancement of recovery had occurred. Analysis of the time constant of the recovery function confirmed the lack of an effect. In the absence of the high ATP pulse, the average time constant of recovery was 7.0 ± 1.1 minutes and in its presence the time constant was 12.9 ± 1.7 minutes (N = 5 each).

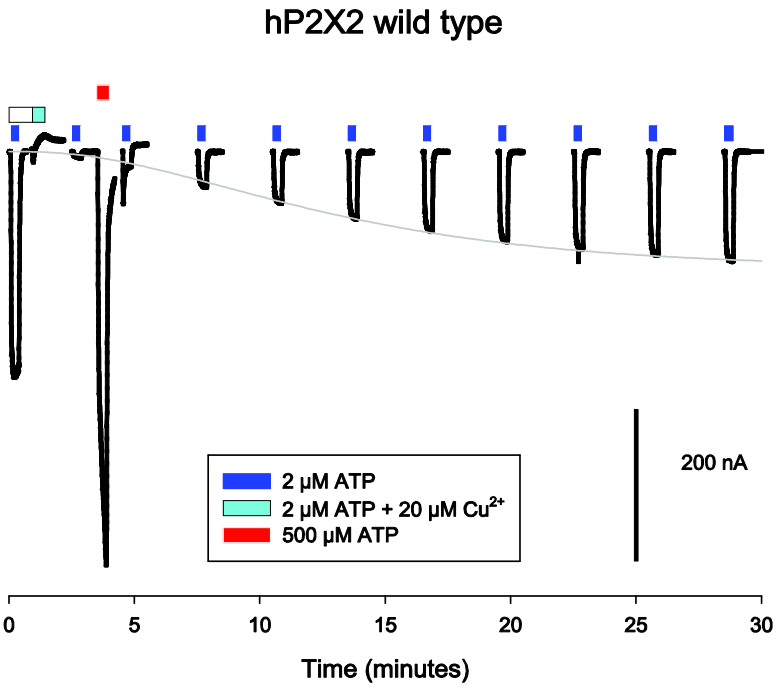

Figure 3.7: Recovery from copper inhibition of hP2X2 is not enhanced by channel opening. Recovery from copper was monitored by applying test pulses of ATP every few minutes. After 9 minutes only every other pulse is illustrated. One minute after treatment with ATP plus copper, a pulse of very high ATP (red bar and trace) was interposed between the first and second recovery test pulses (black bars).

Test of mechanisms for recovery from copper inhibition

The recovery from copper inhibition might arise by several mechanisms. One possibility is that copper is binding to a very high affinity site with a slow dissociation constant (off rate). Another possibility is that copper permanently inactivates the receptors and the rate of recovery represents the rate of insertion of intracellular receptors onto the surface. If recovery is by insertion, then under conditions, in which the intracellular pool is depleted, the rate of recovery should be much slower and the final amplitude of the currents should be much smaller than the initial amplitude because fewer receptors are available to replace the inactivated ones. To deplete the intracellular pool, we treated oocytes with the protein synthesis inhibitor cyclohexamide (CHX) beginning a few hours after RNA was injected. We then compared the rate of recovery from copper in CHX treated and untreated oocytes 24 or 48 hours later.

An essential control was to demonstrate that we were using a dose of CHX that eliminated hP2X2 synthesis, and this indeed was the case, although it required a dose 10 times higher (1 mg/ml = 3.5 mM) than is typically used on mammalian cells in culture. When oocytes were bathed in CHX beginning immediately after RNA injection (t = 0), and then tested for responses to saturating ATP (200 μM) 24 hours later, there were no detectable ATP evoked responses while addition of the vehicle (DMSO) without CHX gave average responses of the same amplitude as oocytes that received no treatment (Untreated = -1,160 ± 140 nA, N = 4, DMSO treated = -1,230 ± 80 nA N = 5, CHX treated = -2 ± 3 nA, N = 20). Interestingly, when CHX applied at t=0, washed off at t = 24 hr and then oocytes tested for ATP responsiveness at t = 48 hr, there also were no ATP detectable responses. This suggests that by 24 hrs after injection, there is too little RNA remaining to direct protein synthesis. As the ATP responses of untreated oocytes increased substantially between 24 and 48 hours (208 ± 39 %, N = 3 experiments), this also indicates that at 24 hours many receptors have been synthesized but not yet delivered to the surface. Stated another way, under control conditions there is a substantial pool of intracellular receptors remaining after protein synthesis is done.

As reported above, in control oocytes, the magnitude of recovery following treatment with saturating copper was 83% ± 6%. In contrast to the predictions of the replacement hypothesis, recovery was just as large as for CHX treated oocytes (78 ± 10%, N = 20). The rate of recovery was similar as well (untreated 19.5 ± 5.1 minutes; CHX treated 25.2 ± 3.7 minutes). As a final control, we conducted an independent set of experiments to assess the effect of CHX on a process that was known to be dependent on insertion of new receptors. Modification of I67C of rat P2X2 by large molecule Alexa 488 maleimide (AM488) blocks access of ATP to its binding site (S Dellal and RI Hume, unpublished), and since this compound does not cross the membrane and the bond is very stable, the rate of recovery of ATP sensitivity is a measure of the replacement rate from the intracellular pool. When we made the homologous mutation of hP2X2 (I79C) we found that recovery from AM488 treatment was different from recovery from copper treatment in several important features. First, it followed an exponential time course, while the recovery from copper had a lag phase and so required an exponential function raised to a power greater than 1. Second, when CHX was added 24 hr after RNA

injection, and recovery tested at 48 hours, ATP responses after recovery from copper reached the pretreatment value (93 ± 7%, N = 7) when sufficient time had elapsed, while the final value for the AM488 treated oocytes reached only 11 ± 2%, (N = 4). Third, after CHX treatment the time constant of the recovery function of AM488 was 3fold slower than for copper. As these experiments demonstrate that ATP responsiveness recovers normally when delivery of internal receptors is severely impaired, we conclude that recovery from copper inhibition is likely to be due to slow unbinding.

Inhibition by copper is allosteric

The ability of 0.5 mM ATP to transiently overcome copper inhibition of hP2X2 that was demonstrated in Figure 3.7 suggested that the mechanism of inhibition is allosteric, rather than by blocking the channel, as the latter effect would not be overcome with additional agonist. We further explored this issue by assessing the ATP concentration response relation of wild type hP2X2 before and after copper treatment. The EC_{50} for ATP immediately after treatment with 20 µM copper was over 200 µM, a right shift of 9.8 ± 2.4fold (N = 7). Furthermore, the maximal current at saturating ATP immediately after copper treatment was only 20 ± 4% of the pretreatment control. Thus, copper makes it harder for ATP to open the channel.

Effects of modifying cysteines on copper inhibition

The most common residues involved in copper binding sites are cysteines and histidines (Rubino and Franz, 2011). We first explored the possible role of the extracellular cysteines, because if any Cu^{1+} was present, it would represent a redox active metal that potentially might promote changes in the disulfide bonding state of the receptor. The only extracellular cystienes of hP2X2 are the ten that are highly conserved across all chordate P2X receptors. Studies of P2X1 and P2X2 strongly suggested that these form five disulfide bonds (Ennion and Evans, 2002; Clyne et al, 2002b). This disulfide bond pattern was confirmed by the crystallization of the zebrafish P2X4.1

receptor (Kawate et al, 2009). The first six cysteines form three disulfide bonds (SS1, SS2 and SS3) located in the "head" region of this dolphin resembling structure, while the last four cysteines forming two disulfide bonds (SS4 and SS5) near the "dorsal fin" region (Kawate et al, 2009). Although it is clear that these residues can form disulfide bonds, there is a suggestion in the literature that under appropriate conditions some bonds become reduced and so their cysteines are available to participate in copper binding (Coddou et al, 2007).

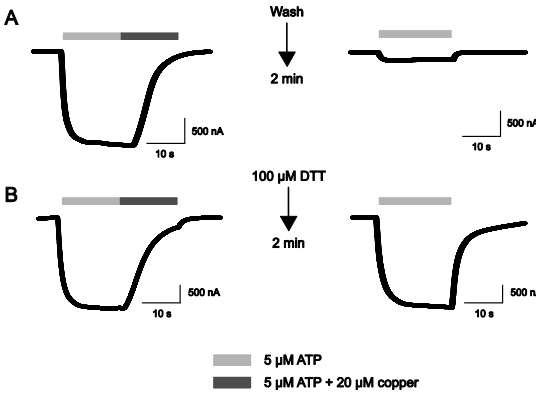

Figure 3.8: Effect of DTT on recovery from copper inhibition.

As an initial test of a potential role for non-disulfide bonded extracellular cysteines, we examined the properties of receptors that had their disulfide bonds chemically reduced by DTT or TCEP. When wild type hP2X2 was treated with DTT, the EC_{50} of the post-treatment ATP concentration response relation was 13.6 ± 2.8 µM (N = 7) which was indistinguishable from untreated oocytes. Similar results had previously been reported for rP2X2 (Li et al, 1997; Rassendren et al, 1997; Clyne et al, 2002b). However, DTT had a huge effect on responses to copper. As noted previously, after a 2 minute wash following treatment with 20 µM copper plus ATP, recovery was minimal. In the batch of control oocytes studied on the same day as the DTT experiments, the average amplitude was 2 ± 1% (N = 7) of the pretreatment value (Fig 3.8A). However, when cells were treated with DTT or TCEP immediately after treatment with copper, by 2 minutes later the responses had returned to 100% of the pre-copper amplitude (DTT 107 ± 5% , N= 7; TCEP 103 ± 5%, N = 3). When the sequence of drug application was reversed (DTT, then copper) the effect was time dependent. When cells were tested with copper within the first five minutes after DTT treatment, the inhibition by copper was less effective (the post copper current was to 17 ± 5% of the pretreatment level rather than the 2% shown without DTT pretreatment) and recovery was complete within 2 minutes. However, if the copper presentation was delayed until 30 minutes after DTT, the extent of inhibition was as great as in untreated oocytes and recovery was just as slow. A likely

explanation for these results is that the cysteines gradually reform their disulfide bonds. Evidence for this is that once recovery had occurred, a second treatment with DTT could return the receptors to the state where copper had low potency and recovery was rapid.

To test whether breaking of a specific disulfide bond was responsible for the effect of reducing agents on copper inhibition, single cysteine to serine mutations were made. No ATP evoked currents could be detected when the final four cysteines were mutated, but mutation of any one of the first six resulted in receptors that responded to ATP. However, mutations at the first four positions had much lower potency than wild type (the EC_{50}s for ATP were C125S = 363.4 ± 76.9, N = 5; C136S = 392.2 ± 66.5, N = 5; C142S = 531.6 ± 117.7, N= 4; C159S = 255.5 ± 9.4, N = 6; C170S = 16.6 ± 2.3, N = 4 and C176S = 13.3 ± 2.6, N = 5). To assess the effect of these mutations on copper inhibition, we measured the amplitude of the currents present at steady state when the bathing solution was changed from EC_{10} ATP only to EC_{10} ATP plus 20 µM ATP. All showed inhibition similar to wild type (Figure 3.9A) and all recovered from application of 20 µM copper very slowly along a sigmoid time course well described by the Chapman equation with a time constant greater than 5 minutes.

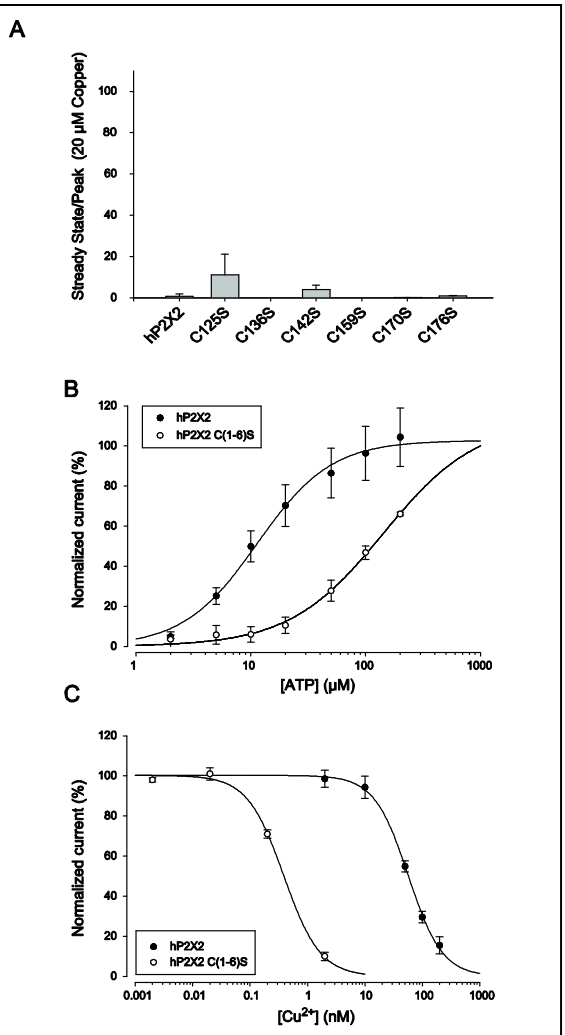

Figure 3.9: Effect of mutation of extracellular cysteines. A) Mutation of each of the first six cysteines to serines on responses to copper. None were significantly different from wild type. Mutation of each of the last four cysteines to serine produced non-functional proteins. B) ATP concentration response relation of the hP2X2 C(1-6)S mutant in which all six cysteines illustrated in A were simultaneously mutated to serine. C) Copper concentration response relation for hP2X2 C(1-6)S.

These single mutations would be expected to break one of three disulfide bonds that are found very close to each other, and so they might not cause much of a structural change. We therefore also studied the hP2X2 C(1-6)S sextuple mutant where the first six cysteines of the extracellular domain of the hP2X2 receptor were all replaced by serines. This mutant had low ATP potency, with its ATP concentration relationship shifted about 10fold to the right (Fig 3.89B). Surprisingly, when studied at its EC_{10} for ATP, this mutant showed higher potency for copper than wild type hP2X2 (Figure 3.8C). As for wild type, the time course of recovery from copper inhibition was very slow and followed a sigmoid time course, with a time constant averaging 11 $\pm$2.1 minutes (N = 5). Thus none of the first six cysteines can be essential participants in copper binding.

We therefore tested the effect of reducing agents on the C(1-6)S mutant. Without treatment by a reducing agent, the response of C(1-6)S to ATP alone after treatment with 20 µM copper plus 20 µM ATP averaged 1.7 ± 0.2% of the precopper control at 1 minute (N = 13) and 3.4 ± 0.5% at 4 minutes (N = 5). However, when a reducing agent was added 2 minutes after copper plus ATP and washed away 3 minutes after copper, the response to ATP alone at 4 minutes had nearly returned to the full control amplitude (10 mM TCEP 77.3 ± 1.8%, N = 4; 10 mM DTT 94.1 ± 3.3%, N = 4). As only the SS4 and SS5 disulfide bonds were present in this mutant, one or both of these is required to maintain the structure that allows high potency copper inhibition.

Effects of modifying histidines on copper inhibition

In contrast, to the lack of effect with cysteine mutagenesis, there were three H to A mutations that showed significantly reduced copper inhibition. When tested with 20 µM copper, the steady state inhibition of H204A, H209A and H330A was much less than for wild type of the other 6 histidine to alanine mutants (Fig 3.10A). We therefore estimated the copper concentration response relations for these mutants. At the EC_{10} for ATP, the respective values for their IC_{50}s were 1.5 µM, 3.6 µM and 4.0 µM (Figure 3.10 B). Thus copper inhibition is present, but is at least 40fold less potent. We also tested the triple histidine to alanine mutant for its effect on copper inhibition and found that similar to its effect on the potency of zinc inhibition (Punthambaker et al, 2012), this mutant was

shifted about a 1000-fold to the right on the concentration-response curve for copper and had an IC_{50} value of 34.0 µM.

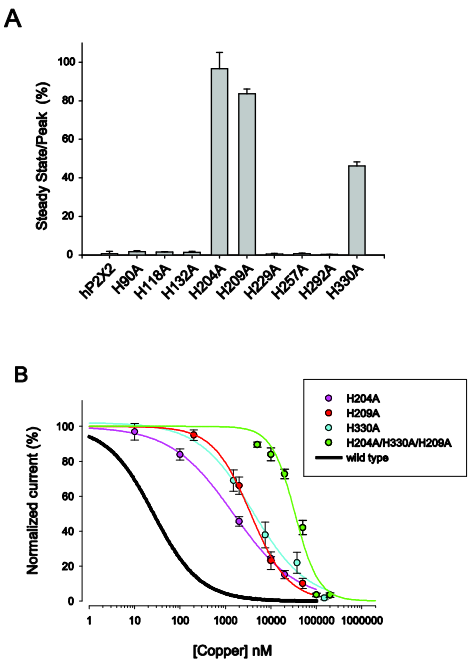

Figure 3.10: Effect of mutation of histidine residues to alanines. A) Bar graph of percentage of recovery from copper inhibition of wildtype and all nine histidine residues in the extracellular domain individually mutated to alanine residues. B,C,D) Copper concentration response relations for H204A, H209A and H330A.

Discussion

In rat P2X2, copper and zinc both strongly potentiate responses to low concentrations of ATP (Xiong et al, 1999; Wildman et al, 1999). We had previously shown that in human P2X2, zinc strongly inhibits responses to low concentrations of ATP (Tittle and Hume, 2008) and our initial goal for this study was to see if copper does so too. We quickly discovered that copper inhibits hP2X2 with a potency approximately 250fold greater than zinc, and that recovery from copper inhibition is extremely slow. The three other divalent metals we tested (cadmium, cobalt and nickel) had effects similar to zinc, with recovery from inhibition complete in just a few minutes. The time course of recovery from copper inhibition could usually be fit well by an exponential function raised to a power greater than 1, with a time constant around 15-20 minutes and a power near 2. These parameters indicated that full recovery will typically require nearly an hour. We therefore tested the possibility that recovery might be due to delivery of new receptors to the surface, but our studies with cyclohexamide suggested that very slow unbinding of copper from a high affinity site is the more likely explanation.

The ability of Apyrase and suramin to suppress copper inhibition suggests that binding ATP promotes copper inhibition (and may even be required). Presumably ATP binding causes a conformational change that makes the site accessible. Therefore, a likely explanation for the high affinity and slow off rate is that copper becomes

conformationally trapped by the receptor once it inhibits it. This model is strikingly similar to results obtained in studies of the ASIC channel, which shares great structural homology with P2X receptors in the pore regions and vestibule cavities (Gonzales et al, 2009). ASIC channels are closed at pH 8 and undergo desensitization at low pH (pH 7 and below) which is accompanied by a substantial conformational change in the receptor. It has been demonstrated that when D79, a residue in the middle vestibule is mutated to a cysteine, it is accessible to cysteine-modifying agents when the channel is closed but not when the channel is desensitized (Cushman, 2007). As the middle vestibule of P2X receptors has been implicated as a potential binding site for divalent and trivalent cations (Kawate et al 2009, Chapter 2), if the mechanism of copper inhibition is promoting entry into the desensitized state, it would explain why the copper is unable to leave its binding site and thus make recovery slow.

Surprisingly, once copper is in its binding site, re-opening the channel with extremely high ATP did not effectively promote recovery, indicating that some other step is rate limiting for unbinding. However, mutations to residues that sit at the entrance to the middle vestibule (H204A, H209A, H330A) promoted rapid recovery. So did treatment with the reducing agents DTT or TCEP. The crystallization of the zebrafish P2X4.1 structure unequivocally confirmed the presence of 5 disulfide bonds between the 10 highly conserved cysteine residues (Kawate et al, 2009), which had been called into question by the claim that one of the cysteines in the cys-rich domain of rat P2X4 receptor played a role in zinc binding (Coddou et al, 2007). One possible explanation for the effect of reducing agents was that breaking of disulfide bonds and reforming them later is part of the normal mechanism for allowing copper to unbind. Indeed, we showed that within half an hour of chemically breaking the endogenous disulfide bonds they appear to spontaneously re-form, as high potency copper inhibition returns. However, the residue homologous to the specific cysteine proposed by Coddou et al cannot be responsible for promoting either binding or unbinding copper in hP2X2, as it is absent in the C(1-6)S mutant which we showed binds copper with even higher potency than wild type hP2X2.

CHAPTER 4

General Discussion

Potential impact of metal inhibition of P2X2 on normal and pathological human brain function

Considerable evidence suggests that in the mammalian central nervous system P2X2 receptors are expressed both on neurons and glia (Burnstock and Knight, 2004; Illes and Ribeiro, 2004), but the CNS phenotype of mouse P2X2 knock outs is quite modest (Cockayne et al, 2005). The mutants we have characterized in chapter 2 have several potential uses in understanding the role of P2X receptors, and how this role is modulated by zinc. It is estimated that the typical concentration of free extracellular zinc in the brain is approximately 20 nM (Frederickson et al, 2006), which would have no detectable effect on wild type hP2X2 or rP2X2. However, the zinc concentration in the synaptic cleft beneath terminals which express the ZNT-3 vesicular zinc transporter has been estimated to go above 10 µM (Sindreu and Storm, 2011), so any wild type P2X2 receptors on neurons or glia close to such synapses would be expected to be modulated whenever ATP and zinc are simultaneously present. Three mutants seem most promising. First, hP2X2 H204A/H209A/H330A responds normally to ATP, but is effectively zinc insensitive over the range that can occur in the brain. Thus expressing this mutant as a replacement for wild type mouse P2X2 in knock-in replacement animals or in acutely transfected slices from P2X2 knockout mice seems a potentially useful way to explore what occurs without zinc modulation. Conversely, P206H has greatly heightened zinc sensitivity without compromising ATP responsiveness, such that it would be expected to be activated (although not maximally) by basal zinc levels, and thus could be used to chronically lower P2X2 “tone”. Lastly, P206C is sufficiently zinc sensitive that it should

be essentially non-functional at basal zinc levels. However, when modified by MTSET it can be reversibly converted to a state that is nearly zinc insensitive, but has enhanced ATP sensitivity. Thus if a way could be found to express these P206C receptors in a system where access by exogenously applied substances is possible (such as in thin brain slices or in cell culture), it would be possible to observe the same set of interactions with and without functional P2X2 receptors within just a few minutes by manipulating the zinc and MTSET levels.

Based on extrapolations of data measuring release of copper from synaptosomes, the free Cu^{2+} present beneath active synapses has been estimated to be in the range of 2-3 μM (Hopt et al, 2003). The concentration in the absence of activity was not explicitly noted, but given the sensitivity of the assays, it would appear to be at least 10fold lower. However, there are reasons for suspecting that the copper concentration in many brain regions does not get this high. First, when rat hippocampal slices are bathed in 1 μM Cu^{2+}, long term potentiation in CA1 is abolished (Doreulee et al, 1997). As these rats require LTP to learn, it seems unlikely that copper ever gets this high at these excitatory synapses. Similarly, if brain copper levels in humans routinely reached 200 nM Cu^{2+} or higher, the hP2X2 receptors would always be inactive. As nonfunctional genes typically rapidly evolve into pseudogenes, the fact that hP2X2 retains an open reading frame that encodes a functional protein implies that in the regions of the human brain where these receptors are expressed, copper rarely get this high in healthy individuals. However, the high potency of copper inhibition of hP2X2 makes one wonder if these receptors might be affected in humans with Wilson Disease, which is characterized by an excess of copper in the liver that secondarily raises copper levels in other tissues including the brain. If lack of activity via P2X2 signaling plays a role in the pathophysiology of Wilson Disease, it would provide a nice explanation for why mice with mutations in ATP7B show no brain symptoms similar to human Wilson patients. As noted in the introduction, copper potentiates, rather than inhibits the rat and mouse P2X2 receptors, so P2X2 signaling would be enhanced, rather than inhibited in these model organisms.

Potential high impact future experiments

The binding of MTSET to hP206C results in massive potentiation of the ATP-evoked currents. Although in principle if the maximum open probability of this mutant at saturating ATP is extremely low, an increase in open probability alone could account for this result, it seems more likely that an increase in the unitary channel conductance is likely to also play a role. Analysis of the single channel currents from hP206C mutants expressed in HEK cells could clarify which single channel properties of the receptors are altered by MTSET binding at position P206C. An attractive possibility is that the P206C mutation lowers the single channel conductance, and that adding MTSET restores it to its normal level, but it is also possible that MTSET causes the channel to take on a much larger than normal conductance.

The crystal structure of zebrafish P2X4.1 bound to ATP and in an open state was very recently reported (Hattori and Gouaux, 2012). This revealed that the ATP binding site was indeed where mutagenesis had predicted it would be and also showed dramatic conformational changes in the receptor pore as compared to the apo, closed state of the receptor (Kawate et al, 2009). The open state shows an obvious pore large enough for ions to traverse through the membrane, but equally dramatic conformational changes occurs in the lower two vestibules (Hattori and Gouaux, 2012). Both get much wider in diameter, and the narrow constriction between the two of them disappears, indicating that ions will likely flow unimpeded throughout this entire region. In contrast, the middle and upper vestibules remain separated by a region too thin for ions to pass through. The new ATP bound structure confirms that the ion access pathway is via the fenestrations which open even more widely upon ATP binding, rather than through the central pathway along the axis of symmetry (Hattori and Gouaux, 2012). The widening of the entire lower half of the receptor after binding ATP is consistent with our predictions in Chapters 2 and 3 that zinc and copper only can easily gain access a putative middle vestibule binding site once a major structural alteration occurs on channel opening. Thus the additional middle vestibule mutations discussed in Chapter 2 seem a very high priority for future experiments.

APPENDIX

At the time, I started thesis research the 3D structure of all P2X receptors was unknown. A number of studies had used site directed mutagenesis to identify possible residues involved in ATP binding and/ or channel gating (Jiang et al, 2000; Roberts et al, 2008; Roberts and Evans, 2004; Roberts et al, 2009; Zemkova et al, 2007) but there was no direct evidence for the ATP binding site. Therefore, the initial goal of my thesis was to develop tools that would allow us to understand the structural properties of the receptor. The approach I planned to pursue was similar to that used successfully for all three classes of glutamate receptors. The first step was to find a way to make a soluble ligand binding domain. For AMPA receptors this was accomplished by fusing two pieces of the extracellular domain with a short linker, thus excluding the transmembrane regions (Kuusinen et al, 1995). This type of construct was then used by the Gouaux lab to solve the structure by of an AMPA receptor binding site by X-ray Crystallography (Armstrong, 1998). I decided that a sequence encoding just the extracellular domain (ECD) of rP2X2 (with a C-terminal His-tag) might be an appropriate starting material. This construct contained residues from Val48 to Pro330. I then expressed it using the Baculovirus infected inset cells.

The recombinant rat P2X2 ECD protein was expressed by infecting 8L of HI5 cells grown

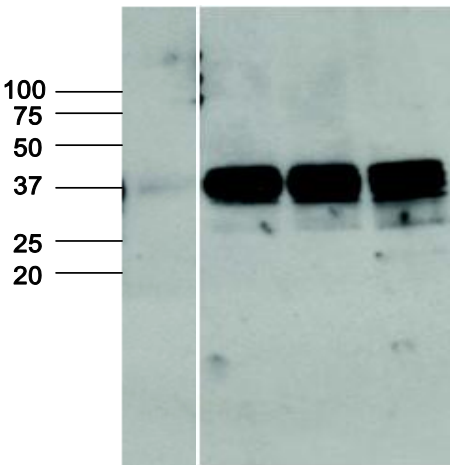

Appendix Figure 1: Expression of P2X2 ECD from Baculovirus infected Sf9 cells: Immunoblot using anti-His antibody showing P2X2-His in medium at different time points of baculovirus infection. The molecular weight standards are shown in kD.

in Sf921 medium (Expression systems) at a cell density of $0.65X10^6$ cells/ml containing (1:100 antibiotics and antimycotics) and 1:100 of 200 mM L-Glutamine with 1.0 or 1.5pfu/ml MOI and incubated for 60 – 64 hrs at 28 °C at 145 rpm. The expressed soluble rP2X2 ECD protein was detected using an anti-Penta-His antibody on a western blot (Appendix Figure 1). All three durations of infection gave a large band at the size predicted for a soluble extracellular domain.

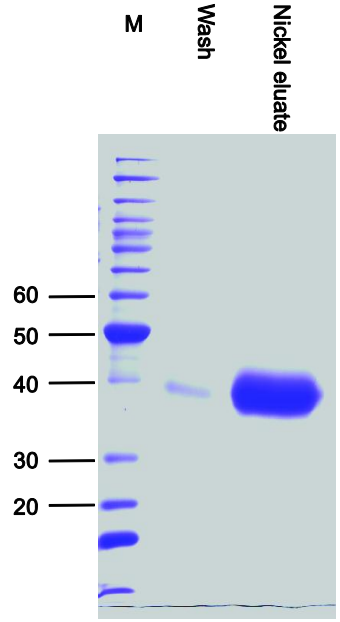

Appendix Figure 2: Affinity column purified P2X2 ECD: SDS-PAGE gel stained with coomassie blue showing purified P2X2 ECD protein expressed from Sf9 cells infected with recombinant baculovirus.

The supernatant was concentrated and affinity purified on a Ni column and was finally eluted with 25 mM Sodium Phosphate pH 8, 500 mM NaCl and increasing concentrations of 500 mM Imidazole using the AKTA FPLC (GE Healthcare). Protein purity was assessed by Coomassie Blue staining on 12% SDS-PAGE gels (Appendix Figure 2). The Ni eluate was diluted 5 times with 25 mM Tris pH 8 and stored at -80 °C. Protein identity was confirmed by N-terminal sequencing (Michigan State University).

Size exclusion chromatographic analysis was performed on the purified protein by taking

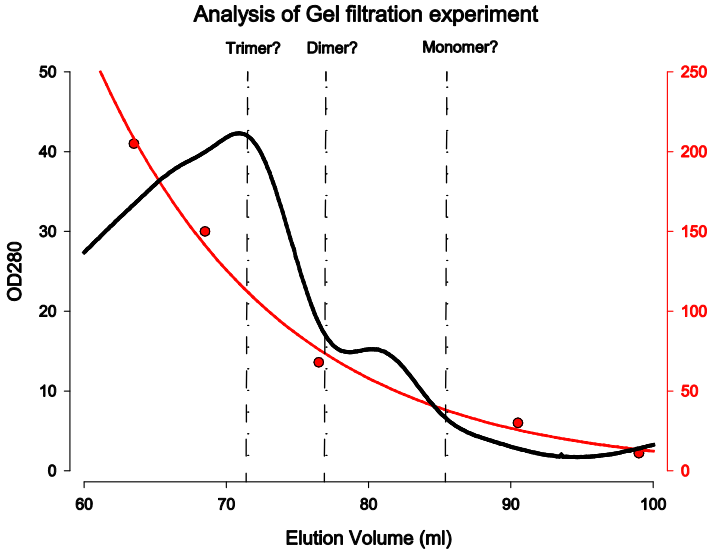

Appendix Figure 3: Gel filtration of P2X2 ECD post Ni column elution. The y axis (milliabsorbance units, mAU) plots absorbance at 280nm, the x axis plots elution volume in ml.

an aliquot of the Ni-eluate (3 mg), concentrating the protein using an Amicon Ultra (molecular weight cut off of 5Kd) and diluted 25X to 3 ml with the Gel-filtration buffer (20 mM Tris and 50 mM NaCl) to reduce the salt concentration. This was applied to a Superdex 200 16/60 GL gel-filtration column. The overlay graph shown in red represents elution data of proteins of known molecular weight. Most of the ECD protein eluted at a volume predicted to be of the trimer size (Appendix Figure 3).

Thus I succeeded in preparing the raw material that might have led to crystallization of a soluble extracellular domain of a P2X receptor. However, at this point the crystal structure of zP2X4.1 was published, and it did not seem that the time necessary to pursue this would lead to sufficient new information to justify the effort.

REFERENCES

Abbracchio, M. P. and G. Burnstock. (1994). Purinoceptors - Are There Families of P2x and P2y Purinoceptors. Pharmacology & Therapeutics 64: 445-475.

Acuna-Castillo, C., B. Morales and J. P. Huidobro-Toro. (2000). Zinc and copper modulate differentially the P2X(4) receptor. J Neurochem 74: 1529-1537.

Acuna-Castillo, C., C. Coddou, P. Bull, J. Brito and J. P. Huidobro-Toro. (2007). Differential role of extracellular histidines in copper, zinc, magnesium and proton modulation of the P2X7 purinergic receptor. J Neurochem 101: 17-26.

Adlard, P. A., J. M. Parncutt, D. I. Finkelstein and A. I. Bush. (2010). Cognitive loss in zinc transporter-3 knock-out mice: a phenocopy for the synaptic and memory deficits of Alzheimer's disease? J Neurosci 30: 1631-1636.

Akabas, M. H., D. A. Stauffer, M. Xu and A. Karlin. (1992). Acetylcholine receptor channel structure probed in cysteine-substitution mutants. Science 258: 307-310.

Alberts, I. L., K. Nadassy and S. J. Wodak. (1998). Analysis of zinc binding sites in protein crystal structures. Protein Sci 7: 1700-1716.

Andreini, C., I. Bertini and G. Cavallaro. (2011). Minimal functional sites allow a classification of zinc sites in proteins. PLoS One 6: e26325.

Aniksztejn, L., G. Charton and Y. Ben-Ari. (1987). Selective release of endogenous zinc from the hippocampal mossy fibers in situ. Brain Res 404: 58-64.

Armstrong, N. and E. Gouaux. (2000). Mechanisms for activation and antagonism of an AMPA-sensitive glutamate receptor: crystal structures of the GluR2 ligand binding core. Neuron 28: 165-181.

Armstrong, N., Y. Sun, G. Q. Chen and E. Gouaux. (1998). Structure of a glutamate-receptor ligand-binding core in complex with kainate. Nature 395: 913-917.

Assaf, S. Y. and S. H. Chung. (1984). Release of endogenous Zn2+ from brain tissue during activity. Nature 308: 734-736.

Awapara, J., A. J. Landua, R. Fuerst and B. Seale. (1950). Free gamma-aminobutyric acid in brain. J Biol Chem 187: 35-39.

Bian, X., J. Ren, M. DeVries, B. Schnegelsberg, D. A. Cockayne, A. P. Ford and J. J. Galligan (2003). Peristalsis is impaired in the small intestine of mice lacking the P2X3 subunit. The Journal of physiology 551: 309-322.

Barajas-Lopez, C., L. M. Montano and R. Espinosa-Luna. (2002). Inhibitory interactions between 5-HT3 and P2X channels in submucosal neurons. Am J Physiol Gastrointest Liver Physiol 283: G1238-1248.

Barajas-Lopez, C., R. Espinosa-Luna and Y. Zhu. (1998). Functional interactions between nicotinic and P2X channels in short-term cultures of guinea-pig submucosal neurons. J Physiol 513 (Pt 3): 671-683.

Bastian, C. and Y. V. Li. (2007). Fluorescence imaging study of extracellular zinc at the hippocampal mossy fiber synapse. Neurosci Lett 419: 119-124.

Birinyi, A., D. Parker, M. Antal and O. Shupliakov. (2001). Zinc co-localizes with GABA and glycine in synapses in the lamprey spinal cord. J Comp Neurol 433: 208-221.

Blakemore, L. J. and P. Q. Trombley. (2004). Diverse modulation of olfactory bulb AMPA receptors by zinc. Neuroreport 15: 919-923.

Bloomenthal, A. B., E. Goldwater, D. B. Pritchett and N. L. Harrison. (1994). Biphasic modulation of the strychnine-sensitive glycine receptor by Zn2+. Mol Pharmacol 46: 1156-1159.

Bo, X., L. H. Jiang, H. L. Wilson, M. Kim, G. Burnstock, A. Surprenant and R. A. North (2003). Pharmacological and biophysical properties of the human P2X5 receptor. Molecular pharmacology 63: 1407-1416.

Bocquet, N., H. Nury, M. Baaden, C. Le Poupon, J. P. Changeux, M. Delarue and P. J. Corringer. (2009). X-ray structure of a pentameric ligand-gated ion channel in an apparently open conformation. Nature 457: 111-114.

Bocquet, N., L. Prado de Carvalho, J. Cartaud, J. Neyton, C. Le Poupon, A. Taly, T. Grutter, J. P. Changeux and P. J. Corringer. (2007). A prokaryotic proton-gated ion channel from the nicotinic acetylcholine receptor family. Nature 445: 116-119.

Bordoli, L., F. Kiefer, K. Arnold, P. Benkert, J. Battey and T. Schwede. (2009). Protein structure homology modeling using SWISS-MODEL workspace. Nat. Protoc. 4: 1-13.

Boue-Grabot, E., C. Barajas-Lopez, Y. Chakfe, D. Blais, D. Belanger, M. B. Emerit and P. Seguela. (2003). Intracellular cross talk and physical interaction between two classes of neurotransmitter-gated channels. J Neurosci 23: 1246-1253.

Boyer, J. L., I. E. Zohn, K. A. Jacobson and T. K. Harden. (1994). Differential effects of P2-purinoceptor antagonists on phospholipase C- and adenylyl cyclase-coupled P2Y-purinoceptors. Br J Pharmacol 113: 614-620.

Brake, A. J., M. J. Wagenbach and D. Julius. (1994). New structural motif for ligand-gated ion channels defined by an ionotropic ATP receptor. Nature 371: 519-523.

Brooks-Kayal, A. R., M. D. Shumate, H. Jin, T. Y. Rikhter, M. E. Kelly and D. A. Coulter. (2001). gamma-Aminobutyric acid(A) receptor subunit expression predicts functional changes in hippocampal dentate granule cells during postnatal development. J Neurochem 77: 1266-1278.

Brown, D. R., K. Qin, J. W. Herms, A. Madlung, J. Manson, R. Strome, P. E. Fraser, T. Kruck, A. von Bohlen, W. Schulz-Schaeffer, A. Giese, D. Westaway and H. Kretzschmar. (1997). The cellular prion protein binds copper in vivo. Nature 390: 684-687.

Budde, T., A. Minta, J. A. White and A. R. Kay. (1997). Imaging free zinc in synaptic terminals in live hippocampal slices. Neuroscience 79: 347-358.

Burnstock, G. and G. E. Knight. (2004). Cellular distribution and functions of P2 receptor subtypes in different systems. Int Rev Cytol 240: 31-304.

Burnstock, G., D. G. Satchell and A. Smythe. (1972). A comparison of the excitatory and inhibitory effects of non-adrenergic, non-cholinergic nerve stimulation and exogenously applied ATP on a variety of smooth muscle preparations from different vertebrate species. Br J Pharmacol 46: 234-242.

Burnstock, G., J. O'Shea and M. Wood. (1963). Comparative Physiology of the Vertebrate Autonomic Nervous System. I. Innervation of the Urinary Bladder of the Toad (Bufo Marinus). The Journal of experimental biology 40: 403-419.

Chang, M. M. and S. E. Leeman. (1970). Isolation of a sialogogic peptide from bovine hypothalamic tissue and its characterization as substance P. J Biol Chem 245: 4784-4790.

Charton, G., C. Rovira, Y. Ben-Ari and V. Leviel. (1985). Spontaneous and evoked release of endogenous Zn2+ in the hippocampal mossy fiber zone of the rat in situ. Experimental brain research. Experimentelle Hirnforschung. Experimentation cerebrale 58: 202-205.

Chaumont, S. and B. S. Khakh. (2008). Patch-clamp coordinated spectroscopy shows P2X2 receptor permeability dynamics require cytosolic domain rearrangements but not Panx-1 channels. Proc Natl Acad Sci U S A 105: 12063-12068.

Chaumont, S., L. H. Jiang, A. Penna, R. A. North and F. Rassendren. (2004). Identification of a trafficking motif involved in the stabilization and polarization of P2X receptors. J Biol Chem 279: 29628-29638.

Chen, L., A. El-Husseini, S. Tomita, D. S. Bredt and R. A. Nicoll. (2003). Stargazin differentially controls the trafficking of alpha-amino-3-hydroxyl-5-methyl-4-isoxazolepropionate and kainate receptors. Mol Pharmacol 64: 703-706.

Chen, L., D. M. Chetkovich, R. S. Petralia, N. T. Sweeney, Y. Kawasaki, R. J. Wenthold, D. S. Bredt and R. A. Nicoll. (2000). Stargazin regulates synaptic targeting of AMPA receptors by two distinct mechanisms. Nature 408: 936-943.

Chen, L., S. Bao, X. Qiao and R. F. Thompson. (1999). Impaired cerebellar synapse maturation in waggler, a mutant mouse with a disrupted neuronal calcium channel gamma subunit. Proc Natl Acad Sci U S A 96: 12132-12137.

Choi, Y. B. and S. A. Lipton. (1999). Identification and mechanism of action of two histidine residues underlying high-affinity Zn2+ inhibition of the NMDA receptor. Neuron 23: 171-180.

Clark, A. K., A. A. Staniland, F. Marchand, T. K. Kaan, S. B. McMahon and M. Malcangio (2010). P2X7-dependent release of interleukin-1beta and nociception in the spinal cord following lipopolysaccharide. J Neurosci 30: 573-582.

Clyne, J. D., L. D. LaPointe and R. I. Hume. (2002). The role of histidine residues in modulation of the rat P2X(2) purineceptor by zinc and pH. Journal of Physiology-London 539: 347-359.

Clyne, J. D., L. F. Wang and R. I. Hume. (2002). Mutational analysis of the conserved cysteines of the rat P2X2 purinoceptor. J Neurosci 22: 3873-3880.

Clyne, J. D., T. C. Brown and R. I. Hume. (2003). Expression level dependent changes in the properties of P2X2 receptors. Neuropharmacology 44: 403-412.

Cockayne, D. A., P. M. Dunn, Y. Zhong, W. Rong, S. G. Hamilton, G. E. Knight, H. Z. Ruan, B. Ma, P. Yip, P. Nunn, S. B. McMahon, G. Burnstock and A. P. Ford. (2005). P2X2 knockout mice and P2X2/P2X3 double knockout mice reveal a role for the P2X2 receptor subunit in mediating multiple sensory effects of ATP. J Physiol 567: 621-639.

Cockayne, D. A., S. G. Hamilton, Q. M. Zhu, P. M. Dunn, Y. Zhong, S. Novakovic, A. B. Malmberg, G. Cain, A. Berson, L. Kassotakis, L. Hedley, W. G. Lachnit, G.

Burnstock, S. B. McMahon and A. P. Ford (2000). Urinary bladder hyporeflexia and reduced pain-related behaviour in P2X3-deficient mice. Nature 407: 1011-1015.

Coddou, C., B. Morales, J. Gonzalez, M. Grauso, F. Gordillo, P. Bull, F. Rassendren and J. P. Huidobro-Toro. (2003). Histidine 140 plays a key role in the inhibitory modulation of the P2X4 nucleotide receptor by copper but not zinc. J Biol Chem 278: 36777-36785.

Coddou, C., C. Acuna-Castillo, P. Bull and J. P. Huidobro-Toro. (2007). Dissecting the facilitator and inhibitor allosteric metal sites of the P2X4 receptor channel: critical roles of CYS132 for zinc potentiation and ASP138 for copper inhibition. J Biol Chem 282: 36879-36886.

Coddou, C., S. S. Stojilkovic and J. P. Huidobro-Toro. (2011). Allosteric modulation of ATP-gated P2X receptor channels. Reviews in the neurosciences 22: 335-354.

Cole, T. B., A. Martyanova and R. D. Palmiter. (2001). Removing zinc from synaptic vesicles does not impair spatial learning, memory, or sensorimotor functions in the mouse. Brain Res 891: 253-265.

Cole, T. B., H. J. Wenzel, K. E. Kafer, P. A. Schwartzkroin and R. D. Palmiter. (1999). Elimination of zinc from synaptic vesicles in the intact mouse brain by disruption of the ZnT3 gene. Proc Natl Acad Sci U S A 96: 1716-1721.

Colquhoun, D., P. Jonas and B. Sakmann. (1992). Action of brief pulses of glutamate on AMPA/kainate receptors in patches from different neurones of rat hippocampal slices. J Physiol 458: 261-287.

Cousins, R. J., J. P. Liuzzi and L. A. Lichten. (2006). Mammalian zinc transport, trafficking, and signals. J Biol Chem 281: 24085-24089.

Curtis, D. R. and J. C. Watkins. (1960). The excitation and depression of spinal neurones by structurally related amino acids. J Neurochem 6: 117-141.

Cushman, K. A., J. Marsh-Haffner, J. P. Adelman and E. W. McCleskey. (2007). A conformation change in the extracellular domain that accompanies desensitization of acid-sensing ion channel (ASIC) 3. J Gen Physiol 129: 345-350.

Dale, H. H. and H. W. Dudley. (1929). The presence of histamine and acetylcholine in the spleen of the ox and the horse. J Physiol 68: 97-123.

Doreulee, N., Y. Yanovsky and H. L. Haas. (1997). Suppression of long-term potentiation in hippocampal slices by copper. Hippocampus 7: 666-669.

Dreixler, J. C. and J. P. Leonard. (1994). Subunit-specific enhancement of glutamate receptor responses by zinc. Brain Res Mol Brain Res 22: 144-150.

Emsley, P., B. Lohkamp, W. G. Scott and K. Cowtan. (2010). Features and development of Coot. Acta. Crystallogr. D. Biol. Crystallogr. 66: 486-501.

Ennion, S. J. and R. J. Evans. (2002). Conserved cysteine residues in the extracellular loop of the human P2X(1) receptor form disulfide bonds and are involved in receptor trafficking to the cell surface. Mol Pharmacol 61: 303-311

Ennion, S., S. Hagan and R. J. Evans. (2000). The role of positively charged amino acids in ATP recognition by human P2X(1) receptors. J Biol Chem 275: 29361-29367

Farrant, M. and Z. Nusser. (2005). Variations on an inhibitory theme: phasic and tonic activation of GABA(A) receptors. Nat Rev Neurosci 6: 215-229.

Fayyazuddin, A., A. Villarroel, A. Le Goff, J. Lerma and J. Neyton. (2000). Four residues of the extracellular N-terminal domain of the NR2A subunit control high-affinity Zn2+ binding to NMDA receptors. Neuron 25: 683-694.

Finger, T. E., V. Danilova, J. Barrows, D. L. Bartel, A. J. Vigers, L. Stone, G. Hellekant and S. C. Kinnamon. (2005). ATP signaling is crucial for communication from taste buds to gustatory nerves. Science 310: 1495-1499.

Fountain, S. J., K. Parkinson, M. T. Young, L. Cao, C. R. Thompson and R. A. North. (2007). An intracellular P2X receptor required for osmoregulation in Dictyostelium discoideum. Nature 448: 200-203.

Frederickson, C. J. (1989). Neurobiology of zinc and zinc-containing neurons. Int Rev Neurobiol 31: 145-238.

Frederickson, C. J. and A. I. Bush. (2001). Synaptically released zinc: physiological functions and pathological effects. Biometals 14: 353-366.

Frederickson, C. J., L. J. Giblin, 3rd, R. V. Balaji, R. Masalha, Y. Zeng, E. V. Lopez, J. Y. Koh, U. Chorin, L. Besser, M. Hershfinkel, Y. Li, R. B. Thompson and A. Krezel. (2006). Synaptic release of zinc from brain slices: factors governing release, imaging, and accurate calculation of concentration. J Neurosci Methods 154: 19-29.

Frederickson, C. J., L. J. Giblin, A. Krezel, D. J. McAdoo, R. N. Mueller, Y. Zeng, R. V. Balaji, R. Masalha, R. B. Thompson, C. A. Fierke, J. M. Sarvey, M. de Valdenebro, D. S.

Prough and M. H. Zornow. (2006). Concentrations of extracellular free zinc (pZn)e in the central nervous system during simple anesthetization, ischemia and reperfusion. Exp Neurol 198: 285-293.

Galligan, J. J. (2004). Enteric P2X receptors as potential targets for drug treatment of the irritable bowel syndrome. Br J Pharmacol 141: 1294-1302.

Garcia-Colunga, J., M. Gonzalez-Herrera and R. Miledi. (2001). Modulation of alpha2beta4 neuronal nicotinic acetylcholine receptors by zinc. Neuroreport 12: 147-150.

Gendreau, S., J. Schirmer and G. Schmalzing. (2003). Identification of a tubulin binding motif on the P2X2 receptor. J Chromatogr B Analyt Technol Biomed Life Sci 786: 311-318.

Gielen, M., A. Le Goff, D. Stroebel, J. W. Johnson, J. Neyton and P. Paoletti. (2008). Structural rearrangements of NR1/NR2A NMDA receptors during allosteric inhibition. Neuron 57: 80-93.

Gill, C. H., J. A. Peters and J. J. Lambert. (1995). An electrophysiological investigation of the properties of a murine recombinant 5-HT3 receptor stably expressed in HEK 293 cells. Br J Pharmacol 114: 1211-1221.

Gitlin, J. D. (2003). Wilson disease. Gastroenterology 125: 1868-1877.

Gollan, J. L. and D. J. Deller. (1973). Studies on the nature and excretion of biliary copper in man. Clin Sci 44: 9-15.

Gonzales, E. B., T. Kawate and E. Gouaux. (2009). Pore architecture and ion sites in acid-sensing ion channels and P2X receptors. Nature 460: 599-604.

Gordon, J. L. (1986). Extracellular ATP: effects, sources and fate. Biochem J 233: 309-319.

Hartter, D. E. and A. Barnea. (1988). Evidence for release of copper in the brain: depolarization-induced release of newly taken-up 67copper. Synapse 2: 412-415.

Harvey, R. J., P. Thomas, C. H. James, A. Wilderspin and T. G. Smart. (1999). Identification of an inhibitory Zn2+ binding site on the human glycine receptor alpha1 subunit. J Physiol 520 Pt 1: 53-64.

Hattori, M. and E. Gouaux. (2012). Molecular mechanism of ATP binding and ion channel activation in P2X receptors. Nature 485: 207-212.

Hechler, B., N. Lenain, P. Marchese, C. Vial, V. Heim, M. Freund, J. P. Cazenave, M. Cattaneo, Z. M. Ruggeri, R. Evans and C. Gachet (2003). A role of the fast ATP-gated P2X1 cation channel in thrombosis of small arteries in vivo. The Journal of experimental medicine 198: 661-667.

Hilf, R. J. and R. Dutzler. (2008). X-ray structure of a prokaryotic pentameric ligand-gated ion channel. Nature 452: 375-379.

Hilf, R. J. and R. Dutzler. (2009). A prokaryotic perspective on pentameric ligand-gated ion channel structure. Current opinion in structural biology 19: 418-424.

Hirzel, K., U. Muller, A. T. Latal, S. Hulsmann, J. Grudzinska, M. W. Seeliger, H. Betz and B. Laube. (2006). Hyperekplexia phenotype of glycine receptor alpha1 subunit mutant mice identifies Zn(2+) as an essential endogenous modulator of glycinergic neurotransmission. Neuron 52: 679-690.

Holton, P. (1959). The liberation of adenosine triphosphate on antidromic stimulation of sensory nerves. J Physiol 145: 494-504.

Howell, G. A., M. G. Welch and C. J. Frederickson. (1984). Stimulation-induced uptake and release of zinc in hippocampal slices. Nature 308: 736-738.

Hsiao, B., D. Dweck and C. W. Luetje. (2001). Subunit-dependent modulation of neuronal nicotinic receptors by zinc. J Neurosci 21: 1848-1856.

Hsiao, B., K. B. Mihalak, S. E. Repicky, D. Everhart, A. H. Mederos, A. Malhotra and C. W. Luetje. (2006). Determinants of zinc potentiation on the alpha4 subunit of neuronal nicotinic receptors. Mol Pharmacol 69: 27-36.

Huang, Y. A., L. M. Stone, E. Pereira, R. Yang, J. C. Kinnamon, G. Dvoryanchikov, N. Chaudhari, T. E. Finger, S. C. Kinnamon and S. D. Roper (2011). Knocking out P2X receptors reduces transmitter secretion in taste buds. J Neurosci **31**: 13654-13661.

Hubbard, P. C. and S. C. Lummis. (2000). Zn(2+) enhancement of the recombinant 5-HT(3) receptor is modulated by divalent cations. Eur J Pharmacol 394: 189-197.

Hughes, J. (1975). Isolation of an endogenous compound from the brain with pharmacological properties similar to morphine. Brain Res 88: 295-308.

Hughes, J., T. W. Smith, H. W. Kosterlitz, L. A. Fothergill, B. A. Morgan and H. R. Morris. (1975). Identification of two related pentapeptides from the brain with potent opiate agonist activity. Nature 258: 577-580.

Huster, D., M. J. Finegold, C. T. Morgan, J. L. Burkhead, R. Nixon, S. M. Vanderwerf, C. T. Gilliam and S. Lutsenko. (2006). Consequences of copper accumulation in

the livers of the Atp7b-/- (Wilson disease gene) knockout mice. Am J Pathol 168: 423-434.

Iglesias, R., S. Locovei, A. Roque, A. P. Alberto, G. Dahl, D. C. Spray and E. Scemes. (2008). P2X7 receptor-Pannexin1 complex: pharmacology and signaling. Am J Physiol Cell Physiol 295: C752-760.

Illes, P. and J. Alexandre Ribeiro. (2004). Molecular physiology of P2 receptors in the central nervous system. Eur. J. Pharmacol. 483: 5-17.

Inscho, E. W., A. K. Cook, J. D. Imig, C. Vial and R. J. Evans (2004). Renal autoregulation in P2X1 knockout mice. Acta physiologica Scandinavica 181: 445-453.

Jasti, J., H. Furukawa, E. B. Gonzales and E. Gouaux. (2007). Structure of acid-sensing ion channel 1 at 1.9 A resolution and low pH. Nature 449: 316-323.

Jiang, L. H., F. Rassendren, A. Surprenant and R. A. North. (2000). Identification of amino acid residues contributing to the ATP-binding site of a purinergic P2X receptor. J Biol Chem 275: 34190-34196.

Jonas, P. (2000). The Time Course of Signaling at Central Glutamatergic Synapses. News Physiol Sci 15: 83-89.

Jones, A. K., A. N. Bera, K. Lees and D. B. Sattelle. (2010). The cys-loop ligand-gated ion channel gene superfamily of the parasitoid wasp, Nasonia vitripennis. Heredity 104: 247-259.

Kaneda, M., M. Mochizuki, K. Aoki and A. Kaneko. (1997). Modulation of GABAC response by Ca2+ and other divalent cations in horizontal cells of the catfish retina. J Gen Physiol 110: 741-747.

Kardos, J., I. Kovacs, F. Hajos, M. Kalman and M. Simonyi. (1989). Nerve endings from rat brain tissue release copper upon depolarization. A possible role in regulating neuronal excitability. Neurosci Lett 103: 139-144.

Kawate, T. and E. Gouaux. (2006). Fluorescence-detection size-exclusion chromatography for precrystallization screening of integral membrane proteins. Structure 14: 673-681.

Kawate, T., J. C. Michel, W. T. Birdsong and E. Gouaux. (2009). Crystal structure of the ATP-gated P2X(4) ion channel in the closed state. Nature 460: 592-598.

Kawate, T., J. L. Robertson, M. Li, S. D. Silberberg and K. J. Swartz. (2011). Ion access pathway to the transmembrane pore in P2X receptor channels. J Gen Physiol 137: 579-590.

Kay, A. R. (2003). Evidence for chelatable zinc in the extracellular space of the hippocampus, but little evidence for synaptic release of Zn. J Neurosci 23: 6847-6855.

Keen, C. L., J. Y. Uriu-Hare, S. N. Hawk, M. A. Jankowski, G. P. Daston, C. L. Kwik-Uribe and R. B. Rucker. (1998). Effect of copper deficiency on prenatal development and pregnancy outcome. Am J Clin Nutr 67: 1003S-1011S.

Khakh, B. S. and R. A. North. (2006). P2X receptors as cell-surface ATP sensors in health and disease. Nature 442: 527-532.

Khakh, B. S., J. A. Fisher, R. Nashmi, D. N. Bowser and H. A. Lester. (2005). An angstrom scale interaction between plasma membrane ATP-gated P2X2 and alpha4beta2 nicotinic channels measured with fluorescence resonance energy transfer and total internal reflection fluorescence microscopy. J Neurosci 25: 6911-6920.

Khakh, B. S., X. R. Bao, C. Labarca and H. A. Lester. (1999). Neuronal P2X transmitter-gated cation channels change their ion selectivity in seconds. Nat Neurosci 2: 322-330.

Khakh, B. S., X. Zhou, J. Sydes, J. J. Galligan and H. A. Lester. (2000). State-dependent cross-inhibition between transmitter-gated cation channels. Nature 406: 405-410.

Kim, M., L. H. Jiang, H. L. Wilson, R. A. North and A. Surprenant. (2001). Proteomic and functional evidence for a P2X7 receptor signalling complex. EMBO J 20: 6347-6358.

Koizumi, S., M. Ikeda, K. Inoue and K. Nakazawa. (1995). Enhancement by zinc of ATP-evoked dopamine release from rat pheochromocytoma PC12 cells. Brain Res 673: 75-82.

Koles, L., A. Leichsenring, P. Rubini and P. Illes. (2011). P2 receptor signaling in neurons and glial cells of the central nervous system. Adv Pharmacol 61: 441-493.

Komatsu, K., K. Kikuchi, H. Kojima, Y. Urano and T. Nagano. (2005). Selective zinc sensor molecules with various affinities for Zn2+, revealing dynamics and regional distribution of synaptically released Zn2+ in hippocampal slices. Journal of the American Chemical Society 127: 10197-10204.

Kozma, M., P. Szerdahelyi and P. Kasa. (1981). Histochemical detection of zinc and copper in various neurons of the central nervous system. Acta Histochem 69: 12-17.

Krieger, D. T. (1983). Brain peptides: what, where, and why? Science 222: 975-985.

Kühne, W. (1862). Über dieperipherischen Endorgane der motorischen Nerven. Engelmann Leipzig

Kühne, W. (1871). In: Stricker S (ed) Handbuch der Lehre von den Geweben. Engelmann Leipzig: 12.

Kuusinen, A., M. Arvola and K. Keinanen. (1995). Molecular dissection of the agonist binding site of an AMPA receptor. The EMBO journal 14: 6327-6332.

Labasi, J. M., N. Petrushova, C. Donovan, S. McCurdy, P. Lira, M. M. Payette, W. Brissette, J. R. Wicks, L. Audoly and C. A. Gabel (2002). Absence of the P2X7 receptor alters leukocyte function and attenuates an inflammatory response. Journal of immunology 168: 6436-6445.

Laube, B., J. Kuhse and H. Betz. (2000). Kinetic and mutational analysis of Zn2+ modulation of recombinant human inhibitory glycine receptors. J Physiol 522 Pt 2: 215-230.

Laube, B., J. Kuhse, N. Rundstrom, J. Kirsch, V. Schmieden and H. Betz. (1995). Modulation by zinc ions of native rat and recombinant human inhibitory glycine receptors. J Physiol 483 (Pt 3): 613-619.

Le, K. T., M. Paquet, D. Nouel, K. Babinski and P. Seguela. (1997). Primary structure and expression of a naturally truncated human P2X ATP receptor subunit from brain and immune system. FEBS Lett 418: 195-199.

Letts, V. A., R. Felix, G. H. Biddlecome, J. Arikkath, C. L. Mahaffey, A. Valenzuela, F. S. Bartlett, 2nd, Y. Mori, K. P. Campbell and W. N. Frankel. (1998). The mouse stargazer gene encodes a neuronal Ca2+-channel gamma subunit. Nat Genet 19: 340-347.

Li, C., R. W. Peoples, Z. Li and F. F. Weight. (1993). Zn2+ potentiates excitatory action of ATP on mammalian neurons. Proc Natl Acad Sci U S A 90: 8264-8267.

Li, Y., C. J. Hough, S. W. Suh, J. M. Sarvey and C. J. Frederickson. (2001). Rapid translocation of Zn(2+) from presynaptic terminals into postsynaptic hippocampal neurons after physiological stimulation. J Neurophysiol 86: 2597-2604.

Lin, D. D., A. S. Cohen and D. A. Coulter. (2001). Zinc-induced augmentation of excitatory synaptic currents and glutamate receptor responses in hippocampal CA3 neurons. J Neurophysiol 85: 1185-1196.

Liu, X., A. Surprenant, H. J. Mao, S. Roger, R. Xia, H. Bradley and L. H. Jiang. (2008). Identification of key residues coordinating functional inhibition of P2X7 receptors by zinc and copper. Mol Pharmacol 73: 252-259.

Liuzzi, J. P. and R. J. Cousins. (2004). Mammalian zinc transporters. Annual review of nutrition 24: 151-172.

Loewi, O. (1921). Über humorale Übertragbarkeit der Herznervenwirkung. Pflügers Arch 189: 4.

Loewi, O. and E. Navratil. (1926). Über humorale Übertragbarkeit der Herznervenwirkunk. X. Über das Schicksal des Vagusstoffs. Pflügers Arch 214: 10.

Lopantsev, V., H. J. Wenzel, T. B. Cole, R. D. Palmiter and P. A. Schwartzkroin. (2003). Lack of vesicular zinc in mossy fibers does not affect synaptic excitability of CA3 pyramidal cells in zinc transporter 3 knockout mice. Neuroscience 116: 237-248.

Lorca, R. A., C. Coddou, M. C. Gazitua, P. Bull, C. Arredondo and J. P. Huidobro-Toro. (2005). Extracellular histidine residues identify common structural determinants in the copper/zinc P2X2 receptor modulation. J Neurochem 95: 499-512.

Lorca, R. A., C. Rozas, S. Loyola, S. Moreira-Ramos, M. L. Zeise, A. Kirkwood, J. P. Huidobro-Toro and B. Morales. (2011). Zinc enhances long-term potentiation through P2X receptor modulation in the hippocampal CA1 region. Eur J Neurosci 33: 1175-1185.

Lovinger, D. M. (1991). Inhibition of 5-HT3 receptor-mediated ion current by divalent metal cations in NCB-20 neuroblastoma cells. J Neurophysiol 66: 1329-1337.

Lu, Y. M., F. A. Taverna, R. Tu, C. A. Ackerley, Y. T. Wang and J. Roder. (2000). Endogenous Zn(2+) is required for the induction of long-term potentiation at rat hippocampal mossy fiber-CA3 synapses. Synapse 38: 187-197.

Lustig, K. D., A. K. Shiau, A. J. Brake and D. Julius. (1993). Expression cloning of an ATP receptor from mouse neuroblastoma cells. Proc Natl Acad Sci U S A 90: 5113-5117.

Ma, B., H. Z. Ruan, G. Burnstock and P. M. Dunn. (2005). Differential expression of P2X receptors on neurons from different parasympathetic ganglia. Neuropharmacology 48: 766-777.

MacDonald, R. S. (2000). The role of zinc in growth and cell proliferation. The Journal of nutrition 130: 1500S-1508S.

Madden, D. R. (2002). The structure and function of glutamate receptor ion channels. Nat Rev Neurosci 3: 91-101.

Masin, M., D. Kerschensteiner, K. Dumke, M. E. Rubio and F. Soto. (2006). Fe65 interacts with P2X2 subunits at excitatory synapses and modulates receptor function. J Biol Chem 281: 4100-4108.

Maske, H. (1955). [Relation between insulin and zinc in the islands of Langerhans, with special reference to blood sugar control and insulin secretion]. Experientia 11: 122-128.

Mathie, A., G. L. Sutton, C. E. Clarke and E. L. Veale. (2006). Zinc and copper: pharmacological probes and endogenous modulators of neuronal excitability. Pharmacology & therapeutics 111: 567-583.

Mayer, M. L. and L. Vyklicky, Jr. (1989). The action of zinc on synaptic transmission and neuronal excitability in cultures of mouse hippocampus. J Physiol 415: 351-365.

Mercer, J. F., J. Livingston, B. Hall, J. A. Paynter, C. Begy, S. Chandrasekharappa, P. Lockhart, A. Grimes, M. Bhave, D. Siemieniak and et al. (1993). Isolation of a partial candidate gene for Menkes disease by positional cloning. Nat Genet 3: 20-25.

Moore, S. F. and A. B. Mackenzie. (2008). Species and agonist dependent zinc modulation of endogenous and recombinant ATP-gated P2X7 receptors. Biochem Pharmacol 76: 1740-1747.

Moroni, M., R. Vijayan, A. Carbone, R. Zwart, P. C. Biggin and I. Bermudez. (2008). Non-agonist-binding subunit interfaces confer distinct functional signatures to the alternate stoichiometries of the alpha4beta2 nicotinic receptor: an alpha4-alpha4 interface is required for Zn2+ potentiation. J Neurosci 28: 6884-6894.

Mosbacher, J., R. Schoepfer, H. Monyer, N. Burnashev, P. H. Seeburg and J. P. Ruppersberg. (1994). A molecular determinant for submillisecond desensitization in glutamate receptors. Science 266: 1059-1062.

Mott, D. D., M. Benveniste and R. J. Dingledine. (2008). pH-dependent inhibition of kainate receptors by zinc. J Neurosci 28: 1659-1671.

Mulryan, K., D. P. Gitterman, C. J. Lewis, C. Vial, B. J. Leckie, A. L. Cobb, J. E. Brown, E. C. Conley, G. Buell, C. A. Pritchard and R. J. Evans (2000). Reduced vas deferens contraction and male infertility in mice lacking P2X1 receptors. Nature 403: 86-89.

Murrell-Lagnado, R. D. and O. S. Qureshi. (2008). Assembly and trafficking of P2X purinergic receptors (Review). Mol Membr Biol 25: 321-331.

Nagaya, N., R. K. Tittle, N. Saar, S. S. Dellal and R. I. Hume. (2005). An intersubunit zinc binding site in rat P2X(2) receptors. J Biol Chem 280: 25982-25993.

Nakazawa, K. and Y. Ohno. (1996). Dopamine and 5-hydroxytryptamine selectively potentiate neuronal type ATP receptor channels. Eur J Pharmacol 296: 119-122.

Newbolt, A., R. Stoop, C. Virginio, A. Surprenant, R. A. North, G. Buell and F. Rassendren. (1998). Membrane topology of an ATP-gated ion channel (P2X receptor). J Biol Chem 273: 15177-15182.

Nicke, A., H. G. Baumert, J. Rettinger, A. Eichele, G. Lambrecht, E. Mutschler and G. Schmalzing. (1998). P2X1 and P2X3 receptors form stable trimers: a novel structural motif of ligand-gated ion channels. The EMBO journal 17: 3016-3028.

Noebels, J. L., X. Qiao, R. T. Bronson, C. Spencer and M. T. Davisson. (1990). Stargazer: a new neurological mutant on chromosome 15 in the mouse with prolonged cortical seizures. Epilepsy Res 7: 129-135.

North, R. A. (2002). Molecular physiology of P2X receptors. Physiological reviews 82: 1013-1067.

North, R. A. (2003). The P2X3 subunit: a molecular target in pain therapeutics. Current opinion in investigational drugs 4: 833-840.

O'Connor, S. E., I. A. Dainty and P. Leff. (1991). Further subclassification of ATP receptors based on agonist studies. Trends Pharmacol Sci 12: 137-141.

Palmiter, R. D. and L. Huang. (2004). Efflux and compartmentalization of zinc by members of the SLC30 family of solute carriers. Pflugers Archiv : European journal of physiology 447: 744-751.

Palmiter, R. D., T. B. Cole, C. J. Quaife and S. D. Findley. (1996). ZnT-3, a putative transporter of zinc into synaptic vesicles. Proc Natl Acad Sci U S A 93: 14934-14939.

Pan, E., X. A. Zhang, Z. Huang, A. Krezel, M. Zhao, C. E. Tinberg, S. J. Lippard and J. O. McNamara. (2011). Vesicular zinc promotes presynaptic and inhibits postsynaptic long-term potentiation of mossy fiber-CA3 synapse. Neuron 71: 1116-1126.

Pelegrin, P. and A. Surprenant. (2006). Pannexin-1 mediates large pore formation and interleukin-1beta release by the ATP-gated P2X7 receptor. EMBO J 25: 5071-5082.

Pena, M. M., J. Lee and D. J. Thiele. (1999). A delicate balance: homeostatic control of copper uptake and distribution. J Nutr 129: 1251-1260.

Peters, S., J. Koh and D. W. Choi. (1987). Zinc selectively blocks the action of N-methyl-D-aspartate on cortical neurons. Science 236: 589-593.

Prohaska, J. R. and B. Brokate. (2002). The timing of perinatal copper deficiency in mice influences offspring survival. J Nutr 132: 3142-3145.

Qian, J. and J. L. Noebels. (2005). Visualization of transmitter release with zinc fluorescence detection at the mouse hippocampal mossy fibre synapse. J Physiol 566: 747-758.

Qu, Y., S. Misaghi, K. Newton, L. L. Gilmour, S. Louie, J. E. Cupp, G. R. Dubyak, D. Hackos and V. M. Dixit. (2011). Pannexin-1 is required for ATP release during apoptosis but not for inflammasome activation. J Immunol 186: 6553-6561.

Que, E. L., D. W. Domaille and C. J. Chang. (2008). Metals in neurobiology: probing their chemistry and biology with molecular imaging. Chem Rev 108: 1517-1549.

Quinta-Ferreira, M. E. and C. M. Matias. (2004). Hippocampal mossy fiber calcium transients are maintained during long-term potentiation and are inhibited by endogenous zinc. Brain Res 1004: 52-60.

Rassendren, F., G. Buell, A. Newbolt, R. A. North and A. Surprenant. (1997). Identification of amino acid residues contributing to the pore of a P2X receptor. EMBO. J. 16: 3446-3454.

Ren, J., X. Bian, M. DeVries, B. Schnegelsberg, D. A. Cockayne, A. P. Ford and J. J. Galligan. (2003). P2X2 subunits contribute to fast synaptic excitation in myenteric neurons of the mouse small intestine. J Physiol 552: 809-821.

Rettinger, J., G. Schmalzing, S. Damer, G. Muller, P. Nickel and G. Lambrecht. (2000). The suramin analogue NF279 is a novel and potent antagonist selective for the P2X(1) receptor. Neuropharmacology 39: 2044-2053.

Roberts, E. and S. Frankel. (1950). gamma-Aminobutyric acid in brain: its formation from glutamic acid. J Biol Chem 187: 55-63.

Roberts, J. A. and R. J. Evans. (2004). ATP binding at human P2X1 receptors. Contribution of aromatic and basic amino acids revealed using mutagenesis and partial agonists. J Biol Chem 279: 9043-9055.

Roberts, J. A., H. R. Digby, M. Kara, S. El Ajouz, M. J. Sutcliffe and R. J. Evans. (2008). Cysteine substitution mutagenesis and the effects of methanethiosulfonate reagents at P2X2 and P2X4 receptors support a core common mode of ATP action at P2X receptors. J Biol Chem 283: 20126-20136.

Roberts, J. A., M. Valente, R. C. Allsopp, D. Watt and R. J. Evans. (2009). Contribution of the region Glu181 to Val200 of the extracellular loop of the human P2X1 receptor to agonist binding and gating revealed using cysteine scanning mutagenesis. J Neurochem 109: 1042-1052.

Rong, W., G. Burnstock and K. M. Spyer (2000). P2X purinoceptor-mediated excitation of trigeminal lingual nerve terminals in an in vitro intra-arterially perfused rat tongue preparation. The Journal of physiology 524 Pt 3: 891-902.

Rui Wang, Craig S. Walker, Penelope J. Brockie, Michael M. Francis, Jerry E. Mellem, David M. Madsen, and Andres V. Maricq. (2008). TARP Proteins Have Fundamental Roles in the Gating of Glutamate Receptors and the Tuning of Synaptic Function Neuron 59: 997–1008.

Samways, D. S., B. S. Khakh, S. Dutertre and T. M. Egan. (2011). Preferential use of unobstructed lateral portals as the access route to the pore of human ATP-gated ion channels (P2X receptors). Proc Natl Acad Sci U S A 108: 13800-13805.

Sato, M., K. Ohtomo, T. Daimon, T. Sugiyama and K. Iijima. (1994). Localization of copper to afferent terminals in rat locus ceruleus, in contrast to mitochondrial copper in cerebellum. J Histochem Cytochem 42: 1585-1591.

Searl, T. J., R. S. Redman and E. M. Silinsky. (1998). Mutual occlusion of P2X ATP receptors and nicotinic receptors on sympathetic neurons of the guinea-pig. J Physiol 510 (Pt 3): 783-791.

Sim, J. A., S. Chaumont, J. Jo, L. Ulmann, M. T. Young, K. Cho, G. Buell, R. A. North and F. Rassendren (2006). Altered hippocampal synaptic potentiation in P2X4 knock-out mice. J Neurosci 26: 9006-9009.

Simon, J. and E. A. Barnard. (2003). The P2Y nucleotide receptors in the human genome. Acta biologica Hungarica 54: 191-201.

Sindreu, C. and D. R. Storm. (2011). Modulation of neuronal signal transduction and memory formation by synaptic zinc. Front. Behav. Neurosci. 5: 68.

Smart, T. G. and A. Constanti. (1990). Differential effect of zinc on the vertebrate GABAA-receptor complex. Br J Pharmacol 99: 643-654.

Smart, T. G., S. J. Moss, X. Xie and R. L. Huganir. (1991). GABAA receptors are differentially sensitive to zinc: dependence on subunit composition. Br J Pharmacol 103: 1837-1839.

Sobolevsky, A. I., M. P. Rosconi and E. Gouaux. (2009). X-ray structure, symmetry and mechanism of an AMPA-subtype glutamate receptor. Nature 462: 745-756.

Sokolova, E., A. Nistri and R. Giniatullin. (2001). Negative cross talk between anionic GABAA and cationic P2X ionotropic receptors of rat dorsal root ganglion neurons. J Neurosci 21: 4958-4968.

Souslova, V., P. Cesare, Y. Ding, A. N. Akopian, L. Stanfa, R. Suzuki, K. Carpenter, A. Dickenson, S. Boyce, R. Hill, D. Nebenuis-Oosthuizen, A. J. Smith, E. J. Kidd and J. N. Wood (2000). Warm-coding deficits and aberrant inflammatory pain in mice lacking P2X3 receptors. Nature 407: 1015-1017.

Sparks, D. L. and B. G. Schreurs. (2003). Trace amounts of copper in water induce beta-amyloid plaques and learning deficits in a rabbit model of Alzheimer's disease. Proc Natl Acad Sci U S A 100: 11065-11069.

Stoop, R., S. Thomas, F. Rassendren, E. Kawashima, G. Buell, A. Surprenant and R. A. North. (1999). Contribution of individual subunits to the multimeric P2X(2) receptor: estimates based on methanethiosulfonate block at T336C. Mol Pharmacol 56: 973-981.

Swanson, G. T., S. K. Kamboj and S. G. Cull-Candy. (1997). Single-channel properties of recombinant AMPA receptors depend on RNA editing, splice variation, and subunit composition. J Neurosci 17: 58-69.

Tasneem, A., L. M. Iyer, E. Jakobsson and L. Aravind. (2005). Identification of the prokaryotic ligand-gated ion channels and their implications for the mechanisms and origins of animal Cys-loop ion channels. Genome biology 6: R4.

Tittle, R. K. and R. I. Hume. (2008). Opposite Effects of Zinc on Human and Rat P2X(2) Receptors. J Neurosci 28: 11131-11140.

Tittle, R. K., J. M. Power and R. I. Hume. (2007). A histidine scan to probe the flexibility of the rat P2X2 receptor zinc-binding site. J Biol Chem 282: 19526-19533.

Tomita, S., L. Chen, Y. Kawasaki, R. S. Petralia, R. J. Wenthold, R. A. Nicoll and D. S. Bredt. (2003). Functional studies and distribution define a family of transmembrane AMPA receptor regulatory proteins. J Cell Biol 161: 805-816.

Tomita, S., M. Fukata, R. A. Nicoll and D. S. Bredt. (2004). Dynamic interaction of stargazin-like TARPs with cycling AMPA receptors at synapses. Science 303: 1508-1511.

Tomita, S., V. Stein, T. J. Stocker, R. A. Nicoll and D. S. Bredt. (2005). Bidirectional synaptic plasticity regulated by phosphorylation of stargazin-like TARPs. Neuron 45: 269-277.

Torres, G. E., T. M. Egan and M. M. Voigt. (1998). N-Linked glycosylation is essential for the functional expression of the recombinant P2X2 receptor. Biochemistry 37: 14845-14851.

Toulme, E., D. Blais, C. Leger, M. Landry, M. Garret, P. Seguela and E. Boue-Grabot. (2007). An intracellular motif of P2X(3) receptors is required for functional cross-

talk with GABA(A) receptors in nociceptive DRG neurons. J Neurochem 102: 1357-1368.

Traynelis, S. F., M. F. Burgess, F. Zheng, P. Lyuboslavsky and J. L. Powers. (1998). Control of voltage-independent zinc inhibition of NMDA receptors by the NR1 subunit. J Neurosci 18: 6163-6175.

Trombley, P. Q. and G. M. Shepherd. (1996). Differential modulation by zinc and copper of amino acid receptors from rat olfactory bulb neurons. J Neurophysiol 76: 2536-2546.

Trombley, P. Q., L. J. Blakemore and B. J. Hill. (2011). Zinc modulation of glycine receptors. Neuroscience 186: 32-38.

Ueno, S., H. Yamada, T. Moriyama, K. Honda, Y. Takano, H. O. Kamiya and T. Katsuragi. (2002). Measurement of dorsal root ganglion P2X mRNA by SYBR Green fluorescence. Brain research. Brain research protocols 10: 95-101.

Ueno, T., S. Ueno, Y. Kakazu, N. Akaike and J. Nabekura. (2001). Bidirectional modulation of P2X receptor-mediated response by divalent cations in rat dorsal motor nucleus of the vagus neurons. J Neurochem 78: 1009-1018.

Uki, M. and T. Narahashi. (1996). Modulation of serotonin-induced currents by metals in mouse neuroblastoma cells. Arch Toxicol 70: 652-660.

Unwin, N. (2005). Refined structure of the nicotinic acetylcholine receptor at 4A resolution. Journal of molecular biology 346: 967-989.

Valentin, G. G. (1836). Über den Verlauf und die letzten Enden der Nerven. Nova Acta Phys-Med Acad Leopoldina Breslau 18: 189.

Valera, S., N. Hussy, R. J. Evans, N. Adami, R. A. North, A. Surprenant and G. Buell. (1994). A new class of ligand-gated ion channel defined by P2x receptor for extracellular ATP. Nature 371: 516-519.

Vallee, B. L. and D. S. Auld. (1993). Cocatalytic zinc motifs in enzyme catalysis. Proc. Natl. Acad. Sci. U S A. 90: 2715-2718.

Vandenberghe, W., R. A. Nicoll and D. S. Bredt. (2005). Stargazin is an AMPA receptor auxiliary subunit. Proc Natl Acad Sci U S A 102: 485-490.

Varea, E., X. Ponsoda, A. Molowny, G. Danscher and C. Lopez-Garcia. (2001). Imaging synaptic zinc release in living nervous tissue. J Neurosci methods 110: 57-63.

Vessey, K. A., A. I. Jobling, U. Greferath and E. L. Fletcher (2012). The role of the P2X7 receptor in the retina: cell signalling and dysfunction. Advances in experimental medicine and biology 723: 813-819.

Vlachova, V., H. Zemkova and L. Vyklicky, Jr. (1996). Copper modulation of NMDA responses in mouse and rat cultured hippocampal neurons. Eur J Neurosci 8: 2257-2264.

Vlaskovska, M., L. Kasakov, W. Rong, P. Bodin, M. Bardini, D. A. Cockayne, A. P. Ford and G. Burnstock (2001). P2X3 knock-out mice reveal a major sensory role for urothelially released ATP. J Neurosci 21: 5670-5677.

Vogt, K., J. Mellor, G. Tong and R. Nicoll. (2000). The actions of synaptically released zinc at hippocampal mossy fiber synapses. Neuron 26: 187-196.

Vorobjev, V. S., I. N. Sharonova, H. L. Haas and O. A. Sergeeva. (2003). Expression and function of P2X purinoceptors in rat histaminergic neurons. Br J Pharmacol 138: 1013-1019.

Vulpe, C., B. Levinson, S. Whitney, S. Packman and J. Gitschier. (1993). Isolation of a candidate gene for Menkes disease and evidence that it encodes a copper-transporting ATPase. Nat Genet 3: 7-13.

Walker, C. S., P. J. Brockie, D. M. Madsen, M. M. Francis, Y. Zheng, S. Koduri, J. E. Mellem, N. Strutz-Seebohm and A. V. Maricq. (2006). Reconstitution of invertebrate glutamate receptor function depends on stargazin-like proteins. Proc Natl Acad Sci U S A 103: 10781-10786.

Wang, R., C. S. Walker, P. J. Brockie, M. M. Francis, J. E. Mellem, D. M. Madsen and A. V. Maricq. (2008). Evolutionary conserved role for TARPs in the gating of glutamate receptors and tuning of synaptic function. Neuron 59: 997-1008.

Webb, T. E., J. Simon, B. J. Krishek, A. N. Bateson, T. G. Smart, B. F. King, G. Burnstock and E. A. Barnard. (1993). Cloning and functional expression of a brain G-protein-coupled ATP receptor. FEBS Lett 324: 219-225.

Wei, W., N. Zhang, Z. Peng, C. R. Houser and I. Mody. (2003). Perisynaptic localization of delta subunit-containing GABA(A) receptors and their activation by GABA spillover in the mouse dentate gyrus. J Neurosci 23: 10650-10661.

Weiser, T. and M. Wienrich. (1996). The effects of copper ions on glutamate receptors in cultured rat cortical neurons. Brain Res 742: 211-218.

Weiss, J. H., S. L. Sensi and J. Y. Koh. (2000). Zn(2+): a novel ionic mediator of neural injury in brain disease. Trends Pharmacol Sci 21: 395-401.

Westbrook, G. L. and M. L. Mayer. (1987). Micromolar concentrations of Zn2+ antagonize NMDA and GABA responses of hippocampal neurons. Nature 328: 640-643.

White, N. and G. Burnstock. (2006). P2 receptors and cancer. Trends Pharmacol Sci 27: 211-217.

Wildman, S. S., B. F. King and G. Burnstock. (1999). Modulation of ATP-responses at recombinant rP2X4 receptors by extracellular pH and zinc. Br J Pharmacol 126: 762-768.

Wildman, S. S., S. G. Brown, M. Rahman, C. A. Noel, L. Churchill, G. Burnstock, R. J. Unwin and B. F. King. (2002). Sensitization by extracellular Ca(2+) of rat P2X(5) receptor and its pharmacological properties compared with rat P2X(1). Mol Pharmacol 62: 957-966.

Williams, K. (1996). Separating dual effects of zinc at recombinant N-methyl-D-aspartate receptors. Neurosci Lett 215: 9-12.

Wilson, H. L., S. A. Wilson, A. Surprenant and R. A. North. (2002). Epithelial membrane proteins induce membrane blebbing and interact with the P2X7 receptor C terminus. J Biol Chem 277: 34017-34023.

Wyllie, D. J., S. F. Traynelis and S. G. Cull-Candy. (1993). Evidence for more than one type of non-NMDA receptor in outside-out patches from cerebellar granule cells of the rat. J Physiol 463: 193-226.

Xie, X. and T. G. Smart. (1994). Modulation of long-term potentiation in rat hippocampal pyramidal neurons by zinc. Pflugers Arch 427: 481-486.

Xie, X. M. and T. G. Smart. (1991). A physiological role for endogenous zinc in rat hippocampal synaptic neurotransmission. Nature 349: 521-524.

Xiong, K., R. W. Peoples, J. P. Montgomery, Y. Chiang, R. R. Stewart, F. F. Weight and C. Li. (1999). Differential modulation by copper and zinc of P2X2 and P2X4 receptor function. J Neurophysiol 81: 2088-2094.

Yamazaki, M., T. Ohno-Shosaku, M. Fukaya, M. Kano, M. Watanabe and K. Sakimura. (2004). A novel action of stargazin as an enhancer of AMPA receptor activity. Neurosci Res 50: 369-374.

Yan, Z., S. Li, Z. Liang, M. Tomic and S. S. Stojilkovic. (2008). The P2X7 receptor channel pore dilates under physiological ion conditions. J Gen Physiol 132: 563-573.

Zemkova, H., Z. Yan, Z. Liang, I. Jelinkova, M. Tomic and S. S. Stojilkovic. (2007). Role of aromatic and charged ectodomain residues in the P2X(4) receptor functions. J Neurochem 102: 1139-1150.

Zhou, X. and J. J. Galligan. (1998). Non-additive interaction between nicotinic cholinergic and P2X purine receptors in guinea-pig enteric neurons in culture. J Physiol 513 (Pt 3): 685-697.